# “NANOPOROUS CARBON FROM CORN COBS AND ITS APPLICATIONS”

---

A Dissertation

presented to

the Faculty of the Graduate School

University of Missouri- Columbia

---

In Partial Fulfillment

of the Requirements for the Degree

Doctor of Philosophy

---

by

Parag S. Shah

Dr. Galen J. Suppes, Dissertation Supervisor

August, 2007

# ACKNOWLEDGEMENTS

First of all I would like to thanks my parents Suresh R Shah and Renuka S Shah for supporting me to pursue my goal of higher studies. And I am sincerely thankful to my dearest brother Virag S Shah for his constant motivation and valuable guidance all the time when I was far away from my cordial family.

I would like to take this opportunity to express my sincere gratitude to Dr. Galen J. Suppes for giving me the opportunity to work on this project and for his invaluable advice and patience throughout my graduate program. His constant suggestions and advice helped incredibly towards my professional development. I would also like to thank Dr Peter Pfeifer for his constant suggestions and advice during the course of this project. The time and efforts of the committee members Drs William Jacoby, Tom Marrero and Eric Doskocil are also highly appreciated.

I owe deep debts of gratitude to my co-researchers Shailesh Lopes, Mohan Dasari, Rusty Sutterlin, and Roger for their excellent support in every aspect at all stages of my research.

Finally I would like to thank my wonderful friends Shailja Vaghela, Janak Dani, Akshay and Ami Patel, Deepak Manjunath, and Bhavin Patel for all the good times I spent with them, cheering and encouraging me whenever needed.

Thank you one and all.

# TABLE OF CONTENTS

**ACKNOWLEDGEMENTS** ..... **II**

**TABLE OF CONTENTS** ..... **III**

**LIST OF TABLES** ..... **VIII**

**LIST OF FIGURES** ..... **X**

**DISSERTATION FORMAT** ..... **XIV**

**CHAPTER 1** ..... **1**

**1. INTRODUCTION** ..... **1**

1.1 INTRODUCTION TO ACTIVATED CARBON ..... 1

1.2 MARKETS FOR ACTIVATED CARBON ..... 3

1.3 CHARACTERIZATION OF CARBON ..... 4

1.4 APPLICATIONS ..... 6

REFERENCES ..... 9

**CHAPTER 2** ..... **10**

**2. NANOPOROUS CARBON FROM CORN COB USING CHEMICAL ACTIVATION PROCESS** ..... **10**

ABSTRACT ..... 11

2.1 INTRODUCTION ..... 12

2.2 EXPERIMENTAL PROCEDURE ..... 16

2.3 RESULT AND DISCUSSION ..... 18

2.3.1 EFFECT OF PHOSPHORIC ACID CONCENTRATION ..... 18

2.3.2 EFFECT OF HEAT TREATMENT TEMPERATURE (HTT)..... 20
2.3.3 EFFECT OF RATE OF HEATING..... 22
2.3.4 EFFECT OF SOAKING TEMPERATURE..... 24
2.3.5 MECHANISM OF PHOSPHORIC ACID ACTIVATION OF CORN COBS EXPLAINED USING THERMOGRAVIMETRIC ANALYSIS (TGA)..... 26
2.3.6 KOH ACTIVATION..... 34
2.4 CONCLUSION..... 40
REFERENCES..... 40
**CHAPTER 3..... 43**
**3. NANOPOROUS CARBON FROM CORN COBS FOR ADSORBED NATURAL GAS APPLICATION..... 43**
ABSTRACT..... 44
3.1 INTRODUCTION..... 45
3.2 EXPERIMENTAL PROCEDURE..... 48
3.3 RESULTS AND DISCUSSION..... 50
3.3.1 EFFECT OF KOH: CHAR RATIO ON METHANE UPTAKE CAPACITY..... 51
3.3.2 EFFECT OF HEAT TREATEMENT TEMPERATURE (HTT) ON METHANE UPTAKE..... 53
3.3.3 DENSIFICATION STUDIES..... 54
3.3.4 VOLUME DISTRIBUTION OF TANK..... 56
3.3.5 TEMPERATURE PROFILES IN CARBON MONOLITHS..... 57
3.3.6 KOH RECYCLE..... 58

3.4 CONCLUSION ..... 59

FIGURES ..... 60

TABLES ..... 68

REFERENCES ..... 71

**CHAPTER 4 ..... 74**

**4. SOYBEAN OIL AS BINDER FOR MAKING NANOPOROUS CARBON MONOLITHS FOR ADSORBED NATURAL GAS APPLICATION ..... 74**

ABSTRACT ..... 75

4.1 INTRODUCTION ..... 76

4.2 EXPERIMENTAL PROCEDURE ..... 77

4.3 RESULTS AND DISCUSSION ..... 79

4.3.1 EFFECT OF COMONOMER CONCENTRATION ..... 79

4.3.2 EFFECT OF CATALYST ..... 81

4.3.3 EFFECT OF % OF SBO PREPOLYMER in MONOLITH ..... 82

4.3.4 COMPARISON BETWEEN SARAN AND SOYBEAN OIL BINDERS ..... 83

4.4 CONCLUSION ..... 85

TABLES ..... 87

FIGURES ..... 90

REFERENCE ..... 94

**CHAPTER 5 ..... 95**

**5 NANOPOROUS CARBON FROM CORN COBS FOR CATALYST SUPPORT APPLICATION ..... 95**

5.1 INTRODUCTION ..... 95

5.2 EXPERIMENTAL PROCEDURE ..... 98
5.2.1 CATALYST PREPARATION ..... 98
5.2.2 CATALYST TESTING ..... 99
5.2.3 PRODUCT ANALYSIS ..... 100
5.3 RESULTS AND DISCUSSION ..... 100
5.4 CONLUSION ..... 104
REFERENCES ..... 105
**CHAPTER 6 ..... 107**
**6 ACTIVATED CARBON FROM CORN COBS FOR REMOVING CU(II) AND CR(III) METALS ..... 107**
ABSTRACT ..... 108
6.1 INTRODUCTION ..... 109
6.2 EXPERIMENTAL PROCEDURE ..... 110
6.2.1 GENERAL PROCEDURE FOR ADSORBENT TESTING ..... 111
6.2.2 METAL ANALYSIS BY ATOMIC EMISSION SPECTROSCOPY ..... 111
6.3 RESULT AND DISCUSSION ..... 112
6.3.1 COPPER (II) REMOVAL ..... 112
6.3.2 CHROMIUM (III) REMOVAL ..... 115
6.4 CONCLUSION ..... 116
TABLES ..... 116
FIGURES ..... 118
REFERENCE ..... 125
**CHAPTER 7 ..... 127**

***7*** **CONCLUSIONS AND FUTURE WORK ..... 127**

7.1 CONCLUSIONS ..... 127

7.2 RECOMMENDED RESEARCH ..... 129

**APPENDIX ..... 131**

A1. Calculation for finding methane uptake capacity using gravimetric method .... 131

A2. Calculation for finding methane uptake capacity volumetric or by using pressure differential method ..... 134

**VITA ..... 136**

# LIST OF TABLES

**Table 1-1 Commercial carbon precursors (source: Bansal et al.) ..... 2**

**Table 2-1 Elemental Analysis of Corn cobs. ..... 13**

**Table 2-2 Characterization of samples prepared with different phosphoric acid concentration ..... 19**

**Table 2-3 Characterization of samples prepared at different HTT ..... 22**

**Table 2-4 Characterization of samples prepared at different rate of heating..... 24**

**Table 2-5 Characterization of samples prepared at different soaking temperature. 26**

**Table 2-6 Characterization of carbon with different KOH: C ratio ..... 37**

**Table 2-7Characterization of carbon prepared with KOH activation at different HTT ..... 39**

**Table 0-1 Pore volume and methane uptake capacity of carbons prepared with varying KOH: C value. ..... 68**

**Table 0-2 Pore volume and methane uptake capacity of carbons prepared at different HTT. ..... 68**

**Table 0-3 Characterization and methane uptake capacity of carbon obtained from pure saran. ..... 69**

**Table 0-4 Effect of binder concentration on compressive strength and density of monolith. ..... 69**

**Table 0-5 Characterization and methane uptake capacity of carbon obtained from corn cobs using recycled KOH..... 70**

**Table 4-1 Effect of varying dicylopendatiene and divinylbenzene amounts on the final polymer..... 87**

**Table 4-2 Effect of divinyl benzene amount on final polymer properties ..... 87**

**Table 4-3 Effect of Catalyst of Final Polymer Properties ..... 87**

**Table 4-4 Effect of amount SBO prepolymer on the final monolith properties ..... 88**

**Table 4-5 Characterization of PVDC and SBO polymer carbon. Comparison between monoliths made with PVDC and SBO polymer..... 89**

**Table 4-6 Comparison between monoliths made with PVDC and SBO polymer….. 89**

**Table 5-1: Comparison of commercial catalyst and catalyst supported on highly porous carbon powder.. ..... 103**

**Table 6-1 Elemental Analysis of Corn cobs[19] ..... 116**

**Table 6-2 Characterization of Adsorbents ..... 117**

**Table 6-3 Adsorbent capacity of adsorbents for Cu (II) and Cr (III)..... 117**

# LIST OF FIGURES

**Figure 1-1Classification of isotherm shapes into six principal classes (Gregg and Sing)..... 6**

**Figure 2-1Graph showing effect of phosphoric acid concentration on BET surface area..... 19**

**Figure 2-2Graph showing effect of phosphoric acid concentration on micropore volume..... 19**

**Figure 2-3 Graph showing effect of HTT on BET surface area..... 21**

**Figure 2-4 Graph showing effect of HTT on micropore volume..... 22**

**Figure 2-5 Graph showing effect of rate of heating on BET surface area..... 23**

**Figure 2-6 Graph showing effect of different rate of heating on micropore volume 24**

**Figure 2-7 Graph showing effect of soaking temperature on BET surface area..... 26**

**Figure 2-8 Graph showing effect of soaking temperature on micropore volume..... 26**

**Figure 2-9 TGA of Corn cobs soaked in 50% vol H3PO4..... 27**

**Figure 2-10 TGA of plain corn cob..... 28**

**Figure 2-11 Reaction of phosphoric acid with cellulose..... 30**

**Figure 2-12 SEM image of an carbon sample prepared using H3PO4 activation at low magnification..... 33**

**Figure 2-13 SEM image of an carbon sample prepared by H3PO4 activation at high magnification..... 33**

**Figure 2-14 Nitrogen isotherms of carbon prepared with different KOH: C ratio.. 35**

**Figure 2-15 Graph showing effect of KOH:C ratio on micropore volume in carbon ..... 36**

**Figure 2-16 Nitrogen Isotherms at 77K for carbon prepared by KOH activation at different HTT ..... 38**

**Figure 2-17 Micro, meso and total pore volume of KOH treated carbon at different HTT ..... 39**

**Figure 0-1 Methane storage value in mass per volume of tank (g/L) with and without adsorbents. ..... 60**

**Figure 0-2 Schematic of Test Fixture used to measure methane uptake on 3.5" carbon monolith. ..... 60**

**Figure 0-3 Nitrogen Isotherms at 77K for carbons prepared with varying KOH:C values. ..... 61**

**Figure 0-4 Methane Isotherms at 298K for carbons prepared with varying KOH:C values. ..... 61**

**Figure 0-5 DFT/Monte Carlo cumulative pore volume graph..... 62**

**Figure 0-6 Effect of KOH :C values on piece density of carbon monoliths. ..... 62**

**Figure 0-7 Nitrogen Isotherms at 77K for carbons prepared at different HTT. ..... 63**

**Figure 0-8 S/S die used to prepare monoliths out of carbon powder. ..... 63**

**Figure 0-9 Effect of pressing force on thedensity of carbon monolith. ..... 64**

**Figure 0-10 Density increase in type-I and type-II PSDs. ..... 64**

**Figure 0-11 Pore size distribution in carbon obtained from pure saran. ..... 65**

**Figure 0-12 Effect of binder concentration on methane uptake capacity..... 65**

**Figure 0-13 Effect of binder concentration on final compressive strength of carbon monlith. ..... 66**

**Figure 0-14 Comparison of volume distribution of tank filled with corn cob derived carbon monolith and monolith made with commercially available MaxSorb carbon and AGLARG carbon..... 66**

**Figure 0-15 Temperature and Pressure profiles during the filling of the ANG tank. ..... 67**

**Figure 4-1 TGA of Saran (PVDC and PVC copolymer) ..... 90**

**Figure 4-2 TGA of SBO polymer with 30% divinylbenzene..... 91**

**Figure 4-3 TGA of SBO Polymer with 10% divinylbenzene and 30% dicyclopentadiene..... 92**

**Figure 4-4 Volume Distribution in Monoliths made with carbon obtained from PVDC ..... 92**

**Figure 4-5 Volume Distribution in Monolith made with carbon obtained from SBO polymer ..... 92**

**Figure 4-6 Volume Distribution in Carbon monoliths made using SBO as binders 93**

**Figure 4-7 Volume Distribution in Carbon monoliths made using PVDC as binders ..... 93**

**Figure 5-1 Schematic diagram of experimental setup to test catalyst..... 99**

**Figure 5-2: *Left:* 2.9-dimensional network of channels created by oxidative removal of carbon by chemical invasion (simulation; invasion from left to right). *Right*: Channel entrances (black areas) in a scanning tunneling micrograph. The entrance marked with an arrow is 11.4 nm wide at that location. ..... 101**

**Figure 5-3 TEM image of bimetallic Cu and Cr deposited on carbon..... 104**

**Figure 6-1 Concentration of $Cu^{2+}$ remaining in solution after treatment of 10 ml of aqueous solution with 1.0g of carbon at 298K..... 118**

**Figure 6-2 Concentration of $Cu^{2+}$ remaining in solution after treatment of 10 ml of aqueous solution with 0.2g of carbon at 298K..... 119**

**Figure 6-3 Concentration of $Cu^{2+}$ remaining in solution after treatment of 10 ml of aqueous solution with 0.5g of carbon at 298K..... 120**

**Figure 6-4 Concentration of $Cu^{2+}$ remaining in solution after treatment of 10 ml of aqueous solution with 1.0g of carbon at 318K..... 120**

**Figure 6-5 Concentration of $Cu^{2+}$ remaining in solution after treatment of 10 ml of aqueous solution with 1.0g of carbon at 298K for case where carbon is treated with nitric acid..... 121**

**Figure 6-6 Impact of mesopore volume on capacity of carbon to remove $Cu^{2+}$ from aqueous solution. ..... 122**

**Figure 6-7 Concentration of Cr(III) remaining in solution after treatment of 10 ml of aqueous solution with 1.0g of carbon at 298K. ..... 122**

**Figure 6-8 Concentration of Cr(III) remaining in solution after treatment of 10 ml of aqueous solution with 0.1g of carbon at 298K. ..... 123**

**Figure 6-9 Concentration of Cr(III) remaining in solution after treatment of 10 ml of aqueous solution with 0.05g of carbon at 298K for case where carbon is treated with nitric acid. ..... 123**

**Figure 6-10 Concentration of Cr(III) remaining in solution after treatment of 10 ml of aqueous solution with 0.05g of carbon at 298K. ..... 124**

# DISSERTATION FORMAT

This dissertation is written as a series of seven chapters. The research can be broadly classified as development of process for manufacturing nanoporous carbon from corn cobs and its applications with emphasis led on storing natural gas for adsorbed natural gas (ANG) technology and extended to other applications such as catalyst support and heavy metal removal from aqueous solution. Chapters 2, 3, and 4 deal with the manufacturing of nanoporous carbon from corn cobs and its application to store natural gas. The Chapter 5 is on the application of carbon produced from corn cobs as catalyst support. Chapter 6 is on the application of carbon for removing heavy metals from aqueous solution. Finally, Chapter 7 summarizes the results of the research and presents some suggestions for future investigations.

# CHAPTER 1

# 1. INTRODUCTION

## 1.1 INTRODUCTION TO ACTIVATED CARBON

The term "Activated Carbon" defines a group of materials with highly developed internal surface area and porosity and hence a large capacity for adsorbing chemicals from gases and liquids. Activated carbon are extremely versatile adsorbents of major industrial significance and are used in a wide range of applications which are concerned principally with removal of species by adsorption from liquids or gas phase in order to effect purification or recovery of chemicals. They also find use as catalysts or catalyst supports.

Because of the large scale applications of activated carbon the cost of activated carbon has to be low. The yield of activated carbon production is usually very low. Hence the process economics are normally dictated by the selection of readily available low cost feed stocks. Common examples of commercial feed stocks are materials of botanical origin (e.g. wood, coconut shell & nut kernels) and degraded or coalified plant matter (e.g. peat, lignite and all ranks of coal). The price of the end product depend both on the cost of precursors and the degree of processing required achieving the desired adsorptive properties. The Table 1-1 shows the world's percentage distribution of precursors used for commercial production of activated carbon in.

**Table 1-1 Commercial carbon precursors (source: Bansal et al.[1])**

| Precursor | Use (%) |
|---|---|
| Wood | 35 |
| Coal | 28 |
| Lignite | 14 |
| Coconut shell | 10 |
| Peat | 10 |
| Other | 3 |

Although the selection of processing conditions can allow some degree of latitude in controlling the structure and properties of the final product, the properties of activated carbons are determined to large extent by the nature of the precursor, and also by the particular processing technology. The differences in the adsorptive characteristics of carbons prepared from different starting materials are such that, in many applications, one carbon type will prove to be the most appropriate.

Little pertinent information exists in the open literature on the fundamental relationships between the structures of the precursor and activated carbon products, or the process chemistry. Although the manufacture of activated carbons is a long established industry, it has not experienced anything like the same level of growth as, for example, did the coking industry. Most of the world production is in the hands of a relatively small number of manufacturers. Each of these tends to use different raw materials and/or different process methods, the result of which is that the properties of the activated carbons offered are very different.[2] This means that there are only a few market segments where there is serious competition. Consequently, there has been no great

incentive for major investments in research and development. This position is beginning to change as application become more diverse, concern over environmental issues continues to grow and demand for higher performance adsorbents continues to increase.[3]

## 1.2 MARKETS FOR ACTIVATED CARBON

The world annual production of activated carbon in all forms is estimated to be in the region of 300,000-400,000 tonnes. According to one reference,[4] about 80% of total production (powder, granular and formed carbon) is used in liquid-phase applications and the remaining 20% in gas-phase applications. The highest consumption is in Japan and the USA; per capita annual consumption is 0.5 kg in Japan, 0.4 kg in the USA, 0.2 kg in Europe and 0.03 kg in the rest of the world. The consumption is increasing at a reported rate of about 7% per annum.[5]

The approximate average selling price for granular or formed carbons is between US$1500-4000 per tonne. For powder carbons, it is between US$500-1200 per tonne. The actual price will vary with the level of activity (surface areas commonly fall in the range of 800-1500 $m^2/g$), the strength and attrition resistance and whether impregnants have been added to enhance adsorption selectivity.

**Precursor Selection**

The principal commercial carbon feedstocks and the proportions in which they are used are summarized in Table 1-1. The selection of the precursor essentially determines the range of adsorptive and physical properties that can be attained in the activated carbon products. Important considerations to be made in selecting a source include cost, availability, consistency of quality, and, particularly for coals, peat and lignite, the mineral matter and sulfur contents.

## 1.3 CHARACTERIZATION OF CARBON

Several techniques are available for characterizing the porous carbon which mainly includes estimating the surface area, porosity, pore size and pore size distribution. Two principle types of adsorption processes used to characterize the porous substrates are physical adsorption of gases and chemical adsorption. For porous carbons the physical adsorption of gases is usually used.

**Adsorption Isotherms:**

To quantify the adsorption process, extents of adsorption (mmol/g) are related to the equilibrium partial pressures $P/P_0$ at constant temperature to create the isotherm. Adsorption isotherms are studied to obtain following information.

- Estimates of surface areas;
- Estimates of pore volumes in the various porosities present, i.e. pore-size of potential energy distribution;
- Assessments of the surface chemistry of the adsorbents;
- The fundamentals of adsorption processes, i.e. the nature of the adsorbed phase;
- Assessments of the efficiency of industrial carbons employed in separation/purification techniques.

The shape of isotherms reveals a lot of information about the porosity and surface area of the porous carbon. Adsorption process in micropores is the most difficult to describe accurately. Several theories such as D-R method[6], T-pore analysis, etc discusses the estimation of microporosity in detail. The adsorption processes occurring within mesopores are more easily understood. Macroporosity behaves in the same way as an open surface to adsorption, and accounts for < 1% of the adsorption processes within

microporous carbons. Macropores are mainly considered to be the gateways for gas and liquid molecules to the mesopores and micropores where most of adsorbate molecules adsorb.

Figure 1-1 shows the six major classes of isotherm shape that are obtained from adsorption experiments.

Type I isotherms are typical of microporous solids in that micropore filling occurs significantly at relatively low partial pressures<0.1 $P/P^0$, the adsorption process being complete at ~0.5 $P/P^0$. Examples include adsorption of nitrogen on micropores carbon at 77 K and of ammonia on charcoal at 273 K.

Type II isotherms describe physical adsorption of gases by non porous solids. Monolayer coverage is succeeded by multilayer adsorption at higher $p/p_0$ values. Type II isotherms can also be obtained from carbons with mixed micro- and mesoporosity.

Type III and IV isotherms are convex towards the relative pressure axis. These isotherms are characteristics of weak gas-solid interactions.[7] Type III isotherms originate from both non-porous and microporous solids and Type V isotherms from microporous or mesoporous solids. The weakness of the adsorbent-adsorbate interactions causes the uptakes at low relative pressures to be small; however, once a molecule has become adsorbed at a primary site, the adsorbate-adsorbate forces promote further adsorption in a cooperative process, which is known as cluster theory, e.g. the adsorption of water molecules on oxides of carbon surfaces.

Type IV isotherms possess a hysteresis loop, the shape of which varies from one adsorption system to another. Hysteresis loop are associated with mesoporous solids, where capillary condensation occurs.[8]

The type VI isotherm is a stepwise isotherm and represents complete formation of successive monomolecular layers. Hasley[9] proposed that stepwise isotherms arise from extremely homogeneous, non-porous surfaces and the step height corresponds to monolayer capacity. An example is the adsorption of krypton on carbon black (graphitized at 3000 K) at 90 K.

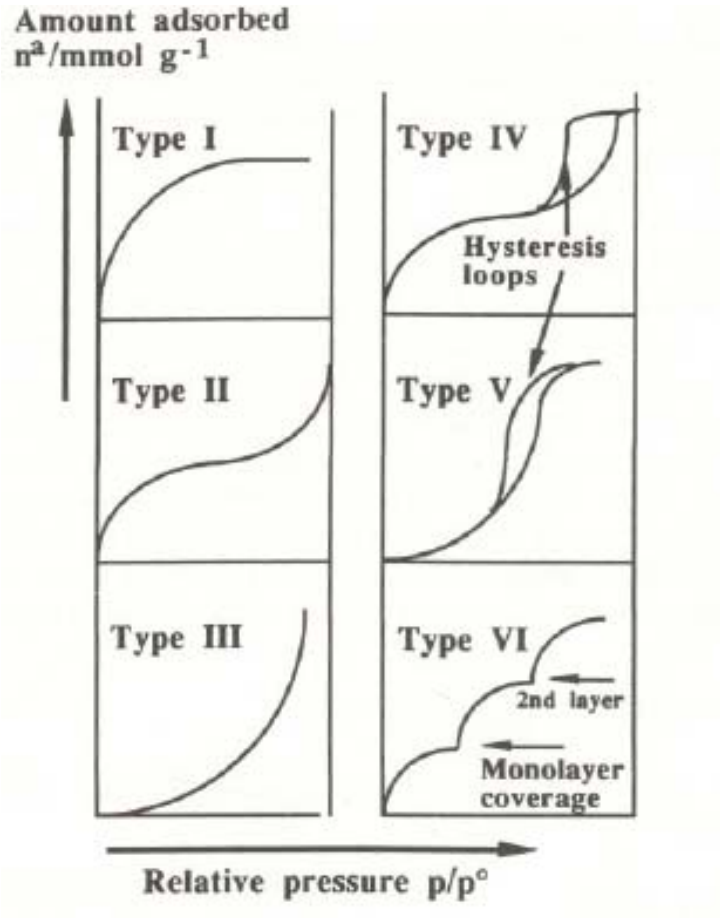


**Figure 1-1Classification of isotherm shapes into six principal classes (Gregg and Sing[10])**

## 1.4 APPLICATIONS

Because of large surface area and pore volume, the activated carbon finds numerous applications in liquid-phase and gas-phase adsorption. The common liquid

phase adsorption application include water treatment, decolorizing, gold and other precious metal recovery, purification of chemicals, pharmaceuticals and food, medicinal uses etc. The common gas phase application includes solvent & VOC recovery (eg. acetone, pentane, methylene chloride, methyl ethyl ketone, tetrahydrofuran (THF), white spirit, benzene, toluene, xylene, etc), as protective filters for military, industrial and nuclear applications, in general air conditioning, gas purification and separation which include land fill gas separation and purification and mercury vapor adsorption and other similar applications.

One of the important applications of carbon which is not used up to its full potential is storing natural gas at low pressures for transportation and vehicular applications. This technology which is called Adsorbed Natural Gas (ANG) uses natural gas in adsorbed phase at low to medium pressures can be very attractive alternative to compressed natural gas (CNG) and liquefied natural gas (LNG) for small to medium scale applications.

In this project corn cobs were used as a precursor for making nanoporous carbon. Activated carbon derived from corn cobs in this project were highly microporous or ultramicroporous and so the activated carbon derived were called nanoporous carbon since it constituted of a large fraction of pores of size between 0.5 to 1.2nm. The research in this project was done under collaborative title of "Alliance for Collaborative Research in Alternative Fuel Technology" or ALLCRAFT. The primary purpose of the nanoporous carbon derived from corn cobs in this project was to use it as an adsorbent for ANG application. The nanoporous carbon obtained in this project has the methane storage capacity of ~178V/V and methane deliverable capacity of 150-160V/V at 25˚C

and 34 atm. Kilogram scale quantities of carbon were produced and were sent to Midwest Research Institute (MRI) at Kansas City to check the performance of the carbon for storing and delivering natural gas in an actual road test done in a Ford 150 pickup truck. The nanoporous carbon synthesized from corn cobs was also tested for its performance in different applications such as storing hydrogen, as catalyst support and as an adsorbent for removing heavy metals from aqueous solutions for water purification. Several papers and presentations to technical journals and meetings have resulted from this work. Considerable media interest (newspapers, magazines, TV) was aroused by the results of this project, resulting in disseminating the knowledge of the successful outcome of the Program to a much wider audience than a purely scientific and technical one.

## REFERENCES

[1] Bansal, R.C., Donnet, D.B. and Stoekli, F. 1988: Active Carbon. New York: Marcel Dekker.

[2] Wilson, J. 1981: 60, 823.

[3] Patrick, J.W., 1995: "Porosity in Carbons: Characterization and Applications" Halsted Press, New York.

[4] Hassler, J.W., "Activated Carbon", 1963.New York: Chemical Publishing Company.

[5] Irving-Monshaw, S. 1990: Chemical Engineering, Feb., 43.

[6] Dubinin, M.M. 1996: Chemistry and Physics of Carbon 2, Marcel Dekker, New York, 51.

[7] Kiselev, A.V. 1968: Journal of Colloid Interface Science 28, 430.

[8] Sing, K.S.W., Everett, D.H., Haul, R.A.W., Moscou, L., Peirotti, R.A., Rouquerol, J. and Siemieniewska, T. 1985: Pure and Applied Chemistry 57, 603.

[9] Hasley, G.D. 1948: Journal of Chemical Physics 16, 931.

[10] Gregg, S.J. and Sing, K.S.W. 1982: Adsoption, Surface Area and Porosity. London: Academic Press, 2nd Edition.

# CHAPTER 2

# 2. Nanoporous Carbon from Corn Cob using Chemical Activation Process

This paper was submitted for publication to CARBON journal as: **"Nanoporous Carbon from Corn Cobs using Chemical Activation Process"** Parag S. Shah [a], Galen J. Suppes [a], Jacob Burress [b] Peter Pfeifer [b]

[a] Department of Chemical Engineering, W2028 Engineering Bldg. East, University of Missouri, Columbia, MO 65211

[b] Department of Physics, University of Missouri, Columbia, MO 65211

## ABSTRACT

In the Midwest there is a huge supply of waste corn cobs. Corn cob can be an excellent starting material to produce nanoporous carbon because of its botanical origin similar to coconut shell and peach pits. Chemical activation of corn cobs using phosphoric acid or potassium hydroxide can lead to nanoporous carbon having surface area in excess of 3800 $m^2/g$ and pore volume of 2.5cc/g.

Dried, crushed, corn cobs were carbonized at temperatures between 450- 900˚C and chemically activated using $H_3PO_4$ and KOH. The effect of different variables of activation such as heat treatment temperature, rate of heating and concentration of activating agent was studied. The mechanism of phosphoric acid activation was studied using thermogravimetric analysis. The carbon was characterized by $N_2$ adsorption at 77 K, and the isotherms were analyzed using BET, T-method and D-R method for determining surface area and pore volume. The structure of porous network in the carbon was observed using scanning electron microscopy.


KEY WORDS: nanoporous carbon, activated carbon, corn cobs, chemical activation, thermogravimetric analysis.

## 2.1 INTRODUCTION

In last few years the growth of corn crop has increased considerably in the US because of the government's policy of promoting alternative fuels derived from agricultural sources. In Midwest there is a huge supply of waste corn cobs. In 2001 Missouri alone produced 350 million bushels of corn. However, after the use of corn for wide variety of applications the corn cobs often leaves in the fields and factories as very low economic value agricultural waste. The efforts of using the corn cobs as a biomass fuel has not given very promising results primarily because of the low calorific value of corn cobs. Another alternate route to convert these waste corn cobs to high economic value product can be to convert them into nanoporous carbon or more commonly called as highly microporous activated carbon. The use of various precursors such as wood, coconut shells, peach stone, and lignite coals for producing activated carbon has been studied in detail by several researchers. However, the use of corn cobs for producing high surface area carbon has not been studied extensively in-spite of its high carbon content. It is the purpose of this project to study comprehensively the routes and procedures to get high surface area nanoporous carbon from corn cobs for variety of applications.

The properties of activated carbon are functions of both the precursor as well as the method of activation. Precursors of activated carbon are cellulosic material of botanical origin or of degraded and coalified plant. The wide array of precursors for activated carbon include wood[11], coconut shells, nut shells, agricultural waste such as apricot stones[12 13 14], peach stones[15 16], olive pits, hulls of soybean and rice[17 18], etc. One of the excellent precursors for activated carbon could be corn cob because of its botanical

origin similar to coconut shells and olive pits. Since the yield of the activated carbon production is usually very low, the cost and availability of the raw material is a very important factor in the economic production of activated carbon. Coconut shell, wood, lignite coals which are often used for commercial production of activated carbon have high price as compared to agricultural waste such as corn cob in US. Corn cob is available in abundance in the US and is relatively cheap. Also the chemical composition of corn cobs suggest that it has less mineral matters, which are often responsible for preferential gasification during the activation process resulting in meso and macropore channeling and pitting, and not the preferred microporosity and repeatability. Because of this reasons corn cobs could be an excellent precursor for the commercial production of activated carbon. Table2-1 shows the elemental analysis of corn cobs which shows high promises of its use as precursor of nanoporous carbon production because of its carbon content up to 45%.

**Table 2-1 Elemental Analysis of Corn cobs[19].**

| ***Element*** | ***%*** |
|---|---|
| Carbon | 43.5 |
| Nitrogen | 0.21 |
| Oxygen | 48.4 |
| Hydrogen | 7.9 |
| Sulphur | 0.013 |
| Ash | 1.2 |
| Moisture | 10+/- 2 |

| | |
|---|---|
| Cellulose | 47.1 |
| Lignin | 6.8 |
| Hemi cellulose | Not Available |

The large internal surface and porosity in activated carbon are due the activation process. There are two common carbon activation schemes; physical activation and chemical activation. Physical activation refers to gasification of the carbon by gases such as $CO_2$ and steam at temperature ranging from 800˚C to 1200˚C[20]. In chemical activation the feed stock is mixed with chemicals such as KOH, $H_3PO_4$, $ZnCl_2$ before carbonization process. With chemical activation more porous and high surface area carbon can be obtained. Chemical activation procedure is usually preferred over physical activation for soft, woody and more cellulosic materials such as pine, sawdust, corn cobs, whereas physical activation is preferred route of activation for hard carbonaceous materials like peach stone, olive pits, date pits, etc.

The characterization of the highly porous activated carbon or nanoporous is often done by physical adsorption of gases such as $N_2$ and $CO_2$. The adsorption of $N_2$ at 77K is the most common technique used for carbon characterization. The internal surface area of the carbon is usually determined using BET equation. Adsorption in micropores does not take place by successive build-up of molecular layers as admitted by BET theory. Nevertheless, the BET method had been, and will continue to be used for microporous solids owing to its simplicity and reasonable predictions[21]. Different methods can be used for micropore analysis. These methods include the V-T method, $\acute{\alpha}_s$ method, Dubinin-Rudeskivich (DR) method, DA method, etc. V-T method involves the measurement of nitrogen adsorbed by the sample at various low pressure values. The procedure is the same as that employed in the BET surface area measurement, but it extends the pressure

range to higher pressures to permit calculation of the matrix or external surface area, that is, the non-microporous part of the material. A t-plot is a plot of the volume of gas adsorbed versus t, the statistical thickness of an adsorbed film. The t values are calculated as a function of the relative pressure using either the de Boer equation[22],

$$t(\dot{A}) = \sqrt{\frac{13.99}{\log(P_0 / P) + 0.034}}$$

or the Halsey equation[23] which, for nitrogen adsorption at 77 K can be expressed as

$$t(\dot{A}) = 3.54 \left[ \frac{5}{2.303 \log(\frac{P_0}{P})} \right]^{1/3}$$

A different approach for isotherm analysis of microporous solids is based on the volume filling of micropores, described by Dubinin and his co-workers. The adsorption of a non polar vapor in micropores gives rise to type I isotherm which can be interpreted by the DR equation. Based on the Polanyi potential theory of adsorption[24] Dubinin and Radushkevich[25] postulated that the fraction of the adsorption volume V occupied by liquid adsorbate at various adsorption potentials ε can be expressed as a Gaussian function:

$$V = V_0 \exp\left[-(A / \beta E_o)\right]^2$$

where A is the free energy of adsorption $RT \ln(P/P)_0$, which in early Dubinin's works was also called adsorption potential ε, $V_0$ represents micropore volume, $E_0$ is the so-called characteristic energy of adsorption and β is the affinity coefficient whose value is 0.35 for N2 at 77 K[26].

The general objective of this work was to demonstrate the use of corn cobs as a precursor for production of high quality activated carbon with high surface area and rich in nanopores. The chemical activation route using phosphoric acid and molten salt method was investigated and the effect of various parameters of activation on the final surface area, pore volume and pore size distribution was determined. The primary application for the nanoporous carbon produced from corn cobs was for adsorbed natural gas technology and hydrogen storage. Thermogravimetric analysis was used to verify and have insight in to the mechanism of activation of corn cobs using phosphoric acid. Nitrogen adsorption at 77 K, scanning electron microscopy (SEM) and transmission electron microscopy (TEM) were used to characterize the carbon. Carbons from other lignocellulosic precursor peach pits were also produced using the same activation process for comparison.

## 2.2 EXPERIMENTAL PROCEDURE

Since corn cob was the selected principle raw material for the study, series of experiments were carried out to understand the impact the different parameters of phosphoric acid and KOH activation on the final carbon pore volume, pore size distribution and surface area. Chemical activation was preferred over physical activation because of the cellulosic and soft nature of corn cobs and because chemical activation gave more micropore volume as compared to physical activation.

The dried crushed corn cobs (particle size between 10 and 20 mesh) were mixed with different concentrations of phosphoric acid ranging from 0-70% (vol) in the weight

ratio of 1:1.5. The corn cobs were soaked at different temperatures in phosphoric acid for about 8 -10 hrs. After that the excess of phosphoric acid was removed by heating the mixture at 165-175˚C for 2 hrs. Then the soaked corn cobs were carbonized at temperature ranging from 450- 800˚C, in nitrogen atmosphere. After carbonization the carbon was washed thoroughly to pH 7 to remove the excess of acid.

In order to get higher pore volume and higher surface areas the carbon obtained by phosphoric acid activation was further treated with a molten salt activation process. The carbon or char was mixed with varying amounts of KOH flakes and water to form thick slurry. This slurry was then heated to temperatures between 700 to 900 ˚C in an inert atmosphere for one hour. The final product was then washed thoroughly with water to remove $K_2CO_3$ formed during the reaction and unreacted KOH, until the pH of 7 was achieved. KOH activation of the char or carbon produced from plain corn cob without treating with phosphoric acid was also carried out. However, the carbon obtained by this method had lower packing density, more mesopores volume and the process had lower yield compared to the process in which phosphoric acid was used.

The thermogravimetric analysis was carried out using TGA Q50 series from TA instruments. The nitrogen flow rate in the TGA was 50mL/hr. The mechanism of the phosphoric acid activation was determined by following the accurate weight loss of the acid soaked corn cobs with different temperatures and different rates of heating.

The characterization of all the carbon produced was done with N2 adsorption at 77 K using the Autosorb 2.0 instrument from Quantachrome. Analysis of isotherms was carried out by applying various methods to obtain different information. The BET equation was used to get the BET surface area from volume of N2 adsorbed at $P/P_0$=

0.95. The T-method was used to find the micropore volume and the external surface area of the mesoporous fraction from the volume of $N_2$ adsorbed up to the $P/P_0 = 0.0315$. The Hitachi S4700 cold-cathode field emission scanning electron microscopy (FESEM) was used to have the better understanding of the pore networks and pore geometry in the carbon. This analysis was done in ultra high resolution mode with working distance of 6300 micrometers and accelerating voltage of 5000 volts.

## 2.3 RESULT AND DISCUSSION

### 2.3.1 EFFECT OF PHOSPHORIC ACID CONCENTRATION

The concentration of phosphoric acid is one of the critical parameters that control the final porosity in the carbon. Experiments were carried out with 0, 30, 50 and 70 volume % of phosphoric acid to know the effect on final porosity and pore size distribution. The Table 2.2 shows the characterization of various carbons at 77K using liquid $N_2$ with Quantachrome Autosorb-1 instrument. As seen from the Figures 2-1 and 2.2, with increases in concentration of phosphoric acid the surface area and micropore pore volume of the final carbon increases. The primary reason of this observation is the higher phosphoric acid concentration leads to higher acid to corn cob ratio which results in better and more effective phosphorylation of the lignin and cellulose molecules present in the corn cobs producing phosphate esters and phosphorous oxides (V) which enhances the porosity in the carbon. The thermogravimetric analysis of the corn cobs impregnated with 70% phosophoric acid shows progressive decrease in total mass loss to 60% compared to 75% in corn cob without any phosphoric acid in it.

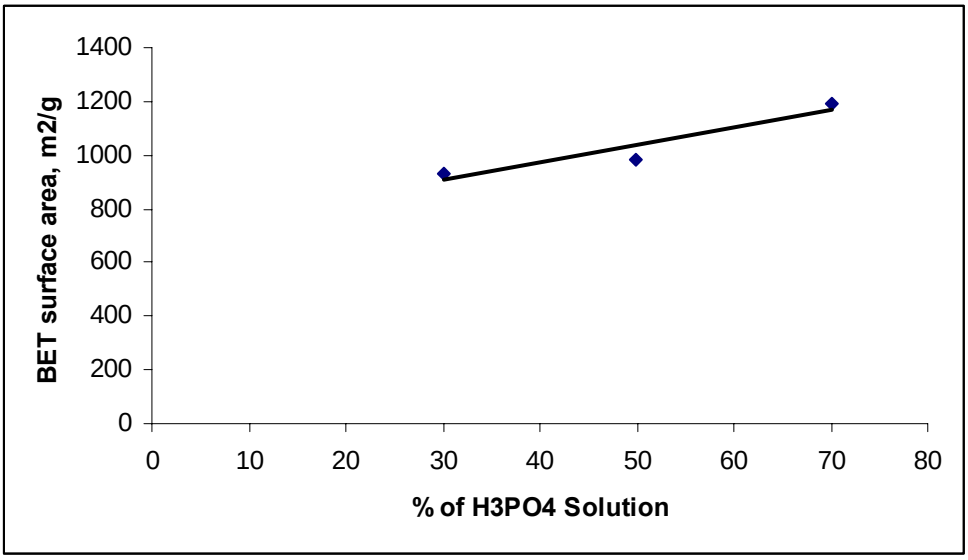


**Figure 2-1 Graph showing effect of phosphoric acid concentration on BET surface area.**

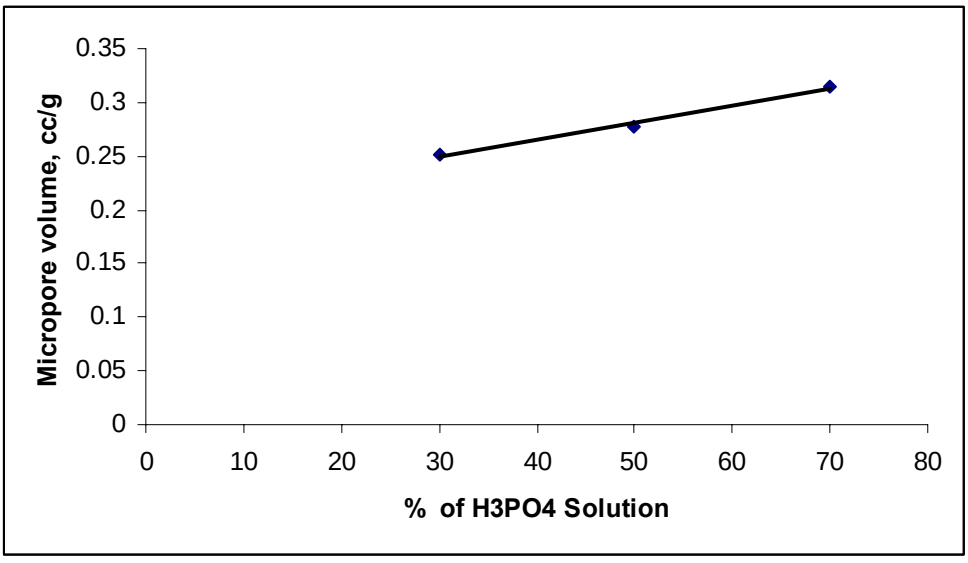


**Figure 2-2 Graph showing effect of phosphoric acid concentration on micropore volume.**

**Table 2-2 Characterization of samples prepared with different phosphoric acid concentration.**

| Sample | % of H3PO4 Solution | Temperature of carbonization ˚C | Rate of Heating ˚C /min | Temperature of Soaking ˚C | BET Surface Area $m^2/g$ | Micropore Volume cc/g |
|---|---|---|---|---|---|---|
| C-1 | 30 | 450 | 1 | 40 | 934 | 0.252 |
| C-2 | 50 | 450 | 1 | 40 | 986 | 0.278 |
| C-3 | 70 | 450 | 1 | 40 | 1195 | 0.315 |

### 2.3.2 EFFECT OF HEAT TREATMENT TEMPERATURE (HTT).

The final BET surface area, pore volume and pore size distribution in the carbon can be conditioned by the final heat treatment temperature. The Figures 2-3 and 2-4 show the BET surface area and micropore volume in carbon samples obtained at different HTTs. Figure 2-3 and 2-4 shows that the carbon with final HTT of 450˚C has more surface area and micropore volume than the carbon with higher HTT. In fact, with increase in HTT beyond 450˚C there is a sharp drop in the BET surface area and the micropore volume. The primary reason of higher surface area and micropore volume in carbon treated up to 450˚C is because up to 450˚C the cross linkages between phosphate esters are stable and the aromatization of the aliphatic chains containing phosphate ester is not to a very high degree to form very large aromatic molecules. The formation of phosphate esters drives a process of expansion of the micro fibers present in the corn cobs[27]. Removal of the acid by washing leaves this matrix in an expanded state hence leaving micropores and mesopores in the structure. However, increasing the HTT beyond 450˚C up to 800˚C, there is a considerable breakage of the cross linkages and phosphate esters, making the char or carbon less stable and increasing the loss of carbon in the form of CO, $CO_2$ and $CH_4$ gases and expansion of the micropores to mesopores. This process does not decrease the surface area considerably; however, there is a major decrease in the micropore volume.

After 650˚C there is a major increase in the aromatization of the aliphatic phosphate ester linkages making the aromatic molecule bigger[28]. As a result of this process there is substantial structural rearrangement decreasing the porosity and increasing the density of the carbon because of more orderly arrangement of the chains and decrease in the cross link density. Because of this process there is sharp fall in the surface area of the carbon at HTT temperatures above 650˚C.

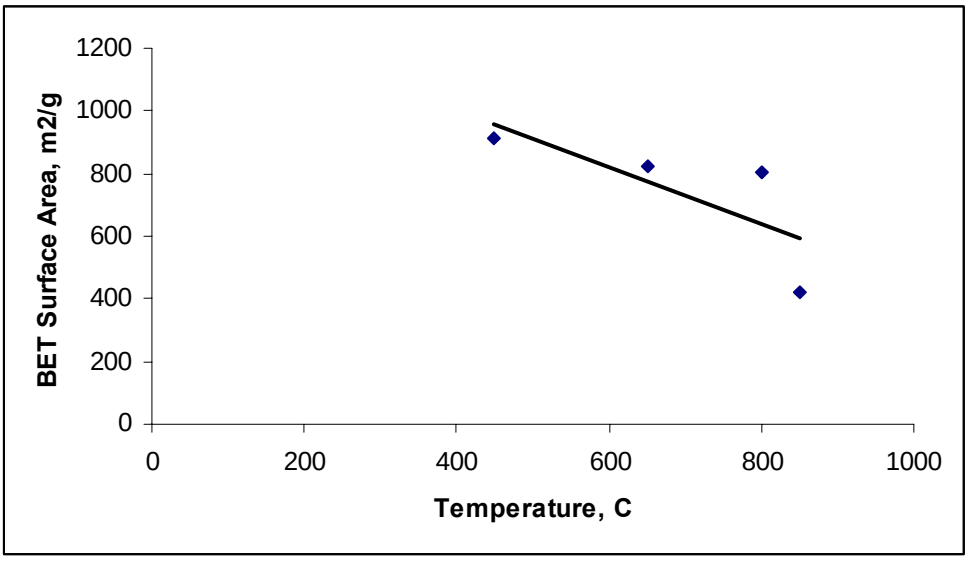


**Figure 2-3 Graph showing effect of HTT on BET surface area.**

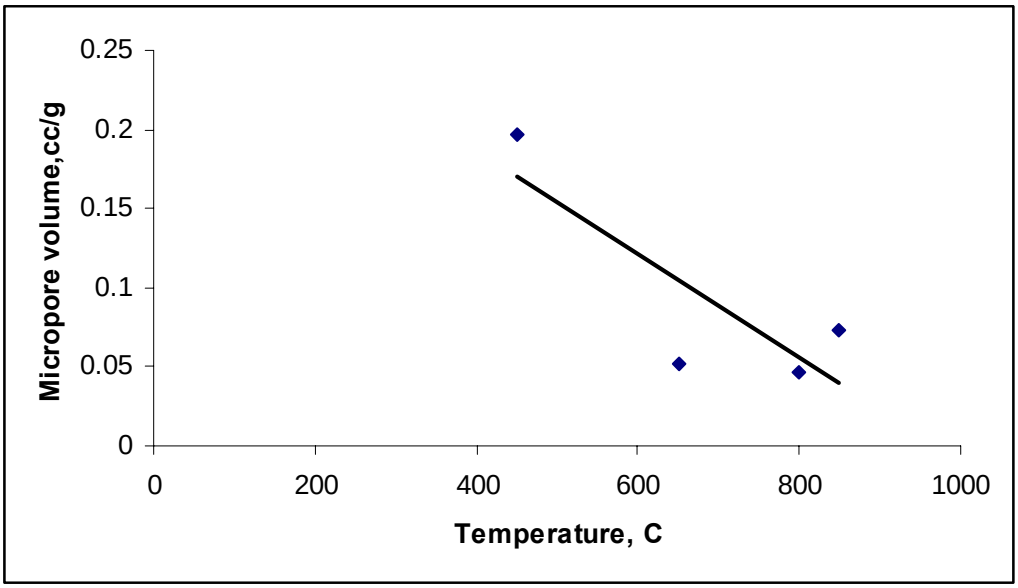


**Figure 2-4 Graph showing effect of HTT on micropore volume.**

| Sample | % of H3PO4 Solution | Temperature of carbonization ˚C | Rate of Heating ˚C/min | Temperature of Soaking ˚C | BET Surface Area $M^2/g$ | Micropore Volume cc/g |
|---|---|---|---|---|---|---|
| HTT-1 | 50 | 450 | 1 | 50 | 910 | 0.197 |
| HTT-2 | 50 | 650 | 1 | 50 | 826 | 0.052 |
| HTT-3 | 50 | 800 | 1 | 50 | 802 | 0.047 |
| HTT-4 | 50 | 850 | 1 | 50 | 424 | 0.073 |

**Table 2-3 Characterization of samples prepared at different HTT.**

### 2.3.3 EFFECT OF RATE OF HEATING

Rate of heating is another parameter that affects the porosity development and final surface area in corn cobs. During the heat treatment of corn cobs the surface area

and pore micropore volume at given temperature also depends on how fast or slow that temperature is reached. Ramping the temperature slowly up to about 450 -500˚C gives more time for the cross linking and phosphorylation of the lignin and cellulose molecules due to the reaction with phosphoric acid. As shown in Figures 2-5 and 2-6 as the rate of heating increases from 0.5˚C/min to 1.5˚C/min, the surface area and pore volume decreases, which indicates that the faster rate of heating doesn't provide enough time for the reaction of phosphoric acid with the lignocellulosic matter in the corn cobs. Whereas when the temperature is increased slowly at a rate of 0.5˚C/min, there is enough time for the development of the porosity due the more crosslinking and esterification of the phosphates.

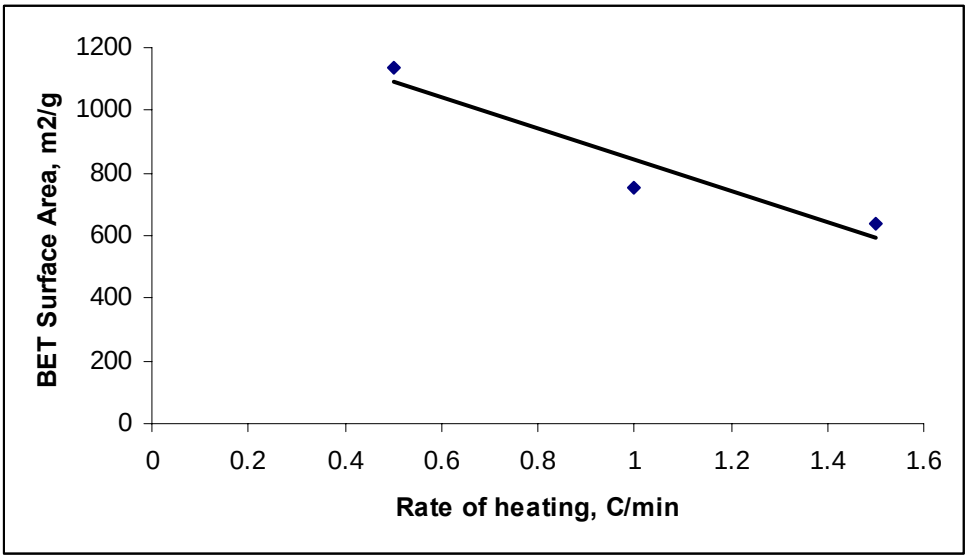


**Figure 2-5 Graph showing effect of rate of heating on BET surface area.**

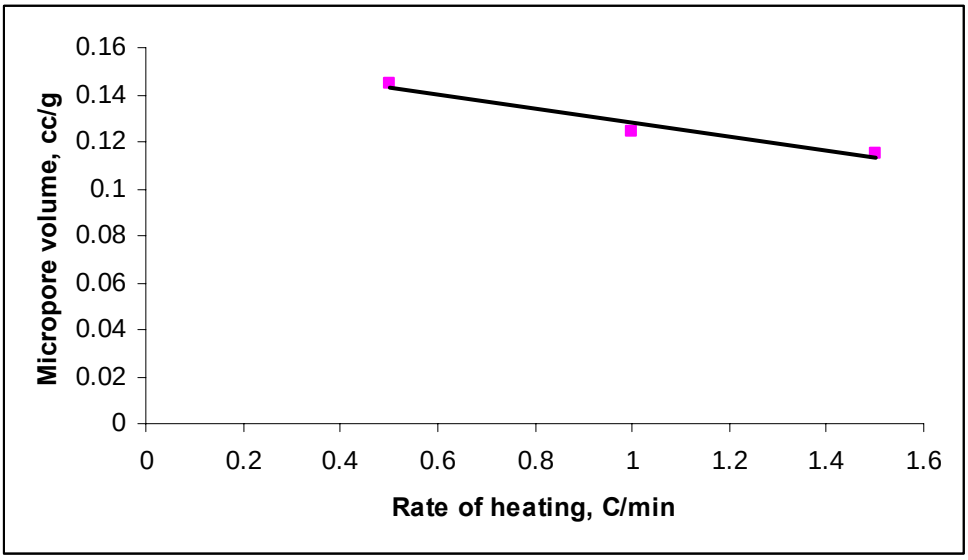


**Figure 2-6 Graph showing effect of different rate of heating on micropore volume.**

**Table 2-4 Characterization of samples prepared at different rate of heating.**

| Sample | % of H3PO4 Solution | Temperature of carbonization ˚C | Rate of Heating ˚C/min | Temperature of Soaking ˚C | BET Surface Area $M^2/g$ | Micropore Volume Cc/g |
|---|---|---|---|---|---|---|
| RH-1 | 50 | 450 | 0.5 | 80 | 1135 | 0.145 |
| RH-2 | 50 | 450 | 1 | 80 | 754 | 0.124 |
| RH-3 | 50 | 450 | 1.5 | 80 | 637 | 0.115 |

## 2.3.4 EFFECT OF SOAKING TEMPERATURE

Samples of activated carbon were prepared at different soaking temperatures of corn cobs in to phosphoric acid solution. Figures 2-7 and 2-8 show the effect of soaking temperature of corn cobs in phosphoric acid solution on final surface area and pore volume. As seen from the graphs and Table 2-5, lower soaking temperature promotes higher surface area and pore volume than higher soaking temperatures which is similar to that observed by Pandey and Nair[29]. This is primarily because of the soft and open morphological structure of the corn cobs [50]. As seen in Figure 2-9 the digestion of lignin

molecules begins at temperature as low as 50˚C. So when the soaking is carried out at 30˚C, the phosphoric acid gets soaked in to the corn cobs; however, its reaction with lignin molecules has not started. So there is no alteration of the cell structure before the actual heat treatment is started. There isn't much alteration in the physical appearance of the corn cobs after 8 hours of soaking and the release of aromatic smell is also less. However, when the soaking is carried out at 80˚C or higher for 8hrs, the physical appearance of the corn cobs changes becoming dark brown to black and a strong aromatic smell is released. This is primarily because the attack of phosphoric acid on lignin part of the corn cob has already started and there is a considerable alteration or depolymerization of the lignin molecules into lighter volatile molecules (hence strong aromatic odor) before the actual cross linking and phosphorylation of the lignin molecules start at the temperature of about 200˚C during the heat treatment. So it is advantageous to soak the corn cobs in phosphoric acid solution at lower temperature to prevent the major attack of phosphoric acid on the lignin and hemicelullosic matter of the corn cobs before the temperature of crosslinking and esterfication is reached.

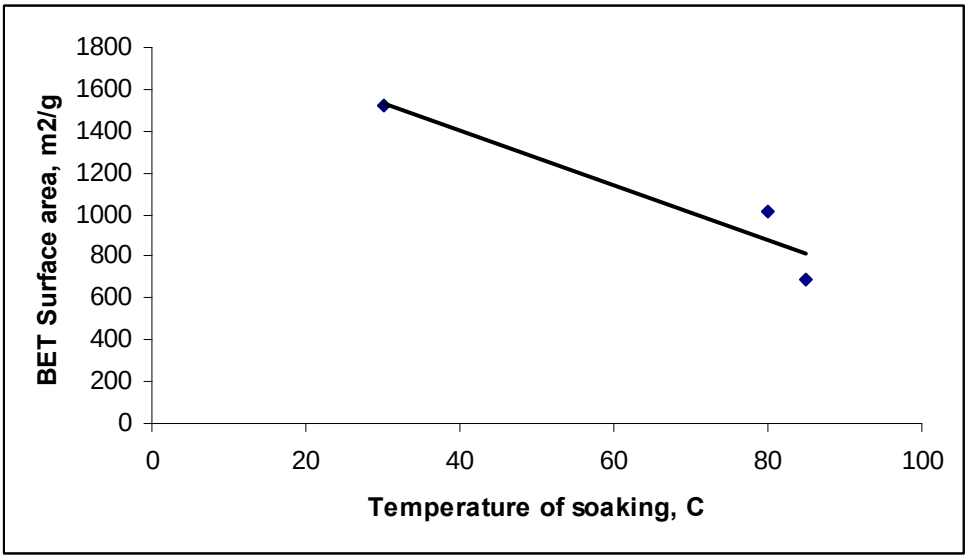

**Figure 2-7 Graph showing effect of soaking temperature on BET surface area.**

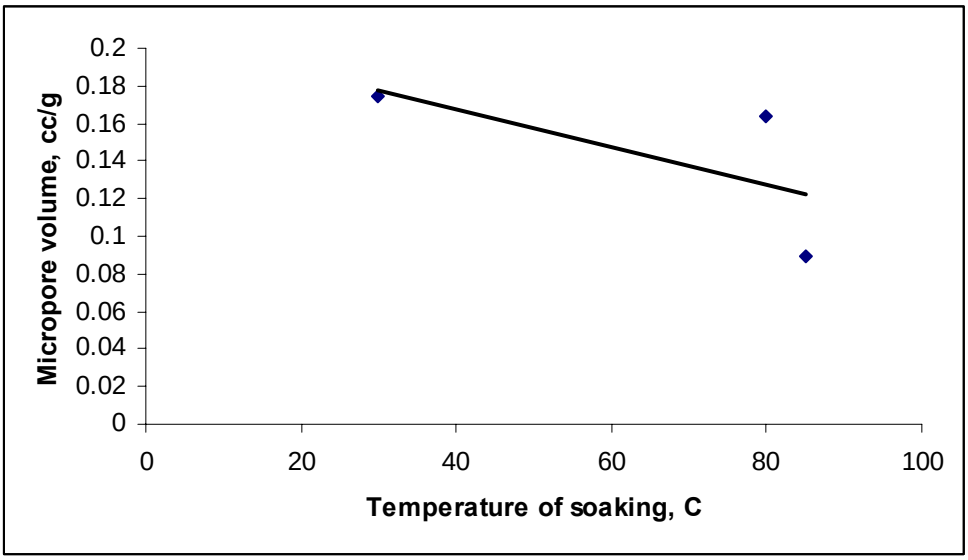


**Figure 2-8 Graph showing effect of soaking temperature on micropore volume.**

**Table 2-5 Characterization of samples prepared at different soaking temperature.**

| Sample | % of H3PO4 Solution | Temperature of carbonization | Rate of Heating | Temperature of Soaking | BET Surface Area | Micropore Volume |
|---|---|---|---|---|---|---|
| | | ˚C | ˚C/min | ˚C | $m^2/g$ | cc/g |
| ST-1 | 50 | 450 | 1 | 30 | 1520 | 0.174 |
| ST-2 | 50 | 450 | 1 | 80 | 1017 | 0.164 |
| ST-3 | 50 | 450 | 1 | 85 | 691 | 0.089 |

### 2.3.5 MECHANISM OF PHOSPHORIC ACID ACTIVATION OF CORN COBS EXPLAINED USING THERMOGRAVIMETRIC ANALYSIS (TGA)

Figures 2.9 and 2.10 show the TGA of corn cobs soaked in phosphoric acid solution and just plain corn cobs i.e. not soaked in phosphoric acid respectively. The rate of heating is 1.5˚C/min and the ratio of phosphoric acid to corn cob is 0.7:1 g/g. This

TGA curves can be divided into 3 segments. Segment A from 30 to 150˚C, segment B from 150 to 450˚C and segment C from 450 to 750˚C, based on the rates of weight loss with temperature.

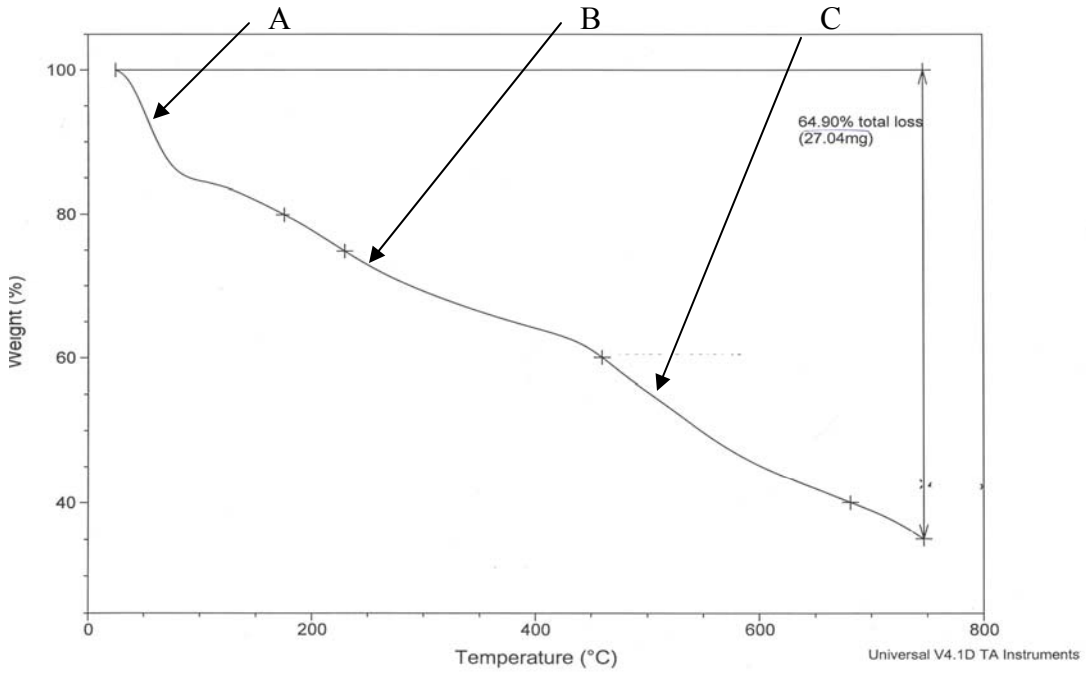


**Figure 2-9 TGA of Corn cobs soaked in 50% vol H3PO4.**

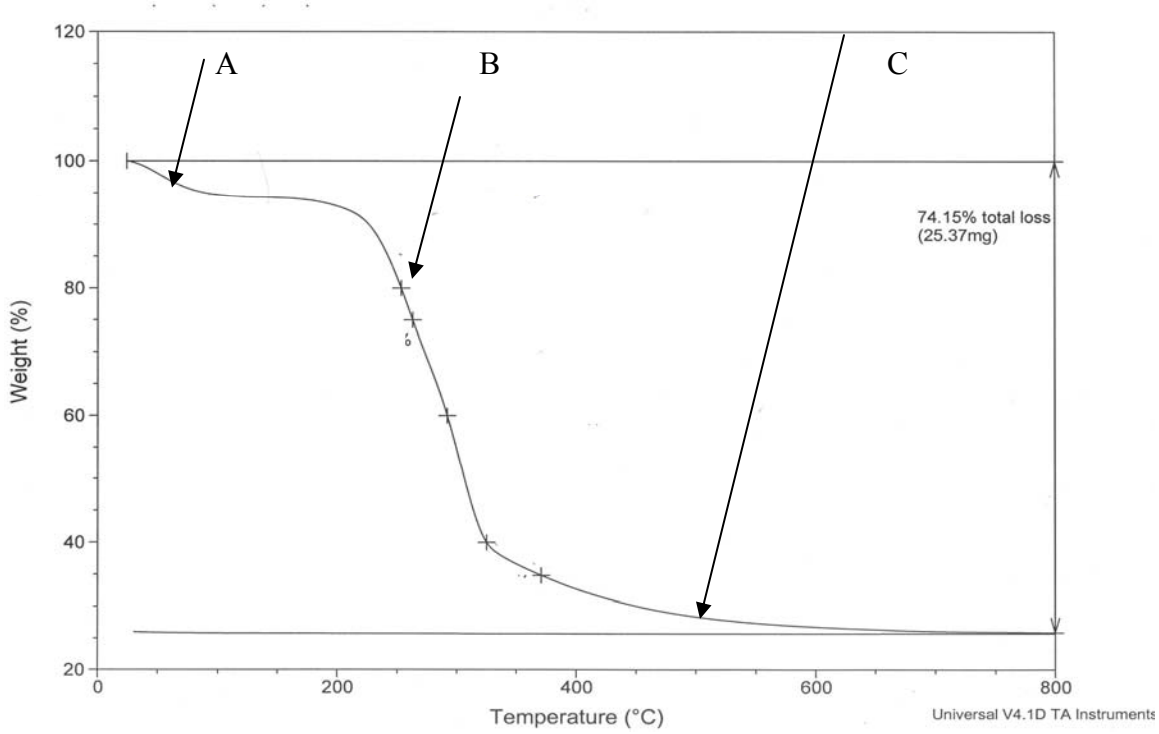


**Figure 2-10 TGA of plain corn cob.**

**Weight Loss for Segment A:** As seen from Figure 2-9, the slope of this segment is very high indicating that the rate of weight loss is high in this region. There is 20% weight loss in temperature interval of 125˚C. As seen from the curve, the loss of weight in corn cobs starts at temperature as low as 30˚C. This indicates the onset of reaction between corn cobs and phosphoric acid. The phosphoric acid seems to react first with the lignin and the hemicellulose present in the corn cobs possibly because of the amorphous nature of this biopolymers and easy access to these biopolymers due to the open morphological structure of the corn cobs[50 34 30]. In this temperature range i.e. up to 150˚C the phosphoric acid does not have much effect on the cellulose because it is not accessible as it is present more in the secondary cell wall of the plant cell wall[30]. Also the crystalline nature of the cellulose provides extra resistance to phosphoric acid attack

at this low temperature, so during the segment A of the curve the primary loss in weight is due to the attack of phosphoric acid on lignin and hemicellulose. The primary effects of acid attack are to hydrolyze glycosidic linkages in polysaccharides (hemicellulose and cellulose) and to cleave aryl ether bonds in lignin. These reactions are accompanied by further chemical transformations that include dehydration, degradation and condensation[31]. Because of this bond cleavage reaction the corn cob losses weight in the form of gases such as CO, $CO_2$, $CH_4$, moisture, and other volatile products that are the results of depolymerization of the lignin and hemicellulose. The cleavage of the bonds starts decreasing the aliphatic nature of the biopolymers and increases the aromaticity.

Such a nature of weight loss in this temperature range is not seen in case of TGA of plain corn cobs as shown in Figure 2-10. The slope of segment A in Figure 2-10 is very low indicating that the rate of weight loss in this temperature range is very slow. It losses just about 7% of weight over temperature interval of 125˚C, which is primarily due to loss of unbound moisture and some degree of thermal cracking of the amorphous biopolymers.

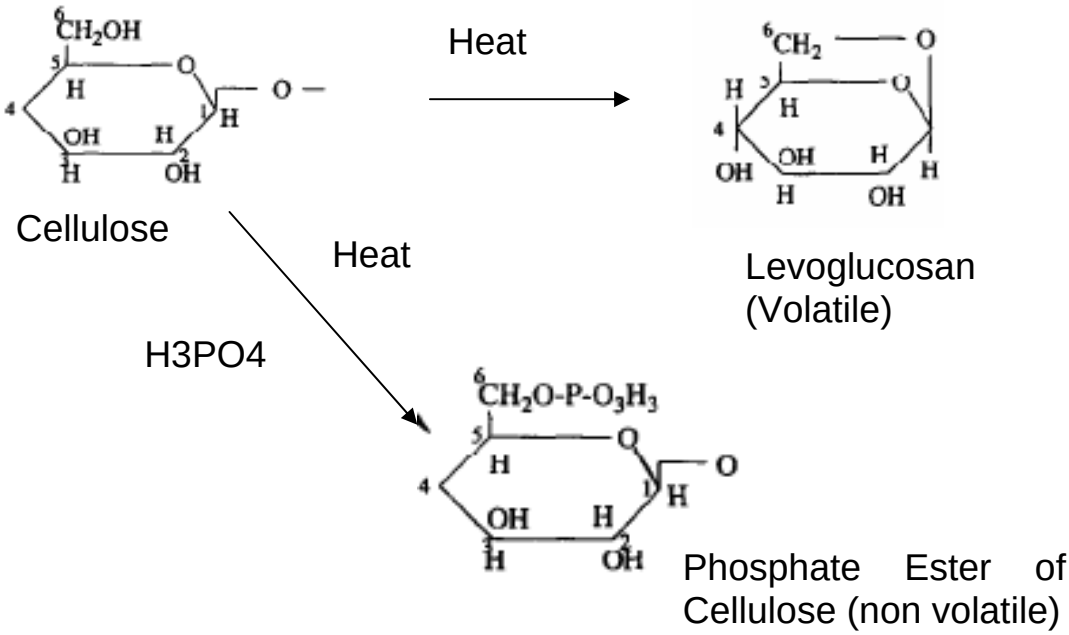

**Figure 2-11 Reaction of phosphoric acid with cellulose[32].**

**Weight Loss for Segment B:** As seen from Figure 2-9, the slope of segment B is much less as compared to the segment A. It losses about 20% of the weight in the temperature interval of 300˚C, indicating a very slow rate of weight loss. The primary reason for such a low rate of weight loss is the dominance of the cross linking of the aliphatic chains that are produced by depolymerization over bond cleavage in this aliphatic chains that has started at lower temperature and also because of the onset of phosphorylation of the lignin and cellulose [28 34]. The increased cross linking process because of the phosphoric acid activity serves to retain relatively low molecular weight species in the solid phase which would be lost if there was no acid action as shown in the segment B of the figure 2-10 for plain corn cobs.

Research on the effect of phosphoric acid on plant cellulose has shown that phosphorous compounds can form ester linkages with –OH groups on cellulose at temperature below 200˚C[33], thus helping to crosslink the cellulosic polymer chains. In absence of phosphoric acid at higher temperature of 250˚C the cellulose starts getting converted to levoglucoson that is relatively more volatile and is lost at those temperatures, which can be seen in the segment B of Figure 2-10 for plain corn cobs. The phosphoric acid stabilizes the cellulose structure by esterfication and thus inhibiting the formation of levoglucosan as shown in Figure 2-11.

Another critical observation in segment-B is between temperatures 300˚C and 425˚C the weight loss is still low as compared to the loss in weight in the range of 150 to 210˚C. This observation is in accordance with that by M. Jagtoyen and F. Derbyshire[34]. Jagtoyen and Derbyshire concluded that at 290-300˚C the cellulose structure consists of

relatively small poly aromatic units that are interconnected by phosphate and polyphosphate bridges. As the temperature is increased above 300˚C the cyclization and condensation reaction lead to an increase in aromaticity and in the size of polyaromatic units, enabled by the scission of P-O-C bonds. But after about 430˚C and above, the continued cleavage of crosslinks leads to a very extensive growth in the size of the aromatic units which results in decrease of the cross link density and decrease in the stability of the phosphate linkages.

The segment B in the case of heat treatment of plain corn cobs looks completely different from the heat treatment of phosphoric acid treated corn cobs. In this case in the temperature range of 150 to 450˚C there is a sharp loss in the weight starting at around 200˚C. This is because at the temperature around 200˚C the breaking of the lignin and hemicellulose into smaller molecules begin. Since there is no crosslinking between these smaller fragments the char starts losing carbon in the form of gases such as CO, $CO_2$, $CH_4$, and other light hydrocarbon gases. At about 250˚C the conversion of cellulose to levoglucoson, which is volatile increases and resulting in to sharp loss of the cellulosic content of the char. Thus in the absence of phosphoric acid, char losses about 70% of its weight at temperature up to 450˚C.

In segment C (see Figure 2-9) the slope of the weight loss curve increases slightly after 450˚C, indicating the breakage of some phosphate linkages. After 450˚C the char becomes more unstable and start shrinking due to the breakage of the phosphate linkage between the phosphate esters as they reach the limit of their thermal stability. From 450 to 750˚C the char keeps on losing weight steadily because of the breaking of the bonds between the cross linked network and the final weight loss is about 75%. After 750˚C

and higher the char does not lose more weight but there are only changes in the pore size distribution and pore volume. After 450˚C with greater loss in weight because of the breaking of the linkages, the micropore volume starts decreasing and there is a corresponding increase in the mesopores and macropore volume. However after 650˚C the size of the polyaromatic clusters grows a lot and the structure starts becoming more and more densely packed and thus decrease the pore volume of the char. So in the segment C the rate of weight loss is stable and slightly greater than segment-B, but there is a major effect on the pore volume and pore size distribution of the char as confirmed by the experimental data shown in Table 2-3 .

**Scanning Electron Microscopy**

Scanning electron microscopy was used to determine visually the surface structure and beginning pore structure in the carbon samples derived from corn cobs. Figure 2-12 shows the surface of a carbon sample at low magnification which indicates that the surface is fairly non porous. However, when it is further magnified, as seen in Figure 2-13, the presence of macropores, mesopores and to some nanopores can be seen. The magnification and resolution limits of Scanning Electron Microscopy did not allow us to clearly distinguish nanopores. However, other analysis techniques such as nitrogen adsorption, confirmed what we were capable of seeing continuing to make SEM a useful analytical tool in this study.

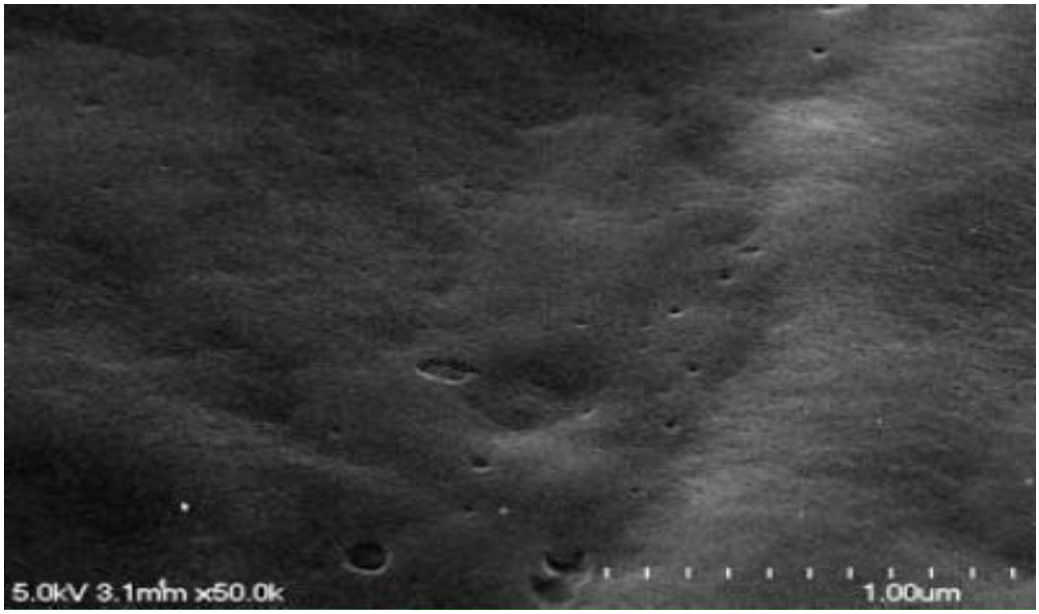


**Figure 2-12 SEM image of an carbon sample prepared using $H_3PO_4$ activation at low magnification.**

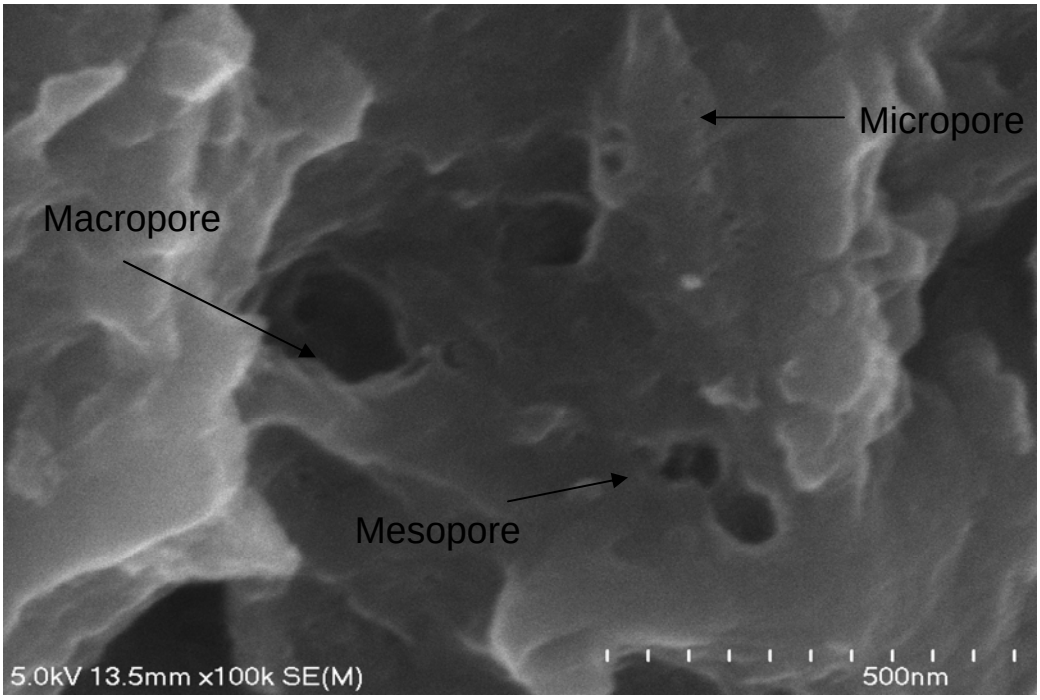


**Figure 2-13 SEM image of an carbon sample prepared by $H_3PO_4$ activation at high magnification.**

### 2.3.6 KOH ACTIVATION

**Effect of KOH to Carbon Ratio:**

The KOH: C ratio is an important parameter that affects the pore volume, pore size distribution and final surface area of the carbon. Different samples of carbon were prepared with varying amount of KOH: C and its effect on final surface area, PSD and pore volume were studied. Figure 2-14 shows the $N_2$ isotherms for carbon samples with KOH: C values varying from 1.5 to 5. As seen from Figure 2-14, the isotherms of carbon prepared with ratio of 1.5:1, 2:1, 3:1 have minimal slope which indicates that this samples are essentially microporous solids having type-1 isotherm. However the slopes of $N_2$ isotherm for sample with KOH: C ratio of 4 and 5 is very high as compared to the 1.5, 2 and 3 indicating the presence of large fraction of mesopores along with micropores.

As seen from Figure 2-14 and Table 2-6, as the KOH: C increases the BET surface area of the final carbon increases thus indicating the action of KOH on char or less porous carbon. The higher amount of KOH drills more pores in the char than lower amount of KOH. However, one important observation to be made in this case is, as shown in Figure 2-15, the micropore volume of the carbon treated with higher amount of KOH actually starts decreasing after some point, and there is a sharp rise in mesopores volume. The micropore volume and the total pore volume of the carbon increases as the KOH: C value increases from 1.5 to 3 indicating that the higher amount of KOH is actually drilling more narrow channels in the char as indicated by lower mesopores volume than micropore volume. However as the KOH: C value is increased above 3, the micropore volume starts dropping sharply and the mesopores volume increases sharply even though the total pore volume increases. This phenomenon shows that after KOH: C

value of 3 the process of widening of the existing micropores to mesopores takes over the process of forming new micropores. Thus as seen from Figure 2-15, the micropore volumes of the samples with KOH:C values of 4 and 5 are less than that for 3 even though their total pore volume and surface area are high. The Table 2-6 shows the packing densities of these carbons. As seen from the table, with increases in the KOH: C the density of the final carbon decreases thus showing the itching action of KOH on carbon. Thus KOH: C is an important parameter to control the final surface area, pore volume and the pore size distribution of the carbon obtained from corn cobs depending on the final application of the carbon.

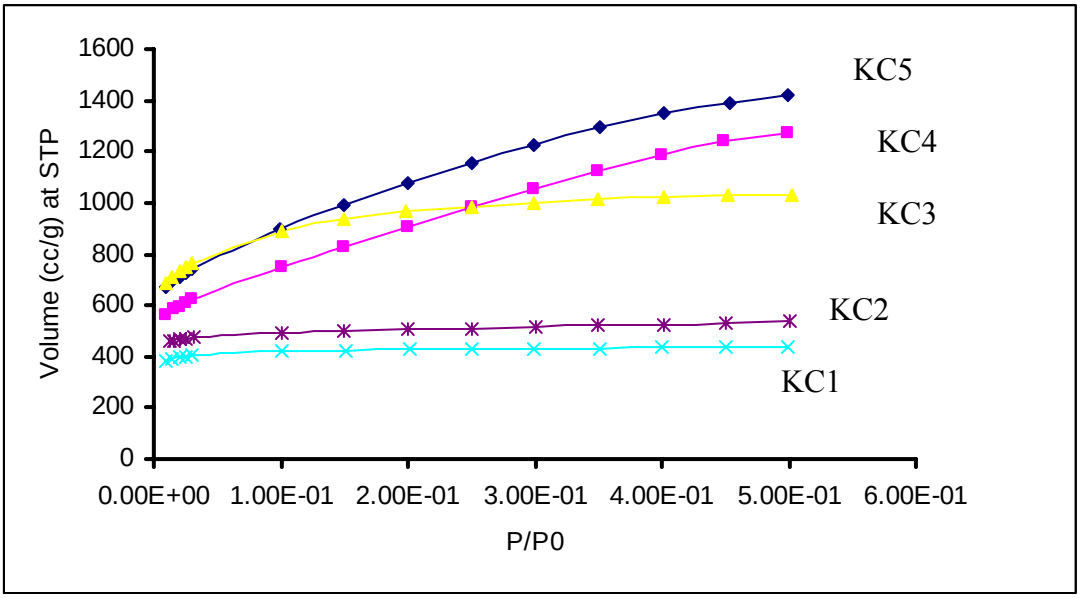


**Figure 2-14 Nitrogen isotherms of carbon prepared with different KOH: C ratio**

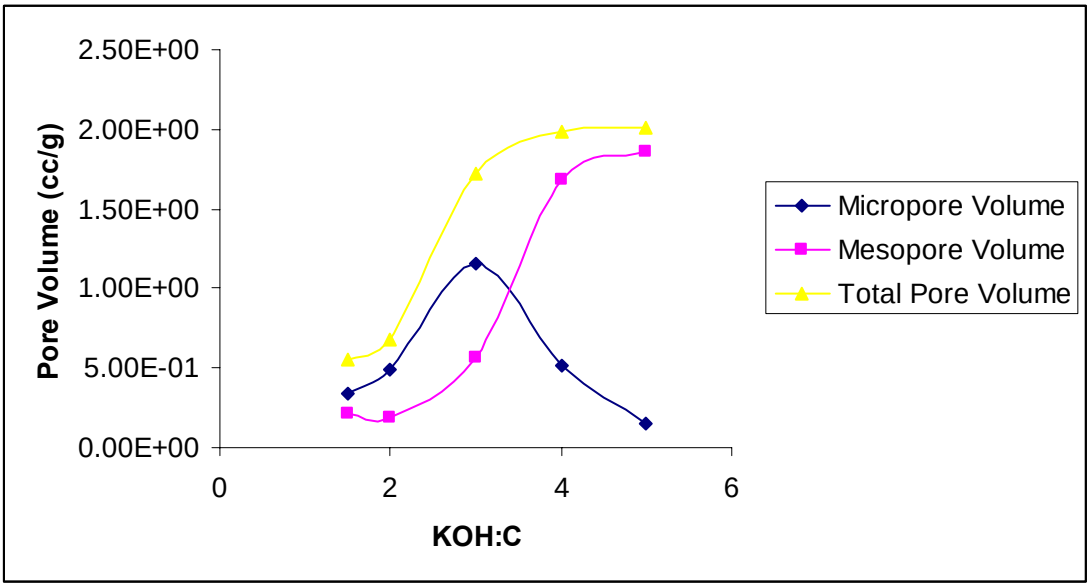


**Figure 2-15 Graph showing effect of KOH:C ratio on micropore volume in carbon.**

**Table 2-6 Characterization of carbon with different KOH: C ratio. The samples were activated at a temperature of 790 °C for 2 hour. The char used for this activation was soaked with 50% phosphoric acid at 50 C for 8 hours, charred at 450 C, and heated to charring temperature at 1 C/min.**

| Sample | KOH X C | BET Surface Area $m^2/g$ | Micropore Volume cc/g | Mesopore Volume Cc/g | Totalpore Volume Cc/g | Particle Density g/cc |
|---|---|---|---|---|---|---|
| KC1 | 1.5 | 1314 | 3.38E-01 | 0.21 | 0.55 | 0.74 |
| KC2 | 2 | 1724 | 4.90E-01 | 0.19 | 0.68 | 0.69 |
| KC3 | 3 | 2997 | 1.16E+00 | 0.56 | 1.72 | 0.47 |
| KC4 | 4 | 3347 | 5.14E-01 | 1.68 | 1.98 | 0.37 |
| KC5 | 5 | 3837 | 3.52E-01 | 1.86 | 2.01 | 0.33 |

**Effect of Heat Treatment Temperature (HTT) during KOH Activation:**

HTT is another important parameter that affects the final quality of the carbon. A series of carbon samples were prepared varying the final HTT from 700 to 900˚C with a KOH: C ratio of 3 and activation time of 1 hr. Figure 2-16 shows the nitrogen isotherm of these samples. The slope at the knee of the isotherm (where the isotherm starts bending) for all the carbon samples up to 800˚C is minimal showing that the carbon is mostly microporous. Also, as seen from the Table 2-7, as the temperature of activation is increased the final BET surface area increases up to 850˚C, thus indicating the higher degree of activation. The BET surface area for carbon at prepared at 700˚C is the lowest whereas it is the highest for one treated at 850˚C. However the BET surface area of the sample prepared at 900˚C is lower which indicates greater attack on the char, drilling bigger pores and hence converting the large fraction of mesopores to macropores. The

Figure 2-17 shows the micropore and mesopore volume of the carbon samples prepared at different HTT. As seen from the graph the micropore volume of carbon is maximum between 750 and 800˚C after which there is a sharp drop in the micropore volume and corresponding increase in the mesopore volume indicating the conversion of micropores to mesopores at higher temperatures. Thus the increasing HTT has an analogous effect of increasing KOH: C value. An explanation is that high values of both lead to the destruction of microporous network making the final carbon more mesoporous with higher surface area.

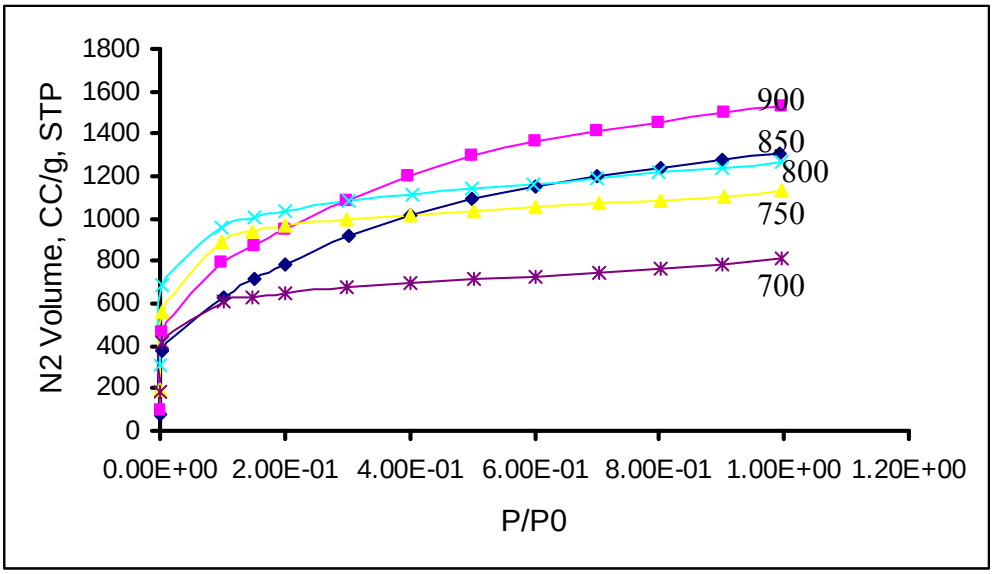


**Figure 2-16 Nitrogen Isotherms at 77K for carbon prepared by KOH activation at different HTT.**

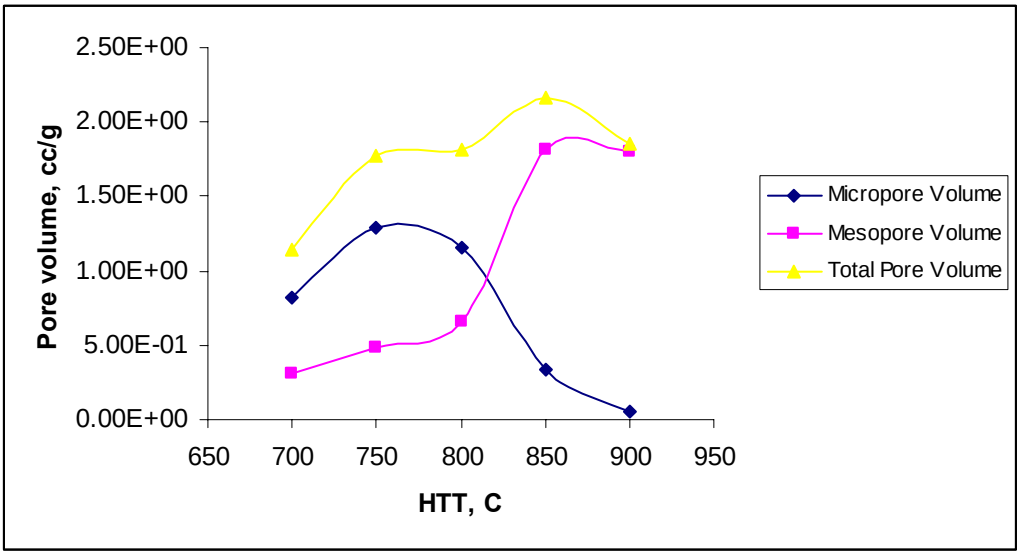


**Figure 2-17 Micro, meso and total pore volume of KOH treated carbon at different HTT.**

**Table 2-7Characterization of carbon prepared with KOH activation at different HTT. Activation was for 1 hour at a [KOH]:[char] mass ratio of 3. The char used for this activation was soaked with 50% phosphoric acid at 50 C for 8 hours, charred at 450 C, and heated to charring temperature at 1 C/min.**

| Sample | HTT ˚C | BET Surface Area $m^2/g$ | Micropore Volume cc/g | Mesopore Volume cc/g | TotalPore Volume cc/g |
|---|---|---|---|---|---|
| KOH-HTT1 | 700 | 1988 | 8.19E-01 | 0.31 | 1.14 |
| KOH-HTT2 | 750 | 3175 | 1.29E+00 | 0.49 | 1.78 |
| KOH-HTT3 | 800 | 2997 | 1.16E+00 | 0.66 | 1.82 |
| KOH-HTT4 | 850 | 3421 | 3.39E-01 | 1.82 | 2.16 |
| KOH-HTT5 | 900 | 2932 | 5.00E-02 | 1.8 | 1.85 |

## 2.4 CONCLUSION

From the above study it can be concluded that nanoporous carbon with micopore volume of 1.3cc/g and BET surface area of 3800+ $m^2$/g can be produced from corn cobs. For phosphoric acid activation of corn cobs, it is advantageous to soak the corn cobs with acid at lower temperatures because of the soft nature of the precursor. Also the heat treatment temperature of 450 -500˚C and acid concentration of 1.1 g/g is appropriate for getting high micropore volume. To produce carbon with high surface area and pore volume KOH treatment followed by phosphoric acid treatment is a preferred route of activation. For KOH activation the KOH: C ratio between 2.5 and 3 and heat treatment temperature between 750-790˚C is optimum for getting nanoporous carbon with pore sizes smaller than 20nm, after which the widening of ultramicropores or nanopores begins and product starts becoming more and more mesoporous.

## REFERENCES

[11] Solum, M. S., Pugmire, R. J., Jagtoycn, M. and Derbyshire, F., "Evolution of carbon structure in chemically activated wood" Carbon, 1995, 33(9). 1247.

[12] K. Gergova, S. Eser, Carbon 34 (1996) 879.

[13] K. Gergova, A. Galushko, N. Petrov, V. Minkova, Carbon 30 (1992) 65.

[14] C. A, Philip, B. S. Girgis, J. Chemical Technology, Biotechnology 67 (1996) 248.

[15] M. Molina-Sabio, F. Rodriguez-Reinoso, F. Caturla, M. J. Selles, Carbon 33 (1995) 1105.

[16] J. A. F. Mc Donald, D. F. Quinn, Journal of Porous Matter. 1 (1995) 43.

[17] M. Ahmedna, M. M. Johns, S. J. Clarke, W. E. Marshall, R. M. Rao, Journal of Science of Food and Agriculture, 75 (1997) 117

[18] L. B. Khalil, B. S. Girgis, Fuel Sci. Technology 13 (1994) 131.

[19] Analysis and use of corn cobs by the Andersons

[20] F. Rodriguez-Reinoso, M. Molina-Sabio and M. T. Gonzalez, "The Use of Steam and CO2 As Activating Agents in The Preparation of Activated Carbon", Carbon, 33(1), (1995) 15-23.

[21] A.M. Goncalves da Silva, V. A. M Soares, J.C. Calado, Journal of Chemical Society, Faraday Trans. 87 (1991) 3799.

[22] J. H. de Boer, B. G. Linsen, Th. van der Plas and G. J. Zondervan, J. Catalysis, 4, 649 (1965).

[23] G.D. Halsey, J. Chem. Phys., 16, 931 (1948).

[24] M. Polanyi, Verh. Dtsch. Phys. Ges., 16, 1012 (1914).

[25] M.M. Dubinin and L.V. Radushkevich, Dokl. Akad. Nauk. SSSR, 55, 331 (1947).

[26] R. Evans, U.M.B. Marconi and P. Tarzona, J. Chem. Soc. Faraday Trans. II, 82, 1763 (1986).

[27] Rowell, R. M., in Wood and Cellulosic Chemistry, Vol. 15, ed. D. N. S. Hon and N. Shirashi. Marcel Dekker, New York, 1991, p. 703.

[28] Solum, M. S., Pugmire, R. J., Jagtoycn, M. and Derbyshire, F.. Evolution of carbon structure in chemically activated wood, Curhon, 1995, 33(9). 1247.

[29] Pandey, S. N. and Nair, P., Effect of phosphoric acid treatment on physical and chemical properties of cotton fiber, ***Textile Res. J.,*** December, 1974, 927.

[30] Jagtoyen. M.. Derbyshire, I:., Rimmer. S. and Rathbone, R., Relationship between reflectance and structure of high surface area carbons, *Fuel,* 1995. 74(4). 610.

[31] Lai, Y. Z., in *Wood and Cellulosic Chemistry,* Vol. IO cd. D. N. S. Hon and N. Shirashi. Marcel Dekker, New York, 1991, p. 455.

[32] Barker, R. H. and Hendrix, J. E., Cotton and other cellulosic polymers, in ***Flame Retardancy of Polymeric Materials,*** Vol. 5, ed. W. C. Kuryla and A. J. Papa. Marcel Dekker, New York, 1979, pp. 35565.

[33] Katsuura, K. and Inagaki, N., Thermal degradation of phsophorus-containing polymers. VIII Relation between the thermal reaction of flame-retardant cellulose and its flammability, Textile Res. J*.,* February, 1975, 103.

[34] Marit Jagtoyen, Frank Derbyshire, " Activated carbon from yellow poplar and white oak using phosphoric acid activation" Carbon 36 (7-8), 1998, 1085-1097.

# CHAPTER 3

# 3. NANOPOROUS CARBON FROM CORN COBS FOR ADSORBED NATURAL GAS APPLICATION

**This paper was submitted for publication to Carbon as: "Nanoporous Carbon from Corn Cobs for Adsorbed Natural Gas Application", Parag S. Shah [a], Galen J. Suppes [a], Jacob Burress [b] Peter Pfeifer [b]**

[a] Department of Chemical Engineering, W2028 Engineering Bldg. East, University of Missouri, Columbia, MO 65211

[b] Department of Physics, University of Missouri, Columbia, MO 65211

## ABSTRACT

Nanoporous carbon was synthesized from corn cobs. The nanoporous carbon was further converted to monolithic form and its capacity to store natural gas at 500psi and 298K was measured using gravimetric and volumetric measuring techniques. Methane capacity as high as 173V/V or 0.21g/g or 108g/L were obtained on the carbon produced from corn cobs. The effect of various parameters of carbon production on the methane storage and delivery capacity was studied. The effect of binder concentration in the monoliths on final methane storage and deliverable capacity was also studied. The carbon characterization was performed using nitrogen adsorption at 77 K.

KEYWORDS: nanoporous carbon, adsorbed natural gas, corn cobs, activated carbon

## 3.1 INTRODUCTION

Since the second oil shock of 1979-1980, interest in alternative fuels has increased as nations look to diversify their fuel options, reduce dependence on volatile oil markets, and meet environmental standards to reduce the growing green house problem.

Natural gas is a relatively inexpensive, clean burning and abundantly available source of energy, which is not utilized to its full potential and availability. One of the applications of natural gas can be as vehicular fuel. However, low volumetric energy density of natural gas at normal temperature and pressure (NTP) limits its use a transport fuel. At NTP the volumetric energy density and hence the mileage per unit volume of fuel tank of natural gas is only 0.12% of that of gasoline.

Liquefied Natural Gas (LNG) has a volumetric density of about 600 times greater than natural gas at NPT. However, the cryogenic conditions required maintaining the LNG makes its unfeasible for vehicular applications.

CNG is natural gas stored as compressed super critical fluid at room temperature and a maximum pressures ranging from 3000-3600 psig[35]. Maximum density of about 230 times greater than at NTP (which is about 26% volumetric energy density of gasoline) can be attained with CNG at about 3000 psig. However, the awkward bulk of the high pressure CNG cylinders take up valuable cargo or trunk space[36]. Further, filling a CNG tank requires an expensive multistage compression facility. Multistage compressor and high pressure metering equipment contribute to as much as 50% of the capital investment required to convert a fleet to CNG operation[35]. Thus the expense of compressors has limited the number of outlet, each of which must be aimed at serving as large a number of vehicles as possible so as to spread the costs around.

The above stated problems have limited the extensive use of CNG as an individual vehicular fuel.

Natural gas as an adsorbed phase in porous materials is referred to as Adsorbed Natural Gas (ANG) and it can overcome the major limitations of CNG and LNG i.e. adequate energy density of natural gas at low pressure and room temperature. Currently ANG can provide up to 80% of energy density as CNG at a low pressure of about 500 psig at room temperature[37 38]. Hence a maximum volumetric energy density of about 20% of that of gasoline can be attained with ANG in the laboratory using some of the best adsorbent materials available currently.

The primary advantage of ANG over CNG is the low pressure. ANG storage tank can be filled with natural gas from domestic pipe-line using an inexpensive single-stage compressor. The small compressors needed for the low pressure filling, particularly for slow overnight filling, would be cheap and reliable enough to place ANG use within the reach of many consumers. Further because of the low pressure, light weight conformable aluminum tanks can be used and can be distributed around the available area of the vehicle with minimal interference with usable space[36]. The feasibility and economics of ANG depends a lot on the methane uptake capacity of the adsorbent comparable to that of CNG at 500 psig and room temperature and the cost of the adsorbent to the end user. A cheaper adsorbent having high methane storage and deliverable capacity will help to switch the economics in favor of ANG over CNG. Hence the search of a suitable porous adsorbent in terms of further improving ANG storage volumetric energy density and lowering the adsorbent cost to the end user is currently an active area of research, that could eventually lead towards home fuelling of natural gas based vehicles.

Figure 3-1 shows the methane storage capacity (mass per volume of tank) with and without adsorbent. The target pressure for a flat ANG tank is 3.44 MPa (500 psi, 34.0 atm; vertical dashed line; all pressures absolute). To store the same amount of methane without adsorbent, the pressure would have to be 15.0 MPa, much more than a flat tank can bear.

Nanoporous or more often called ultramicroporous carbons are better adsorbents for storing natural gas as compared to zeolite[39 40 41 42], silica gel[43] and organic gels[44 45]. Carbons previously tested by researchers that have given higher methane uptake values are usually made from relatively expensive raw materials like saran, wood, coconut shells, peach stones, lignite coals and cokes. Myers and Glandt pointed out that from the economic point of view for activated carbons, maximizing the ANG capacity implies increasing the cost exponentially[46]. Hence in order to keep the adsorbent cost low researchers are investigating the carbons from relatively inexpensive waste materials like landfill tires, newspapers and shredded tires have been investigated for methane uptake but exhibited moderate methane uptake up to 68 to 100 V/V at 500psig and 298K[47 48 49].

One inexpensive and abundantly available precursor for making ANG adsorbent carbon is corn cobs. Corn cob is available in the US at about $5-10/ton, and is available in abundance. In 2002, Missouri alone produced enough corn cobs to produce carbon for all the cars in the US. Also the chemical composition of corn cobs[50] suggest that it has less mineral matter, which are often responsible for preferential gasification during the activation process resulting in meso and macropore channeling and pitting, and not the preferred microporosity and repeatability. Hence, corn cobs could be an excellent precursor for the commercial production of nanoporous carbon for ANG technology.

In this project nanoporous carbon having methane uptake capacity of 0.21g/g and 173 V/V was produced from corn cobs. The carbon that gave highest methane uptake capacity was in the monolithic form made using hydraulic pressing and polymeric binder. The methane uptake and deliverable capacity of the carbon produced were measured using gravimetric and volumetric measurement techniques.

## 3.2 EXPERIMENTAL PROCEDURE

The experimental procedure for making the carbon from corn cob is discussed in detail in our previous publication[51]. This paper discusses the use of nanoporous carbon obtained from corn cobs for ANG application. Experiments were carried out to check the effect of different important parameters of carbon production on the final methane uptake and deliverable capacity. In ANG technology since the density of the carbon storing the methane is an important factor for getting high methane storage values for a given volume, systematic study was performed on densification of the carbon powder. Carbon monoliths were produced from carbon powder by pressing the powder using a 150ton Dake hydraulic press in a metal die. Varying amounts of pressing force and binder concentrations were tried to get optimum crushing strength, density and micropore volume of the final carbon monoliths that gave maximum values of methane uptake both on gravimetric (g/g) and volumetric (V/V) basis.

Methane uptake measurements were made both gravimetrically and by using pressure differential method (volumetrically). The gravimetric measurements were made on 1g of carbon in a stainless steel chamber capable of holding 1000psig pressure. A Denver Instruments M-220D balance was used that was capable of weighing as low as

10microgram. Provisions were made to include the buoyancy effects and the dead volume of the methane in the empty chamber volume during the calculations to give accurately the final methane uptake capacity.

For gravimetric measurements, 1g of powdered carbon or broken pieces of carbon briquettes were first placed in the stainless steel chamber; the remaining empty space was filled with glass wool which prevented the loss of carbon powder during outgasing step that included heating the entire chamber to 140˚C under vacuum for 2hr. After 2 hours the outgased chamber was connected to methane source (99.9% pure methane from Prax Air) and pressurized at the required pressure and left for one hour to attain equilibrium. After 1 hr the chamber was disconnected from the methane source and weighed. In order to determine the deliverable methane capacity of the carbon the pressure from the carbon containing chamber was released and the weight of the chamber was noted after equilibrium was achieved to determine the methane uptake at atmospheric pressure. The difference between the methane uptake at 500psig and atmospheric pressure gave the deliverable methane capacity of the carbon.

To measure the methane uptake volumetrically on the carbon monoliths of 3.5" diameter and to double check the gravimetric measurements, the test apparatus as shown in Figure 3-2 was built by Midwest Research Institute (MRI) that worked on the principle of pressure differential. The test apparatus mainly consisted of two tanks. The storage tank; where the methane was stored at pressures up to 1000psig and the test tank; where the carbon monoliths to be tested were placed. The pressure transducers and pressure gauges were placed in both the tanks. There were two valves separating the test tank from the storage tank, and during methane uptake measurements these valves were

opened in order to connect both the tanks. The test tank was equipped with four thermocouples to measure temperature at four different radial depths in the carbon monoliths during adsorption and desorption process. Provisions were made to outgas the test tank before carrying out methane uptake measurement. After 1 hr of outgasing of the carbon monolith in the test tank, the valves separating the test and the storage tanks were opened and the pressure in the test tank was regulated to the desired values using the pressure regulator. Upon opening the valves the methane flowed from the storage tank that was kept at higher pressure, to the evacuated test tank. After equilibrium was reached (which was indicated by constant pressure and temperature values in the both the tanks) the total pressure differential in the storage tank was noted to determine the methane uptake on the monoliths. The test apparatus was regularly checked for leaks. Provisions were made in the calculations to take care of the dead volume in the test tank and the temperature effects during adsorption.

The characterization of all the carbon produced was done with $N_2$ adsorption at 77K using the Autosorb 2.0 instrument from Quantachrome. Analysis of isotherms was carried out by applying various methods to obtain different information. The BET equation was used to get the BET surface area from volume of $N_2$ adsorbed at $P/P_0$= 0.95. The T-method was used to find the micropore volume and the external surface area of the mesoporous fraction from the volume of $N_2$ adsorbed up to the $P/P_0$ = 0.0315.

## 3.3 RESULTS AND DISCUSSION

A systematic study of the two important parameters the KOH: Char ratio and the heat treatment temperature (HTT) (this affects the final methane uptake capacity of the carbon obtained from corn cobs) were first conducted. It was found that the KOH: Char

ratio had the most significant effect on the final methane uptake capacity of the carbon. After determining values of KOH: Char and HTT that gave highest methane uptake values on the carbon powder, a systematic study of the densification of the carbon powder was performed to get the maximum piece density of the monolithic carbon.

### 3.3.1 EFFECT OF KOH: CHAR RATIO ON METHANE UPTAKE CAPACITY

As showed in our previous paper[51] the KOH: char ratio is an important parameter that affects the pore size distribution of the final carbon from corn cobs. Methane uptake measurements were carried on five different carbons prepared at KOH: Char ratio of 1.5:1, 2.5:1, 3:1, 4:1, and 5:1. Figures 3-3 and 3-4 show the nitrogen and methane isotherms respectively for these carbons.

As seen from Figure 3-2 the isotherms of carbon prepared with ratio of 1.5:1, 2.5:1, 3:1 have minimal slope at the knee of isotherm which indicates that this samples are essentially microporous solids having type-1 isotherms. However the slopes of $N_2$ isotherm for sample with KOH: C ratio of 4 and 5 is very high as compared to the 1.5 to 3 indicating the presence of large fraction of mesopores along with micropores. Looking at the corresponding methane isotherms at pressures from 50 to 500 psig obtained on the monolithic form of the carbons, we can clearly see that the carbon prepared at 2.5: 1 ratio has the highest methane uptake value of 173 V/V.

Table 3-1 shows the micropore volume, methane uptake, methane delivery, and particle and piece densities of these carbons. The carbon with 2.5: 1 has the micropore volume of 1.13cc/g, piece density of 0.62g/cc and has the highest storage and delivery methane values on volume basis and the carbon with 3:1 with micropore volume of 1.23

cc/g and piece density of 0.43g/cc has the highest methane uptake and deliverable capacity of 0.218g/g on the gravimetric basis.

The important observation to be made here is the effect of micropore volume on the methane uptake. The methane uptake value for 5:1 and 4:1 sharply decreases compared to carbons with 1.5 to 3 even though their BET surface area and total pore volume are more. The prime reason for this is the decreased micropore volume than the samples with 1.5 to 3. Figure 3-5 shows the pore size distribution of the sample 2.5/1. As seen from the figure there is a large fraction of the pores with size between 0.7 to 1.9nm. The ideal pore size for getting maximum methane uptake obtained by MonteCarlo simulations is between 0.8 to 1.2nm. Hence the high fraction of pores with size less than 1.9nm leads to high methane adsorption values for sample 2.5/1.

Along with importance of micropore volume for methane uptake Table 3-1 also shows the importance of packing densities, and hence the piece of density of the carbon. Since in ANG application, methane will be stored in a given confined volume of carbon tank it is advantageous to have more carbon in a given volume of the tank or in other words carbon with higher packing density. As seen from table 3-1, the methane uptake value on V/V basis is higher for carbon with higher packing density along with higher micropore volume. As seen from the table, the V/V values of the carbons 5/1 and 4/1 are very low compared to that of carbons 1.5/1 and 2/1 even though the micropore volume is not very different. This is because the packing densities of the 5/1 and 4/1 carbons are low compared to that of 1.5 and 2/1 carbons due to large meso and macropore volume created due to over activation by excess of KOH. Figure 3-6 shows the graph of effect of

KOH: Char ratio on the final packing and piece densities of the carbon and carbon monoliths respectively.

The more practical value for vehicular application of ANG is the deliverable methane capacity of the carbon on V/V basis. The deliverable value for 2.5/1 carbon is 156 V/V which is among the highest values reported in literature for carbons derived from biomass. Table 3-1 shows the deliverable value on V/V basis. These values are lower than the stored methane V/V values for all the carbons, which is due to some of the methane molecules that remain in the nanopores or ultramicropores in the carbon when the pressure is reduced from 500psig to atmospheric pressure. This amount in nanoporous carbons is always around 10% of the stored V/V values.

### 3.3.2 EFFECT OF HEAT TREATEMENT TEMPERATURE (HTT) ON METHANE UPTAKE

The effect of another important variable in preparing carbon from corn cobs for storing methane, the heat treatment temperature, was studied by preparing carbon pyrolyzed at different final heat treatment temperature ranging from 700˚C to 900˚C. Table 3-2 summarizes the characterization details and the methane performance for these carbon samples. Figure 3-7 shows the nitrogen isotherms for these samples. As seen from the figure the slope at the knee of the nitrogen isotherm is minimal for samples prepared up to final temperature of 800˚C, indicating that they are essentially microporous solids. However the slope value increases for carbons prepared at 850˚C and 900˚C showing the presence of large fraction of mesopores and macropores. Table 3-2 shows, as expected, that the samples with higher micropore volume have higher methane uptake values than those with lower micropore volume. The methane uptake

value for the carbon prepared at 790˚C is the highest at 159 V/V and is the lowest for carbon prepared at 900˚C which is 139V/V. Thus it can be concluded that after the activation temperature of 800˚C, the destruction of ultramicropores or nanopores to larger mesopores and macropores starts leading to lower packing density and lower methane storage values. The optimum HTT is between 750 to 800˚C which leads to both higher micropore volume and higher packing density of the carbon powder and ultimately leading to higher methane storage density and capacity.

### 3.3.3 DENSIFICATION STUDIES

As discussed earlier, since the amount of carbon accommodated in a given volume is the most important factor for getting higher methane storage density for vehicular application of ANG, a progressive study was performed on the densification of the carbon powder. Figure 3-8 shows the picture of the SS 316 die used to prepare carbon monoliths of diameter 3.5” and thickness 1” from carbon powder. Figure 3-9 shows the graph illustrating the effect of pressing force on the final piece density of the monolithic carbon. The initial packing density of the carbon was 0.28g/cc corresponding to a carbon prepared with a KOH:Char ratio of 3:1 and HTT of 750˚C. As seen from the graph, as the hydraulic force used to press the powder is increased the density of final monolith also increases. This continues up to the pressure of 16000psig after which additional pressure doesn’t affect the density. Thus a pressure of 16000 psig was used for all the further work on densification to reduce void volume between the carbon particles.

Besides the pressing force the other parameter affecting density and monolith volume is the carbon particle size distribution. Two different types of carbon powder made with same activation procedure, but each having different particle size distribution

(PSD), where used to check the effect of PSD on the final monolith density. Two PSDs were investegated. Type-I PSD mainly consisted of particles of similar size that was between 0.0035 and 0.00295 inches. Type-II PSD consisted of particles sizes distributed as 30% between 0.0035-0.00295, 20% between 0.00295 and 0.0025" and 50% < 0.0021". After using the same process of densification for both types of powder, the final piece density of the monolith with Type-II PSD was about 10% more than with Type-I PSD. Thus it can be concluded that the distributed type of PSD gives greater increase in density or reduction in void volume than non-distributed type of PSD. The methane uptake on the mass basis was not affected by the greater increase in density due to type II PSD but the methane storage density increase by at least 10%. Figure 3-9 shows the density increase for the type-I and type-II PSDs.

Another important factor in the densification of the carbon powder is the type and amount of binder used. The binder used for making the monoliths should be such that it doesn't blind the ultramicropores present in the carbon and at the same time provides sufficient structural integrity so that during adsorption and desorption cycle it doesn't crack and release lot of carbon dust. The binder used in this study was saran which is a co-polymer of polyvinylidene chloride (PVDC) and polyvinyl chloride (PVC). The primary reason to use this polymeric binder was that PVDC and PVC can themselves be converted to highly microporous carbon by pyrolizing them at temperatures upto 750˚C. The advantage of this being the binder will not block the nanoporous network in the carbon monolith and at the same time bind it well to give higher density and excellent compressive and abrasive strengths.

Table 3-3 shows the characterization of carbon obtained from pure saran. As seen from the table saran carbon has a large fraction of micropore with high micropore volume of 0.256 cc/g and BET surface area of 900$m^2$/g. Figure 3-11 shows the pore size distribution of the carbon obtained from pure saran. As seen the large faction of pore volume is microporous of size between 1-2 nm which is ideal for storing methane. Experiments were carried out to find the effect of different concentration of saran used to make monoliths on the final methane storage capacity of the monoliths and the monolith density and compressive strengths. Figure 3-12 shows the monolith methane uptake values on mass basis as a function of binder concentration. Also Table 3-4 shows the compressive strengths of the monoliths made with different concentration of binder. As seen from the table the higher binder concentration leads to higher compressive strengths of the final carbon monolith, however, it decreased the methane uptake capacity simultaneously. Hence it is advantageous to use least amount of binder so that the methane uptake capacity is not reduced still giving good quality briquettes.

### 3.3.4 VOLUME DISTRIBUTION OF TANK

As mentioned earlier the volume distribution of tank is an important factor to be considered in the adsorbed natural gas technology. For storing maximum amount of natural gas in the given volume of the ANG tank ideally the tank volume should just consist of micropore volume in the carbon adsorbent and the carbon particles itself. Hence the adsorbents used for ANG application should have high micropore volume and less meso and macropore volume. Figure 3-14 shows the volume distribution in the tank filled with corn cob derived carbon monoliths of this project and monoliths of carbon obtained from AX-21 and monolith of best carbon obtained in the AGLARG project.

AX-21 from Kansai Coke is considered the best commercial carbon available in the market that has one of the best surface areas (~3100 $m^2/g$) and micropore volume (~1.07 cc/g). The AGLARG project was a comprehensive project on natural gas storage on carbon derived from olive pits and other carbons. As seen from Figure 3-14 the monolith made from carbon from corn cob has the highest micropore volume and minimum meso pore volume as compared to other two carbons. Because of very high fraction of micropore volume in the monolith the methane uptake capacity up to 173V/V was obtained on the carbon of this project.

### 3.3.5 TEMPERATURE PROFILES IN CARBON MONOLITHS

Temperature effect during the filling and discharge of the ANG tank is an important factor to be considered while designing an ANG based fuel system. Temperature affects the adsorption capacity of the adsorbents and the time required to reach equilibrium in ANG tank filling and discharge. Temperature profiles were studied in the monolithic carbon using the same test apparatus designed by MRI used to measure methane uptake values using pressure differential. Temperatures at four locations in the carbon monolith at different radial depths were recorded by drilling thermocouples at these depths during the filling and discharge of the methane in the adsorbent containing tank. The test apparatus designed by the MRI was a very good representation of an actual ANG based fuel system, so the temperature effects seen in the test apparatus are a very good representation of the temperature effects that will be seen in an actual onboard vehicular ANG system. Figure 3-15 shows the temperature and pressure profile of the carbon monolith during the filling and discharge of the test tank. The volumetric flow rate during the filling and discharge were kept to simulate the actual filling and discharge

rates in the ANG vehicle (about 129 CFD). As seen from the figure the temperature at the center of the briquette is the highest (upto 80˚C) during the filling whereas the temperature at the outer section of the monolith where lower due to the heat transfer with the relatively cooler outer wall of the tank. Also, during the discharge the center of the briquette gets the coldest to the temperature of 20˚F whereas the outer part of the briquettes remains at relatively mild temperatures again due to the contact with the outer tank wall. This study indicate that there should be some time gap available between the filling and discharge cycles of the ANG tank depending on the amount of the adsorbent and filling and discharge rates, to utilize the full adsorption capacity of the tank. This study proved to be very useful during the actual road test of the ANG tank in a FORD 150 pick truck performed at MRI (not described in this paper).

### 3.3.6 KOH RECYCLE

To commercialize the ANG technology the cost of the adsorbent (ideally between $2-3/kg) is an important factor. As seen from the previous discussions, to get the maximum methane storage the KOH: Char ratio is between 2.5 to 3. Since KOH is the reagent added in excess it is important to recover this unreacted valuable KOH after the reaction to reduce the cost of carbon production. Experiments were carried out to recover residual KOH from the spent liquid after washing. Up to 50% of initially added fresh KOH was successfully recovered from the washing liquor after the washing step. This recovered KOH was solely used as reactant for producing new carbon at HTT of 790˚C and soaking time of 1hr. Table 3-5 shows the characterization and methane uptake data for this carbon. As seen from the table the pore volume and density of this carbon is similar to that of the carbon prepared from fresh KOH. Also the methane uptake of 142

V/V is in close proximity of the value obtained using fresh KOH. Thus the unused KOH from the process can be recycled and can be successful used solely or mixed with fresh KOH without affecting the carbon quality. Doing so will help to cut the cost related to KOH.

## 3.4 CONCLUSION

From this study it can be concluded that corn cobs are excellent precursors to produce nanoporous carbon for methane storage. The KOH:Char ratio and heat treatment temperature proved to be a very critical parameters for getting high methane storage density on the carbon. After optimizing the various important parameters the carbon adsorbent with micropore volume between 1.2 and 1.4 cc/g and piece density of monoliths between 0.6 and 0.7 were obtained. As result of combination of high micropore volumes and piece density, a high methane storage density of 173 V/V (108 g/L) was repeatedly obtained with this value confirmed by both gravimetric and pressure differential measurement techniques. The deliverable volume of 156 V/V was obtained repeatedly. The use of recycled KOH to produce same quality of carbon as fresh KOH was also demonstrated.

# FIGURES

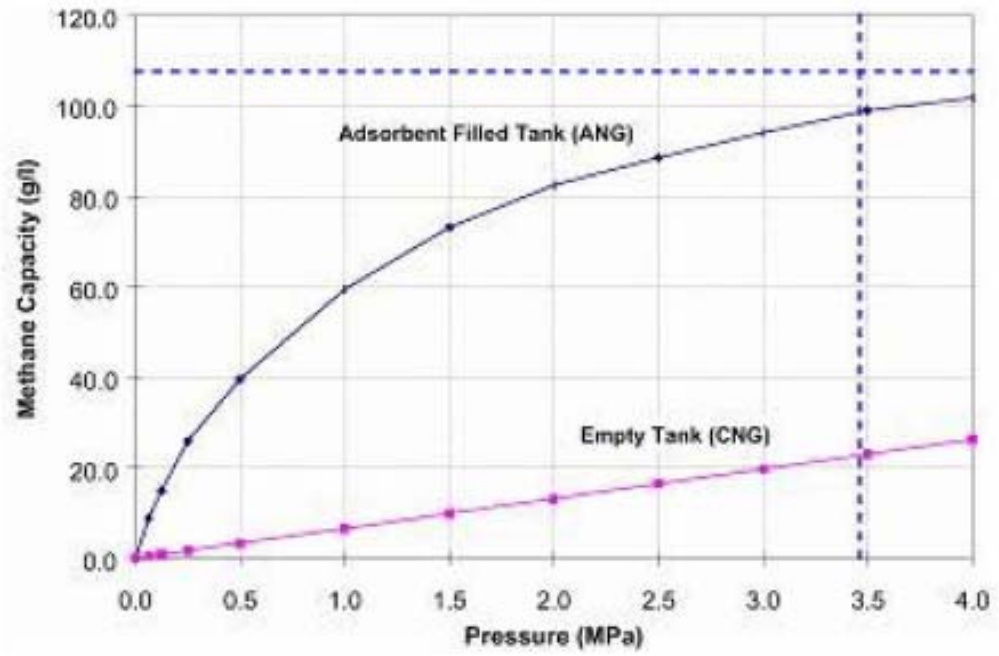


**Figure 0-1 Methane storage value in mass per volume of tank (g/L) with and without adsorbents.[52]**

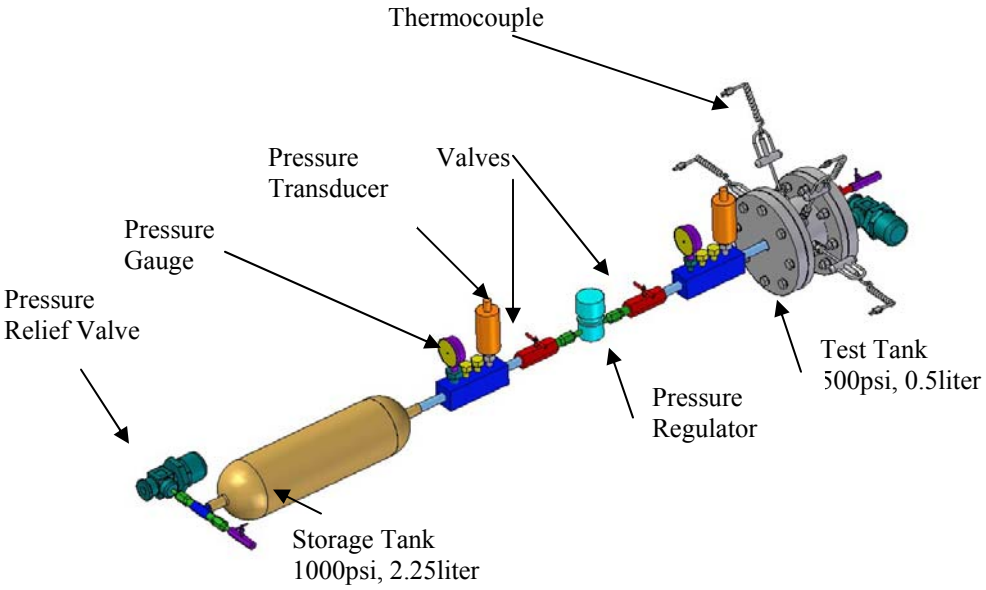


**Figure 0-2 Schematic of Test Fixture used to measure methane uptake on 3.5" carbon monolith.**

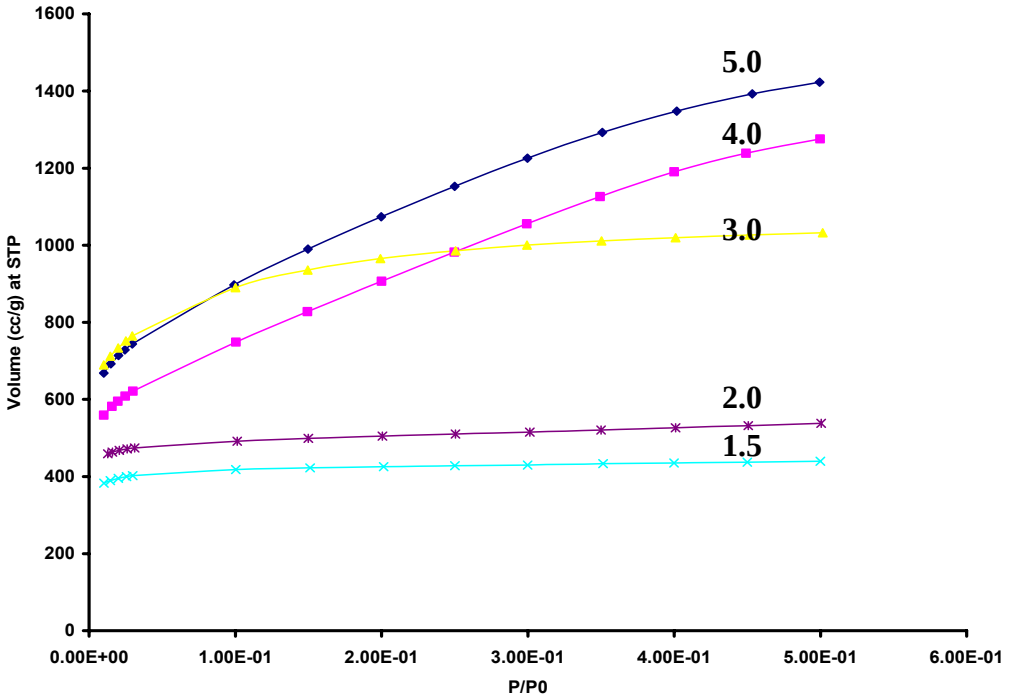


**Figure 0-3 Nitrogen Isotherms at 77K for carbons prepared with varying KOH:C values.**

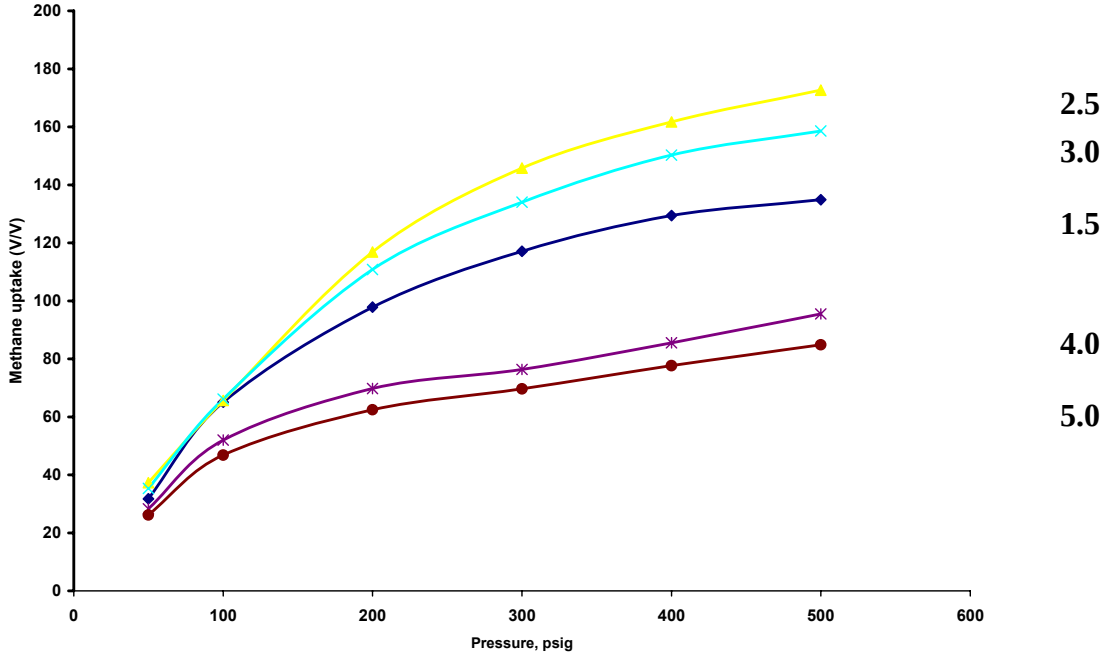


**Figure 0-4 Methane Isotherms at 298K for carbons prepared with varying KOH:C values.**

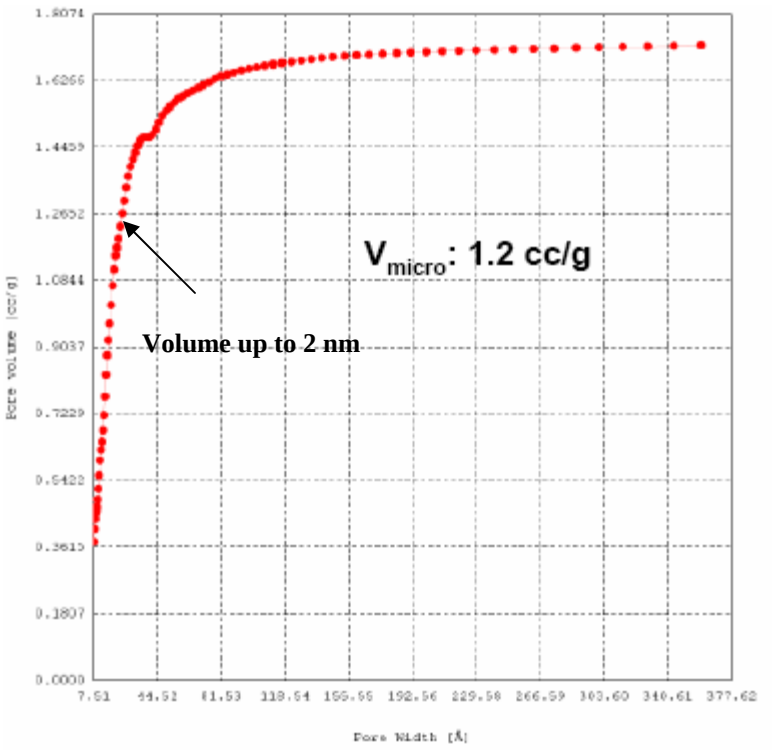


**Figure 0-5 DFT/Monte Carlo cumulative pore volume graph.**

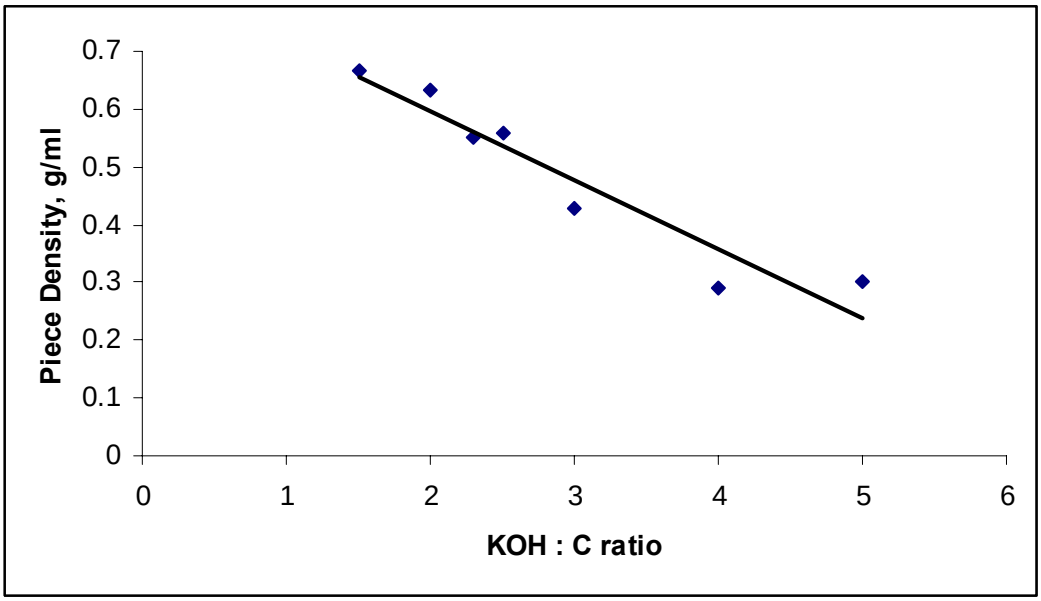


**Figure 0-6 Effect of KOH :C values on piece density of carbon monoliths.**

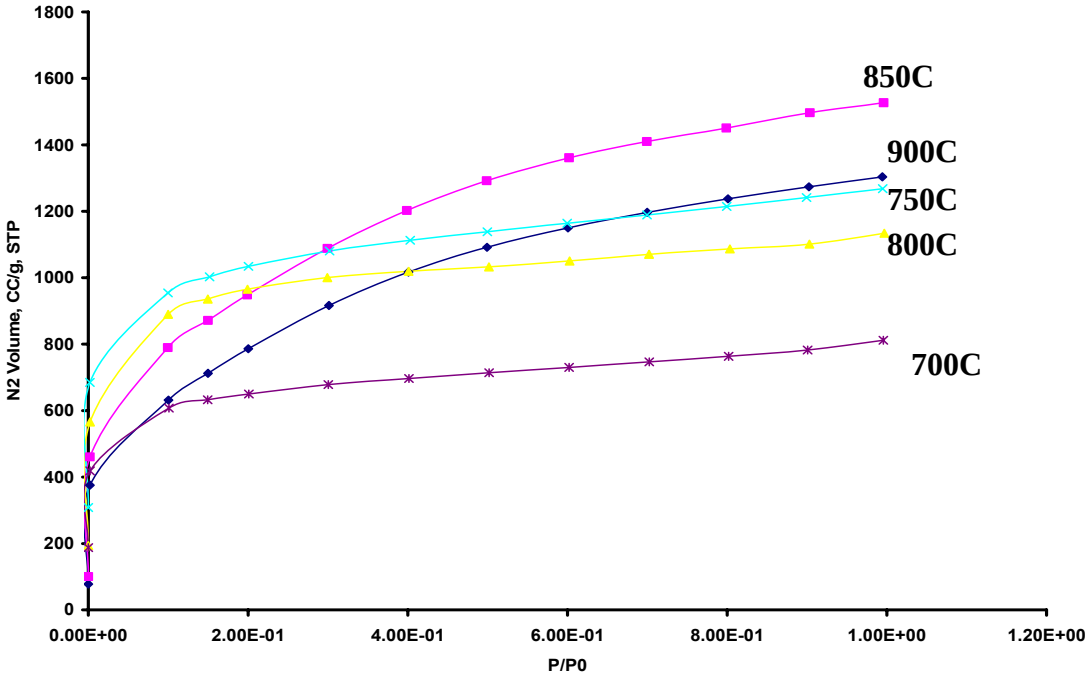


**Figure 0-7 Nitrogen Isotherms at 77K for carbons prepared at different HTT.**

**Figure 0-8 S/S die used to prepare monoliths out of carbon powder.**

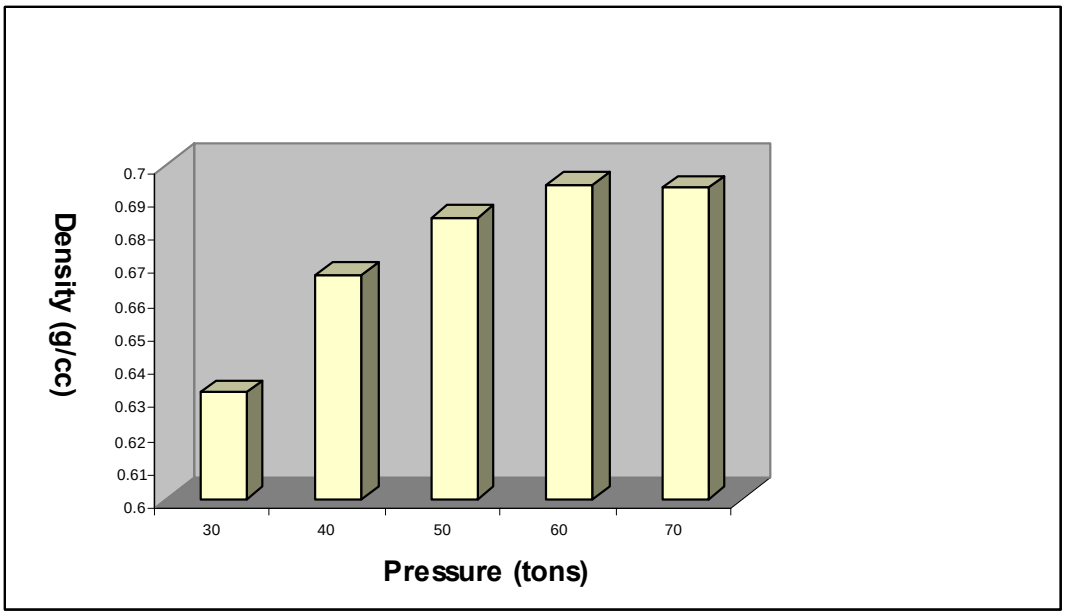


**Figure 0-9 Effect of pressing force on the density of carbon monolith.**

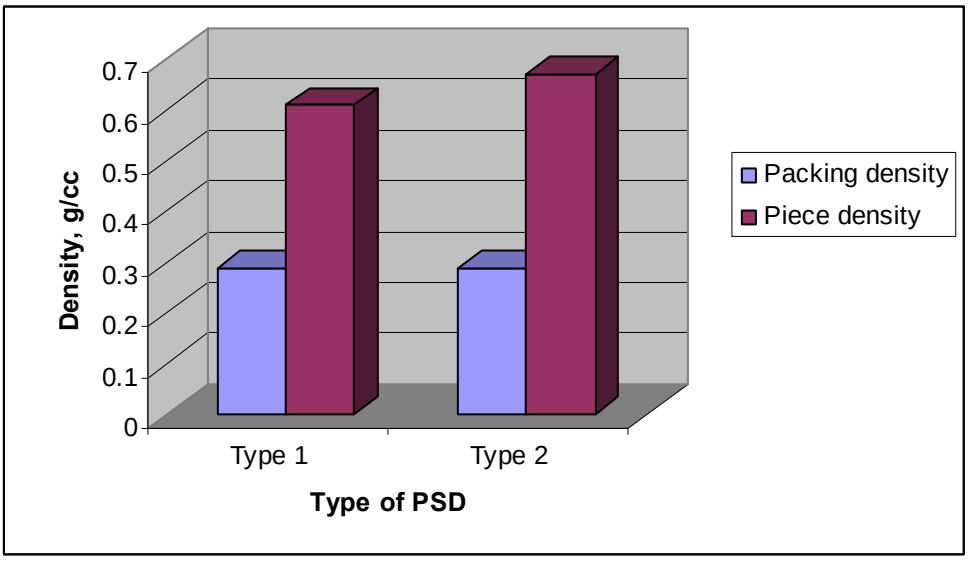


**Figure 0-10 Density increase in type-I and type-II PSDs.**

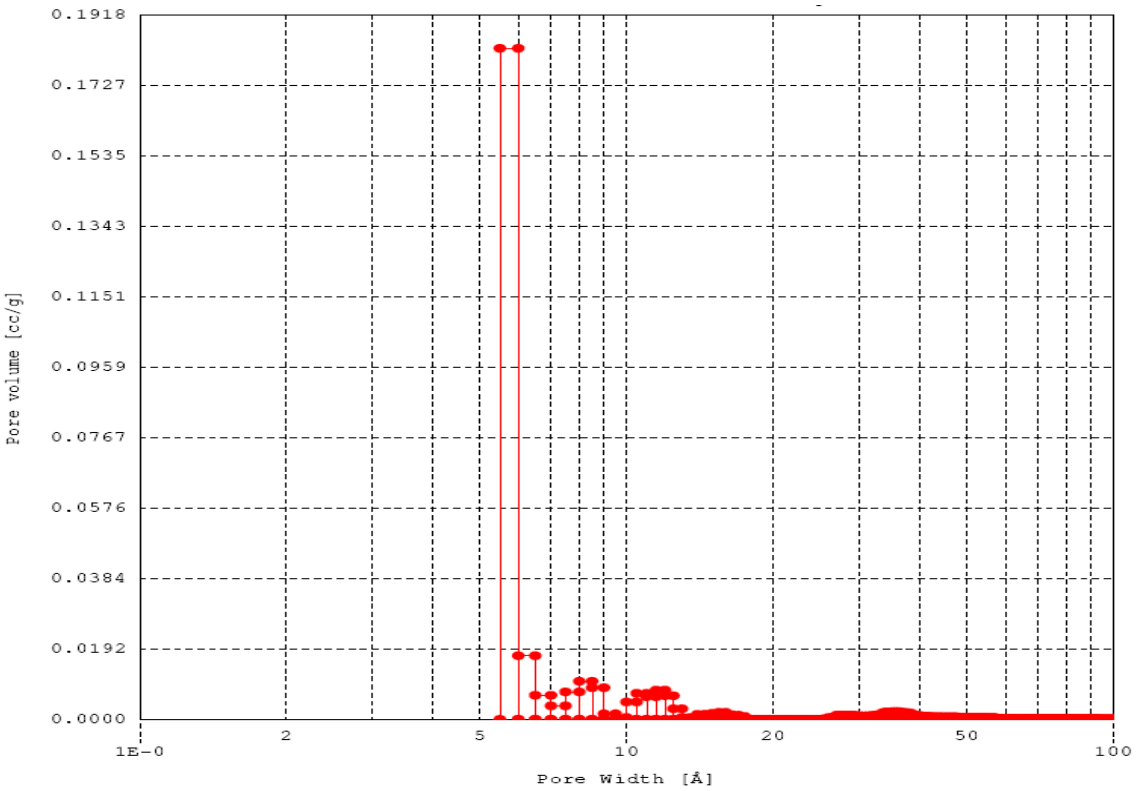


**Figure 0-11 Pore size distribution in carbon obtained from pure saran.**

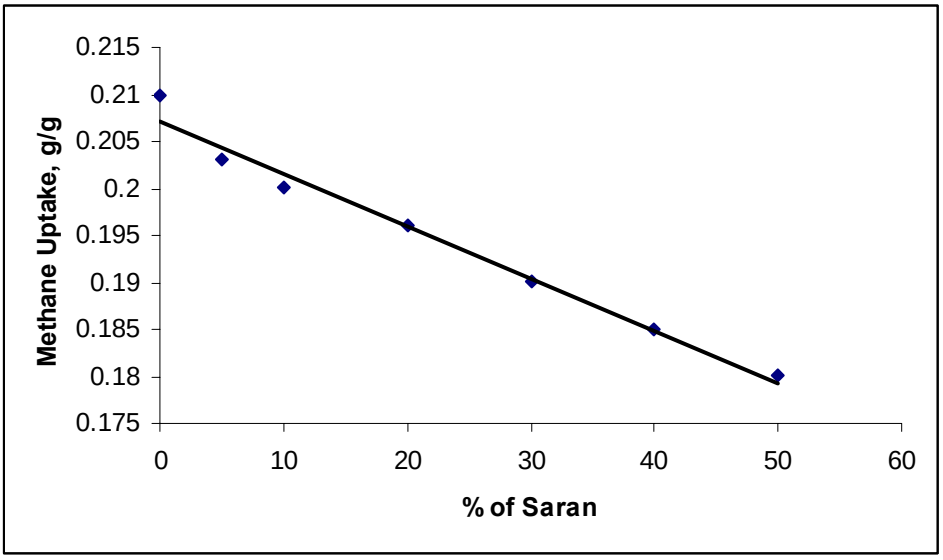


**Figure 0-12 Effect of binder concentration on methane uptake capacity.**

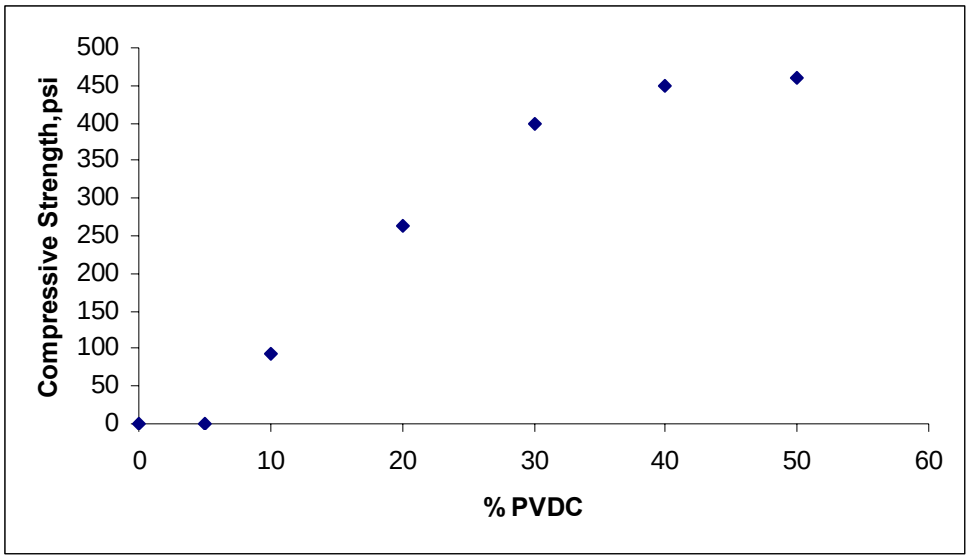


**Figure 0-13 Effect of binder concentration on final compressive strength of carbon monlith.**

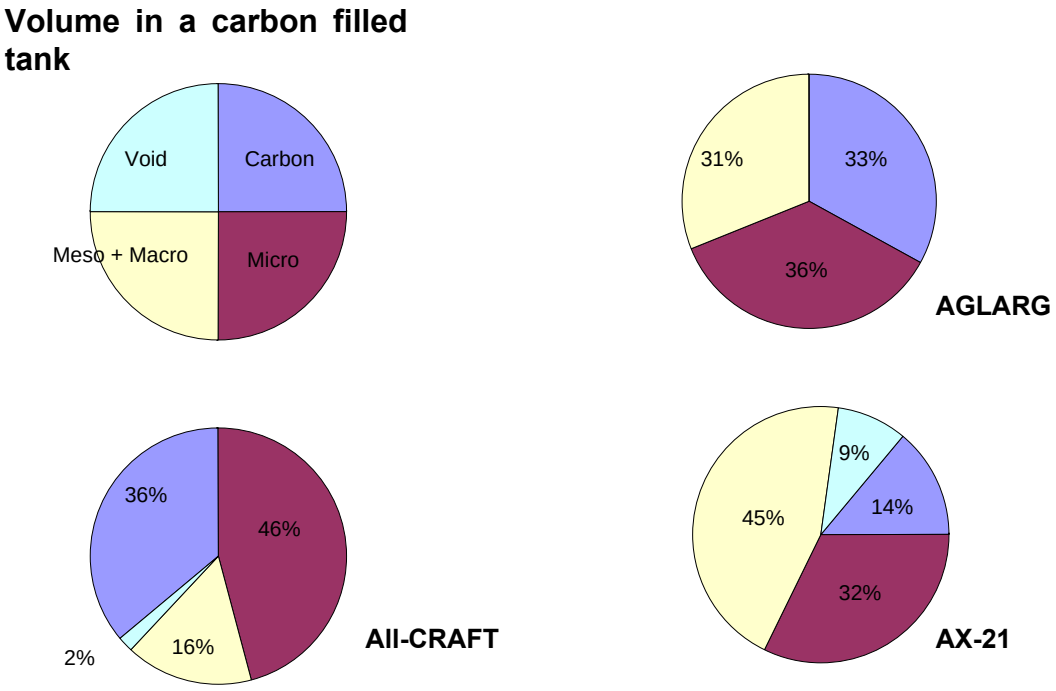


**Figure 0-14 Comparison of volume distribution of tank filled with corn cob derived carbon monolith and monolith made with commercially available MaxSorb carbon and AGLARG carbon.**

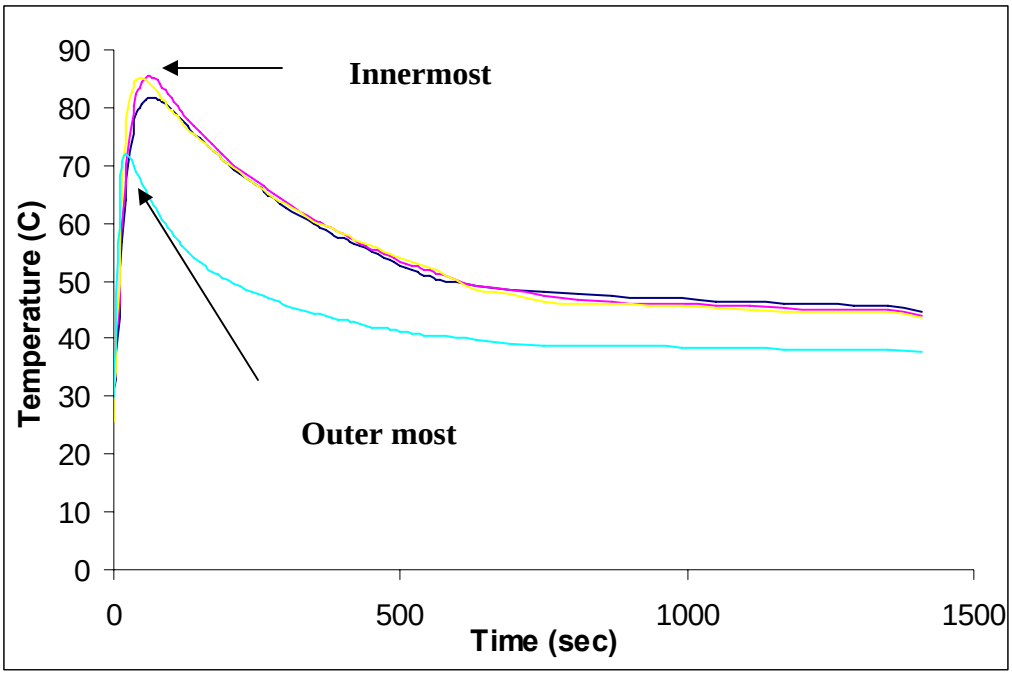


**Figure 0-15 Temperature and Pressure profiles during the filling of the ANG tank.**

# TABLES

**Table 0-1 Pore volume and methane uptake capacity of carbons prepared with varying KOH: C value.**

| KOH/Char | Micropore Volume cc/g | Mesopore volume cc/g | Total pore Volume cc/g | Piece Density g/cc | Methane uptake V/V | Methane Deliverable V/V |
|---|---|---|---|---|---|---|
| 1.5 | 3.38E-01 | 0.21 | 0.55 | 0.74 | 135 | 121 |
| 2 | 4.90E-01 | 0.19 | 0.68 | 0.69 | 128 | 116 |
| 2.5 | 1.10E+00 | 0.38 | 1.48 | 0.62 | **173** | **156** |
| 3 | 1.16E+00 | 0.66 | 1.82 | 0.47 | 159 | 146 |
| 4 | 5.14E-01 | 1.68 | 1.98 | 0.37 | 96 | 89 |
| 5 | 1.52E-01 | 1.86 | 2.01 | 0.33 | 85 | 78 |

**Table 0-2 Pore volume and methane uptake capacity of carbons prepared at different HTT.**

| HTT ˚C | BET Surface Area $M^2/g$ | Micropore Volume cc/g | Mesopore Volume cc/g | Total Pore Volume cc/g | Piece Density | Methane Uptake Value V/V | Methane Deliverable Value |
|---|---|---|---|---|---|---|---|
| 700 | 1988 | 8.19E-01 | 0.31 | 1.14 | 0.6 | 156 | 142 |
| 750 | 3175 | 1.29E+00 | 0.49 | 1.78 | 0.58 | 156 | 143 |
| 800 | 2997 | 1.16E+00 | 0.66 | 1.82 | 0.47 | 159 | 144 |
| 850 | 3421 | 3.39E-01 | 1.82 | 2.16 | 0.4 | 140 | 128 |
| 900 | 2932 | 5.00E-02 | 1.8 | 1.85 | 0.35 | **139** | **128** |

**Table 0-3 Characterization and methane uptake capacity of carbon obtained from pure saran.**

| Carbon Sample | HTT | BET Surface Area | Micropore Volume | Mesopore Volume | Total Pore Volume | Paticle Density | Methane Uptake Value | Methane Deliverable Value |
|---|---|---|---|---|---|---|---|---|
| | ˚C | $m^2/g$ | cc/g | cc/g | cc/g | g/cc | V/V | V/V |
| Made from Saran | 750 | 784 | 2.56E-01 | 0.124 | 0.38 | 0.35 | 97 | 80 |

**Table 0-4 Effect of binder concentration on compressive strength and density of monolith.**

| % Saran | Temperature | Pressure | Compressive Strength at 30% strain | Density | Methane Uptake | Methane Uptake |
|---|---|---|---|---|---|---|
| | C | Psi | psi | g/cc | g/g | V/V |
| 0 | 170 | 15000 | 0 | 0.27 | 0.21 | 87 |
| 5 | 170 | 15000 | 0 | 0.27 | 0.203 | 81 |
| 10 | 170 | 15000 | 93 | 0.4 | 0.2 | 126 |
| 20 | 170 | 15000 | 263 | 0.45 | 0.196 | 140 |
| 30 | 170 | 15000 | 400 | 0.61 | 0.19 | 176 |
| 40 | 170 | 15000 | 450 | 0.67 | 0.185 | 130 |
| 50 | 170 | 15000 | 460 | 0.69 | 0.18 | 126 |

**Table 0-5 Characterization and methane uptake capacity of carbon obtained from corn cobs using recycled KOH.**

| HTT ˚C | BET Surface Area $M^2/g$ | Micropore Volume cc/g | Mesopore Volume Cc/g | Total Pore Volume cc/g | Piece Density | Methane Uptake Value V/V | Methane Deliverable Value |
|---|---|---|---|---|---|---|---|
| 790 | 2429 | 0.91 | 0.445 | 1.355 | | 143 | 130 |

# REFERENCES

[35] R.J. Remick and A.J. Tiller, Advanced methods for low-pressure storage of CNG, in *Proc. of Symposium on Nonpetroleum Vehicular Fuels V* (CNG Fuel, Arlington, 1985), pp. 105–119.

[36] D. Elliot and T. Topaloglu, The development of new adsorbent materials for the storage of natural gas on-board vehicles, in *Conf. Proc. of Gaseous Fuels for Transportation I* (Vancouver, 1986), pp. 489–504.

[37] J. Wegrzyn, H. Wisemann, and T. Lee, Low pressure storage of natural gas on activated carbon, in *SAE Proc. of Annual Automotive Technology Development* (1992), pp. 1–11.

[38] C. Komodromos, S. Pearson, and A. Grint, The potential of adsorbed natural gas (ANG) for advanced on-board storage in natural gas-fuelled vehicles, in *Intl. Gas Research Conf. Proc* (1992), pp. 1917–1926.

[39] P.D. Rolniak and R. Kobayashi., Adsorption of methane and several mixtures and carbon dioxide at elevated pressures and near ambient temperatures on 5A and 13X molecular sieves by tracer perturbation chromatography, AIChE J. **26**(4), 616–625 (1980).

[40] T. Ding, S. Ozawa, T. Yamazaki, I. Watanuki, and Y. Ogino, A Generalized treatment of adsorption of methane onto various zeolites, Langmuir **4**(2), 392–396 (1988).

[41] S.Y. Zhang, O. Talu, and D.T. Hayhurst, High-pressure adsorption of methane in NaX, MgX, CaX, SrX, and BaX, J. Phys. Chem. **95**, 1722–1726 (1991).

[42] 27. O. Talu, S.Y. Zhang, and D.T. Hayhurst, Effect of cations on methane adsorption by NaY, MgY, CaY, SrY, and BaY zeolites, J. Phys. Chem. **97**, 12894–12898 (1993).

[43] J.J. Haydel and R. Kobayashi, Adsorption equilibria in the methane-propane—Silica gel system at high pressures, I & EC Fundamentals **6**(4), 546–554 (1967).

[44] S.C. Ventura, G.P. Hum, and S.C. Narang, Novel strategies for the synthesis of methane adsorbents with controlled porosity and high surface area, GRI Final Report, (1992), p. 37.

[45] S. Komarneni, High Surface Area Silica Aerogels and Xerogels for Natural Gas Storage, U.S. Patent Pending

[46] A.L. Myers and E.D. Glandt, Adsorbed Natural Gas (ANG), Adsorption News, Quantachrome Corp. **4**(1), 3–4 (1993).

[47] J. Sun, T.A. Brady, M.J. Rood, M. Rostam-Abadi, and A.A. Lizzio, Adsorbed natural gas storage with activated carbon, ACS Preprints (Div. of Fuel Chem.), **41**(l), 246–250 (1996).

[48] R.A. Greinke, I.C. Lewis, and D.R. Ball, Process for producing high surface area activated carbon, U.S. Patent 5,102,855, 1992.

[49] I.C. Lewis, R.A. Greinke, and S.L. Strong, Active carbons for natural gas storage, in *Proc. 21st Biennial Conference on Carbon* (1993), Vol. 21, pp. 490–491.

[50] Andersons, "Analysis & Use of Corn cobs" 1970.

[51] Shah P S. Suppes, G J., Pfeifer P, "Nanoporous carbon from corn cobs using Chemical Activation Process", Carbon, 2006 (In Press)

[52] Atlanta Gas Light Adsorbent Research Group, “Low pressure adsorbent natural gas vehicle demonstration—Final Report.” Report to Brookhaven National Laboratory (1997).

# CHAPTER 4

# 4. SOYBEAN OIL AS BINDER FOR MAKING NANOPOROUS CARBON MONOLITHS FOR ADSORBED NATURAL GAS APPLICATION

**This paper was submitted for publication to Journal of AOCS as: "Soybean Oil as Binder for Making Nanoporous Carbon Monoliths for Adsorbed Natural Gas Application",** **Galen J. Suppes[1], Parag S. Shah[1], and Peter Pfeifer[2]**

**[1] Department of Chemical Engineering, W2028 Engineering Bldg. East, University of Missouri, Columbia, MO 65211**

**[2] Department of Physics, University of Missouri, Columbia, MO 65211**

## ABSTRACT

Soybean oil mixed with one or two olefins and a lewis acid catalyst was used as binder to form soybean oil and nanoporous carbon composites or monoliths. Experiments were carried out to find the optimum concentration of olefin comonomer and catalyst to be added to the soybean oil to get optimum monolith quality in terms of strength and methane uptake capacity. Monoliths with compressive strengths and methane uptake capacity close to those made with polymeric polyvinlylidiene chloride and polyvinyl chloride copolymer as binder were obtained.

## 4.1 INTRODUCTION

Previously researchers have used polyvinylidene chloride (PVDC) as binder for making adsorbents for adsorbed natural gas application.[53] [54] The main advantage of using polymeric polyvinylidene chloride as a binder for making monoliths of nanoporous carbon for storing natural gas is that PVDC itself can be converted to porous carbon by pyrolysis so it does not block the micropores in the carbon monolith and hence does not reduce its methane uptake capacity.[55] The carbon obtained from PVDC is highly microporous and has high surface area.[56] Hence it is advantageous to use PVDC as a binder for making carbon monoliths for methane storage, both to get high density of the monoliths and high microporosity in monolith because of no blocking of the pores by the binder. Also the glass transition temperature of PVDC is between 140 and 175˚C which helps to make carbon monoliths at moderate temperatures. Figure 4-1 shows the TGA of the PVDC powder. As seen from this TGA, the powder starts transition to glassy state as about 150˚C.

However, the primary disadvantage of using PVDC as binder for mass production of carbon monoliths for methane storage is that during the pyrolysis of PVDC a large amount of toxic hydrochloric (HCl) gas is released due to the breaking of the polymeric chains which is harmful to humans, the environment, and the materials of processing equipment. As seen from the TGA graph after 200˚C the decomposition of PVDC starts releasing large quantity of HCl gas which continues until all the chlorine is released.

Several researchers have demonstrated the use of soybean oil for making plastics[57] [58] and polymer[59] [60]; however no researcher has previously successfully used soybean oil as a binder for making shaped adsorbents for gas or liquid applications. In

this work soybean oil was successfully used as binder instead of PVDC for making carbon monoliths for natural gas storage. Soybean oil was first mixed with one or two comonomers which could be styerene, divinylbenzene or dicyclopentadiene and a catalyst to form a prepolymer. This prepolymer was then mixed with the varying amounts of carbon powder and then heated and pressed in a die to form a carbon monolith. The advantage of this approach is monoliths with same physical quality as made with PVDC can be obtained at less severe conditions of temperature and pressure and that soybean oil polymer that holds the carbon powder in the monolithic form can also be converted to porous carbon by pyrolysis. The monolith is formed without releasing the toxic halogen gases since there is a very small fraction of halide compounds used to form the polymer.

The carbon obtained from soybean oil is also porous and it does not block the micropores present in the carbon monolith. One of the probable disadvantage of soybean oil polymer as binder compared to PVDC is that carbon obtained from soybean oil polymer is not as microporous as the carbon obtained from PVDC which may slightly decrease the methane uptake capacity of the carbon monoliths. Nevertheless, carbon monoliths with methane uptake capacity greater than the targeted capacity of 150 V/V were obtained using soybean oil as binder.

## 4.2 EXPERIMENTAL PROCEDURE

Soybean oil was first mixed varying amounts divinyl benzene, dicyclopendaiene dimer and boron triflouride diethyl ether complex to form a prepolymer. This prepolymer was than mixed with carbon powder in different ratios. This mixture was then pressed in 3.5” stainless steel die at a force of 50-60 tons using the hydraulic press

from DAKE at temperature of 120˚C for 1hour. After one hour the carbon monolith was removed from the die and heated at 120˚C in an oven for 12-24 hours. After that the monolith was pyrolyzed in inert atmosphere up to 550˚C at a rate of 0.5˚C/min up to 400˚C and than 1.5˚C/min up to 550˚C. The temperature was held for 30 minutes at 550˚C and then the monolith was allowed to cool. The final monolith was checked for methane uptake capacity and for compressive strength.

Methane uptake measurements were made gravimetrically. The gravimetric measurements were made on 1g of carbon in a stainless steel chamber capable of holding 1000 psig pressure. A Denver Instruments M-220D balance was used that was capable of weighing as low as 10microgram. Provisions were made to include the buoyancy effects and the dead volume of the methane in the empty chamber volume during the calculations to give final methane uptake measurements. One gram of powdered carbon or broken pieces of carbon briquettes were first placed in the stainless steel chamber and the remaining empty space was filled with glass wool which prevented the loss of carbon powder during outgasing step that included heating the entire chamber to 140˚C under vacuum for 2hr. After 2 hours the outgased chamber was connected to methane source (99.9% pure methane from Prax Air) and pressurized at the required pressure and left for one hour to attain equilibrium. After 1 hr the chamber was disconnected from the methane source and weighed. In order to determine the deliverable methane capacity of the carbon the pressure from the carbon containing chamber was released and the weight of the chamber was noted to determine the methane uptake at atmospheric pressure. The difference between the methane uptake at 500psig and atmospheric pressure gave the deliverable methane capacity of the carbon.

The compressive strength of the monoliths was measured using the Sigma automated load test system from Geotac. The 2000 psig load cell was used and the strain rate was fixed at 30%/hr. The raw data were processed using the Sigma-1 UU Version 5.3.3 tester software.

## 4.3 RESULTS AND DISCUSSION

The final hardness and thermal stability of the polymer formed from soybean oil that holds the carbon powder as monolith depends on the amount of catalyst and amount of comonomer added to the soybean oil to form the prepolymer. It was found that the degree of cross linking in the thermoset polymer formed from soybean oil which ultimately affects the quality of the carbon monoliths, depend on the concentration of comonomer and the catalyst added to soybean oil to form the prepolymer mixture. Systematic parametric study was performed in order to determine the concentration of comonomer and catalyst to be added to the soybean oil which will give maximum cross linking in the final polymer. The degree of cross linking and hardness of the polymer were checked by dissolving the final polymers in the solvents such as tetrahydrofuran (THF) or methylene dichloride and the thermal stability and the final carbon yield checked using TGA.

### 4.3.1 EFFECT OF COMONOMER CONCENTRATION

A variety of thermosets were made by adding different amounts of two olefins to the soybean oil keeping the concentration of catalyst constant. The olefins added to soybean oil were divinyl benzene and dicyclopentadiene dimer and the catalyst used was benzene triflouro diethyl ether complex. The physical appearance and nature of the

thermoset polymer after the reaction and dissolving in tetrahydrofuran (THF) solvent were used to determine the extent of crosslinking and polymerization in the final polymer qualitatively. Also, thermal stability of the polymer and final carbon yield were checked using thermogravimetric analysis (TGA).

Table 4-1 shows the appearance and nature of the polymer made with varying amounts of dicyclopentadiene and divinyl benzene. As seen from the table, as the amount of dicyclopentadiene increases and the amount of divinyl benzene decreases simultaneously, the polymer becomes more soft and rubbery in nature. Also, the amount of polymer dissolved in THF increases as the amount of dicyclopentadiene increases and amount of divinylbenzene decreases indicating lower degrees of crosslinking in the polymer. Hence, it was concluded that the dicyclopentadiene was responsible for the rubbery and soft nature of the thermoset polymer while divinylbenzene leads to more crosslinking in the final thermoset polymer making it harder and more insoluble in THF.

Because the final application of the polymer required it to be harder and more crosslinked to make the carbon monoliths with higher compressive strength, only divinylbenzene was added as comonomer to the soybean oil and catalyst to form the prepolymer that worked as binder. Table 4-2 shows the appearance, nature and solubility in THF for the polymers made by adding different amounts of divinylbenzene to soybean oil. As seen from the table, when the amount of divinylbenzene in the soybean oil and catalyst mix is 30% the resulting polymer has the maximum hardness and minimum solubility in the THF showing the high degree of cross linking in the polymer. As the amount of divinylbenzene decreases the resulting polymer starts becoming softer and gel type indicating the lower degree of polymerization and lower crosslinking in the polymer.

Also, the blooming of the unpolymerized oil increased indicating lower extent of polymerization and lower stability in the THF.

To check the thermal stability of the thermosetting polymers obtained from soybean oil, thermogravimetric analysis was performed on the insoluble polymer obtained after dissolving the polymer obtained from soybean oil in THF. Figures 4-2 and 4-3 show the TGA curve of the two different polymers obtained with 30% and 10% of divinylbenzene as comonomer. As seen from the curves at temperature of 300˚C, both the polymers has retained about 90% of their mass indicating the stability of the polymeric chains. However, after 350˚C the rate of weight loss increases sharply indicating the breakage of the polymeric chains and degradation of the polymer. The degradation of the polymer continues until 450˚C after which the formation of carbon begins. It is believed that the higher carbon yield is due to higher crosslinking of the soybean oil molecules that prevents the loss of carbon molecules in the form of gases as in case of less crosslinked or shorter polymeric chains and hence lower carbon yields. As seen from Figures 4-2 and 4-3, the amount of carbon remained after degradation of the polymer made with 30% divinylbenzene is about 10% which is more than twice of what remained in case of polymer with 10% divinylbenzene.

Hence on the basis of the above mentioned observations divinylbenze was used as comonomer for making carbon composite monoliths with soybean oil and its concentration was fixed to 30% in the prepolymer mix that was added to carbon powder.

### 4.3.2 EFFECT OF CATALYST

Experiments were carried out to find the effect of catalyst which was boron triflouride diethyl ether complex on the hardness and the thermal stability of the polymer

obtained from soybean oil. Table 4-3 shows the same information as Table 4-1 but for polymers made with fixed amount of divinylbenzene and different amount of catalyst. The catalyst ranging from 5% to 0.5% were added to polymer mixture. As seen from the table there was not much effect of the catalyst loading on the final hardness and solubility of the final polymer up to 1% loading. Below 1% loading i.e. at 0.5% loading the polymer started becoming very soft and tacky and large amount of the polymer was lost in the THF dissolution, indicating the higher amount of unpolymerized soybean oil in the polymer. Hence catalyst amounts between 1 and 5% were found to be favorable to get desirable degree of crosslinking of the final polymer.

### 4.3.3 EFFECT OF % OF SBO PREPOLYMER in MONOLITH

Once the amount of monomers and catalyst to be added to soybean oil and the proper reaction temperature were determined, soybean oil mixture was used as a binder to form carbon monoliths out of carbon powder. In this process the amount or the concentration of the soybean oil binder in the monolith is important for the final methane uptake capacity, physical strength and density of the monolith. Carbon monoliths were made from carbon powder with soybean oil binder concentration varying from 25% to 70%. Table 4-4 summarizes the results of this experiment.

Table 4-4 compares the methane uptake capacity, compression strength and density of the carbon monoliths made with different soybean oil polymer concentration. As seen from the table as the amount of soybean oil prepolymer is increased the compressive strength of the monolith decreases. The monolith with 70% of binder has the maximum compressive strength and the one with 25% of binder has the lowest compressive strength. However the methane uptake capacity of the monoliths is

inversely proportional to the amount of binder concentration. The methane uptake capacity of monolith made with 30% of binder has more methane uptake capacity than the one with 70% binder monolith made with same type of carbon. The primary reason for this is that carbon formed from soybean oil polymeric binder after pyrolysis is not as porous as the nanoporous carbon itself.

Table 4-5 shows the characterization of the carbon obtained from pyrolysis of the soybean oil polymer. Because the carbon is not very porous it blinds and blocks the nanopores present in the carbon powder which are necessary for higher methane uptake capacity. More binder apparently blinds more micropores and leaves more less porous carbon in the monolith. Combined, these greatly decrease the methane uptake capacity of the carbon monolith.

### 4.3.4 COMPARISON BETWEEN SARAN AND SOYBEAN OIL BINDERS

Comparison was made between the mechanical properties and methane uptake capacities of the carbon monoliths obtained using saran and soybean oil binders. Table 4-4 shows the comparison of the properties of the monoliths made using saran and soybean oil binders. The mechanical properties of the monoliths made with same concentrations of each binder are very similar. The compressive strength of the monoliths are 410 and 380 psi which show that both the binders give monoliths with almost similar compressive strengths saran giving slightly better strength than soybean oil. Table 4-6 shows the comparison of methane uptake values, which shows that the methane uptake capacity is reduced slightly by replacing saran by soybean oil based binder. The monolith made with saran binder had the uptake capacity of 167V/V while

that made with soybean oil had capacity of 156 V/V. Table 4-5 also shows the characterization of the carbons obtained by pyrolysis of the saran and soybean oil polymer. As seen from the table, the carbon obtained from saran is comparatively more porous with higher surface area and micropore volume of 850$m^2$/g and 0.26cc/g respectively than 300$m^2$/g and 0.08g/cc for carbon obtained from soybean oil polymer. Figures 4-1 and 4-2 show the TGA curves of the saran and soybean oil polymer. Both this materials are pyrolyzed up to 650˚C at 1.5˚C/min. As seen from the TGA curves, after pyrolysis the total yield of carbon is 20-25% for saran while it is 10-15% for soybean oil polymer. Carbon from soybean oil contributes to a lower fraction of the carbon in the monolith when applied at the same rates as saran.

After pyrolysis of the monolith and in case of saran binder, 3.4% of micropore volume and 6.2% carbon volume is added to the original micropore and carbon fraction of the powder that is converted to monolith. For soybean oil binder, the contributions are 5.4%and 1.2% respectively. Hence even though less carbon (which blinds the important existing micropores) is added to the monolith volume in case of soybean oil, higher percentage of micropore volume (which is favorable for higher methane uptake capacity) is added in case of saran.

Figures 4-4 and 4-5 show the volume distribution in a monolith made from carbon obtained entirely from pyrolysis of saran and soybean oil polymer respectively. The micropore volume is higher in case of saran carbon (30%) than carbon obtained from soybean oil polymer (16.5%). Figure 4-6 and 4-7 show respectively the volume distribution in two monoliths made from same type of carbon but with soybean oil and saran binder each. The difference in the micropore volume and carbon volume fraction

in two monoliths is less as compared to this difference in case of Figure 4-4. Hence, using soybean oil as binder instead of saran decreases the methane uptake capacity on the monolith by approximately 10% even though carbon obtained from soybean oil pyrolysis is not as porous as that obtained from saran

Other than the methane uptake capacity, the other monolith properties such as density and compressive strengths are very similar for monoliths made using saran and soybean oil binder. However, there are other process advantages and hence economic advantages associated with using soybean oil as binder over saran. The process condition for making monoliths using soybean oil is less time and temperature intensive than using saran. The temperature for making monolith using soybean oil binder is 120˚C while for saran the temperature required is 175˚C. Also the pressing time for soybean oil based monoliths is less than PVDC based monoliths by 45 minutes (refer Table 4-6). This is primarily because the mechanisms by which both binders work are different. In case of PVDC binder at 175˚C the PVDC polymer reaches its glass transition temperature and transforms to a glassy state and while in its glassy state binds the carbon powder together. While in case of soybean oil polymer the soybean oil prepolymer added to the carbon powder as binder starts polymerizing at the temperature of 110˚C and during the process of polymerization binds the carbon powder along with the soybean oil chains. After about 1hr, hard carbon filled thermosetting polymer is obtained.

## 4.4 CONCLUSION

Soybean oil was successfully demonstrated as a binder for making carbon monolith. The compressive strengths of the monoliths made with soybean oil were close

to the monoliths made using saran as binder. The methane uptake capacities of the monoliths made with soybean oil were about 5% less than that made with saran, primarily due to a lower fraction of micropores in the carbon derived from soybean oil polymer than the carbon derived from saran. When considering the environmental, safety, and processing advantages of using soybean oil as binder justifies its use. The amount of divinyl benzene added as co monomer and amount of catalyst added to the soybean oil prepolymer significantly affects the final strength of the monoliths.

# TABLES

**Table 4-1 Effect of varying dicylopendatiene and divinylbenzene amounts on the final polymer.**

| SBO G | Dicyclo-pentadiene G | Divinyl-benzene G | Boron Trifluoride G | Appearance & State | Wt. Before Solvent Wash g | Wt. After Solvent Wash g | Amt lost in washing g |
|---|---|---|---|---|---|---|---|
| 6.506 | 0 | 3.011 | 0.5 | Hard | 9.61 | 6.51 | 2.57 |
| 6.501 | 0.501 | 2.501 | 0.505 | Very Hard | 10.07 | 6.99 | 2.08 |
| 6.501 | 1.003 | 2.008 | 0.507 | Hard | 9.64 | 5.9 | 3.08 |
| 6.501 | 1.5 | 1.503 | 0.502 | Hard | 9.73 | 6.27 | 3.46 |
| 6.5 | 2.003 | 1.002 | 0.516 | Hard | 9.75 | 6.1 | 3.65 |
| 6.501 | 2.5 | 0.5 | 0.508 | Soft & Rubbery | 9.61 | 7.04 | 3.74 |
| 6.5 | 3 | 0 | 0.509 | Very Soft & Rubbery | 9.27 | 7.23 | 3.75 |

**Table 4-2 Effect of divinyl benzene amount on final polymer properties.**

| SBO g | Dicyclo-pentadiene g | Divinyl-benzene G | Boron Trifluoride G | Appearance & State | Wt. Before Solvent Wash G | Wt. After Solvent Wash g | Amt lost in washing g |
|---|---|---|---|---|---|---|---|
| 7.002 | 0 | 3.004 | 0.515g | Very Hard | 9.65 | 6.02 | 1.07 |
| 7.5 | 0 | 2.51 | 0.523g | Hard | 9.68 | 6.2 | 1.72 |
| 8.019 | 0 | 2.01 | 0.522g | Soft | 9.79 | 6.32 | 3.47 |
| 8.507 | 0 | 1.506 | 0.504g | Soft | 9.25 | 7.53 | 3.48 |
| 9 | 0 | 1.007 | 0.502g | Soft & Rubbery | 9.51 | 8.44 | 3.63 |
| 9.504 | 0 | 0.505 | 0.532g | Very Soft | 10.55 | 5.78 | 4.77 |

**Table 4-3 Effect of Catalyst of Final Polymer Properties.**

| SBO | Dicyclo-pentadiene | Divinylbenzene | Boron Trifluoride | Appearance & State | Weight Before Solvent Wash | Weight After Solvent Wash | Amt lost in washing |
|---|---|---|---|---|---|---|---|
| g | g | g | g | | g | g | g |
| 6.507 | 0 | 3.012 | 0.52 | Very Hard | 9.65 | 6.13 | 2.81 |
| 6.504 | 0 | 3.008 | 0.42 | Very Hard | 9.59 | 6.52 | 3.07 |
| 6.505 | 0 | 3 | 0.3 | Very Hard | 9.65 | 6.84 | 3.52 |
| 6.503 | 0 | 3.018 | 0.2 | Hard | 10.18 | 6.93 | 3.25 |
| 6.506 | 0 | 3.005 | 0.1 | Hard | 9.98 | 6.16 | 3.82 |
| 6.505 | 0 | 3.001 | 0.05 | Soft | 10.28 | 4.37 | 5.91 |

**Table 4-4 Effect of amount SBO prepolymer on the final monolith properties .**

| % Binder | Temperature | Pressure | Time of Curing | Compressive Strength | Density | Methane Uptake | Methane Uptake |
|---|---|---|---|---|---|---|---|
| | C | Psi | Hr | Psi | g/cc | g/g | V/V |
| 70 | 120 | 15000 | 24 | 415 | 0.68 | 0.12 | 126 |
| 65 | 120 | 15000 | 24 | 411 | 0.67 | 0.125 | 128 |
| 60 | 120 | 15000 | 24 | 410 | 0.66 | 0.128 | 129 |
| 45 | 120 | 15000 | 24 | 389 | 0.65 | 0.145 | 144 |
| 40 | 120 | 15000 | 24 | 380 | 0.65 | 0.148 | 147 |
| 30 | 120 | 15000 | 24 | 380 | 0.65 | 0.155 | 154 |
| 25 | 120 | 15000 | 24 | 150 | 0.45 | NA | NA |

**Table 4-5** Characterization of PVDC and SBO polymer carbon. Comparison between monoliths made with PVDC and SBO polymer.

| Binder | SA | Micropore Volume Cc/g | Mesopore Volume Cc/g | Total pore Volume cc/g | Density of Carbon g/cc | % yield of Carbon |
|---|---|---|---|---|---|---|
| SBO | 300 | 0.08 | 0.04 | 0.12 | 0.455 | 5-10 |
| Saran | 783 | 0.256 | 0.126 | 0.382 | 0.35 | 18-20 |

**Table 4-6** Comparison between monoliths made with PVDC and SBO polymer.

| Binder | Methane Uptake V/V | Methane Uptake gm/l | Monolith Density g/cc | Amount needed (%) | Temp C | Compressive Strength Psi | Duration Min |
|---|---|---|---|---|---|---|---|
| SBO | 156 | 102 | 0.68 | 30% | 110 | 380 | 30-60 |
| Saran | 167 | 110 | 0.65 | 33% | 175 | 410 | 120 |

# FIGURES

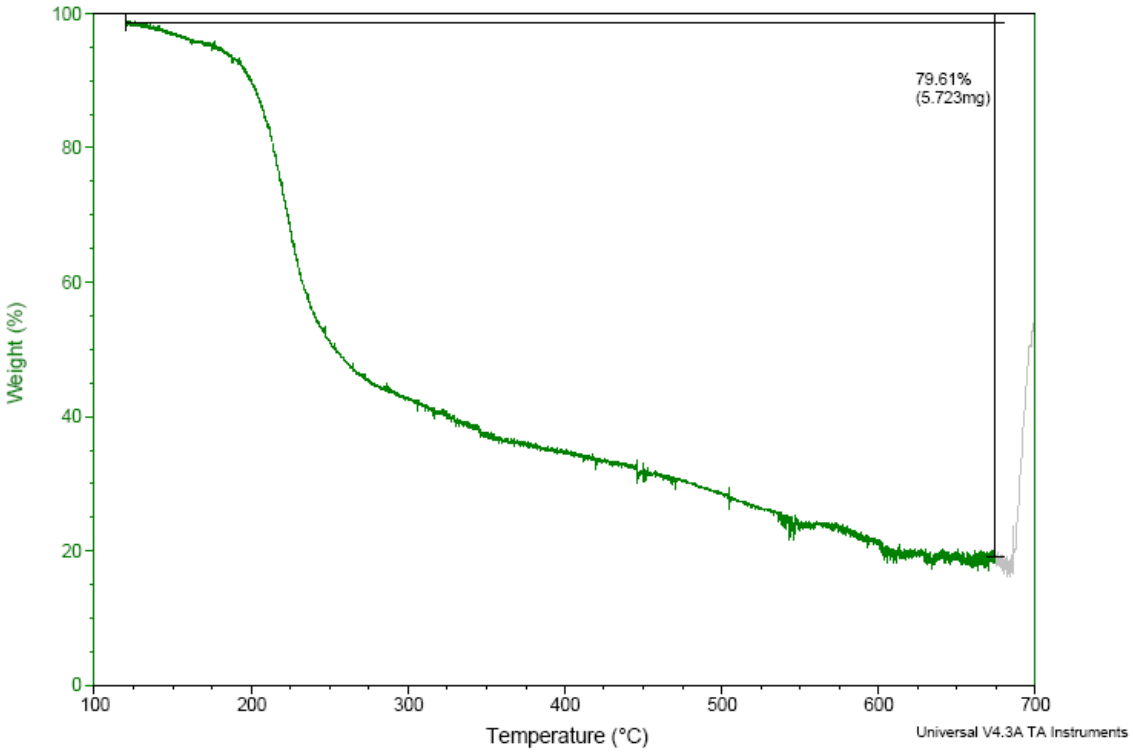


**Figure 4-1 TGA of Saran (PVDC and PVC copolymer).**

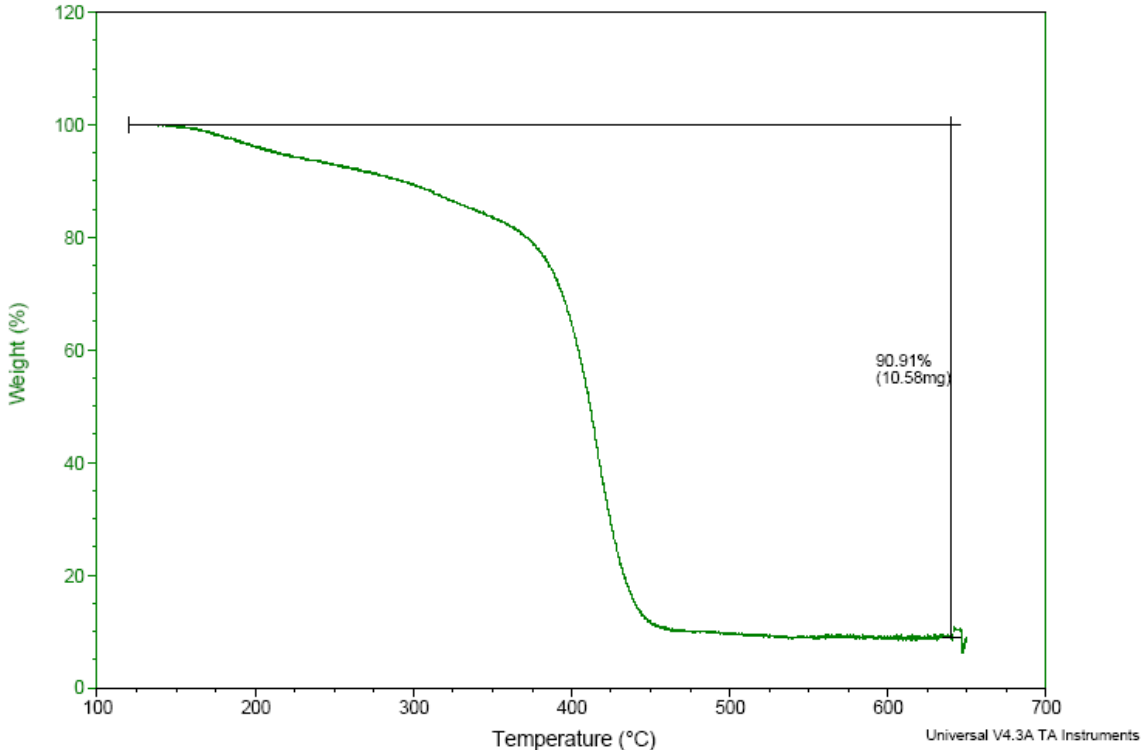


**Figure 4-2 TGA of SBO polymer with 30% divinylbenzene.**

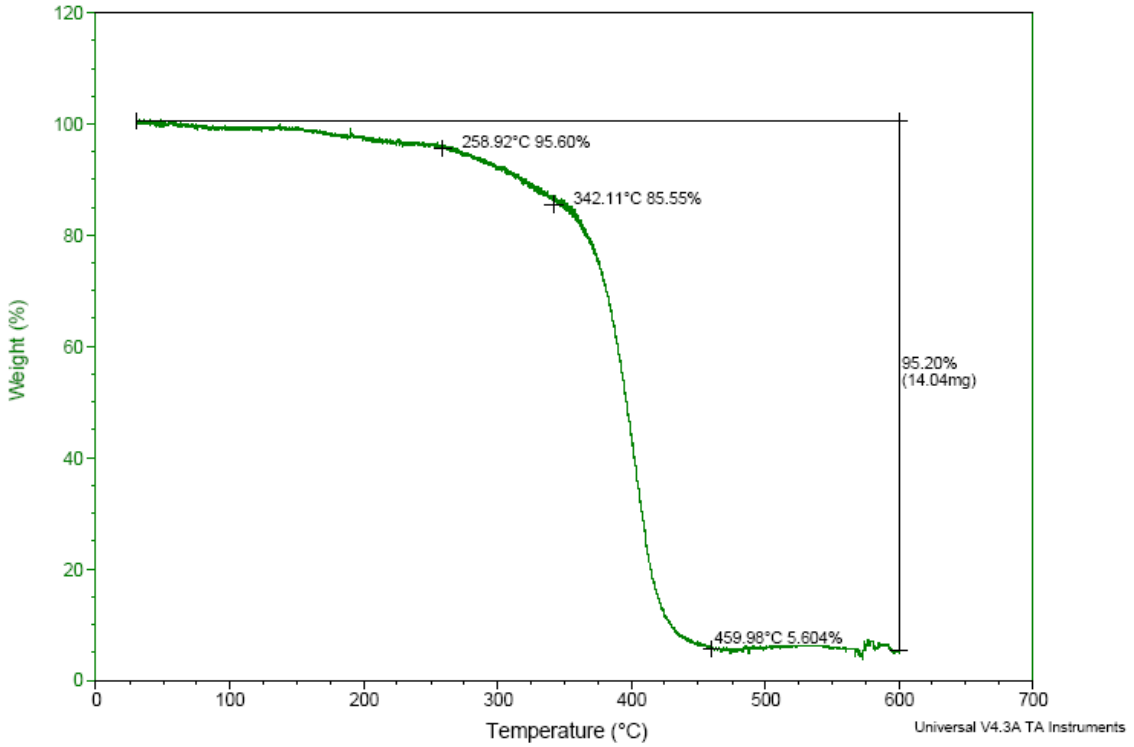

**Figure 4-3 TGA of SBO Polymer with 10% divinylbenzene and 30% dicyclopentadiene.**

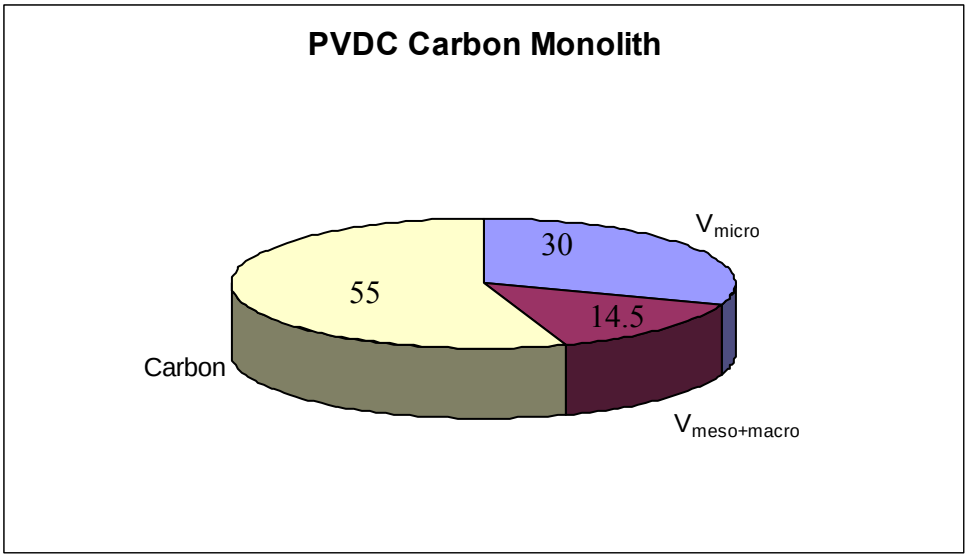


**Figure 4-4** Volume Distribution in Monoliths made with carbon obtained from PVDC.

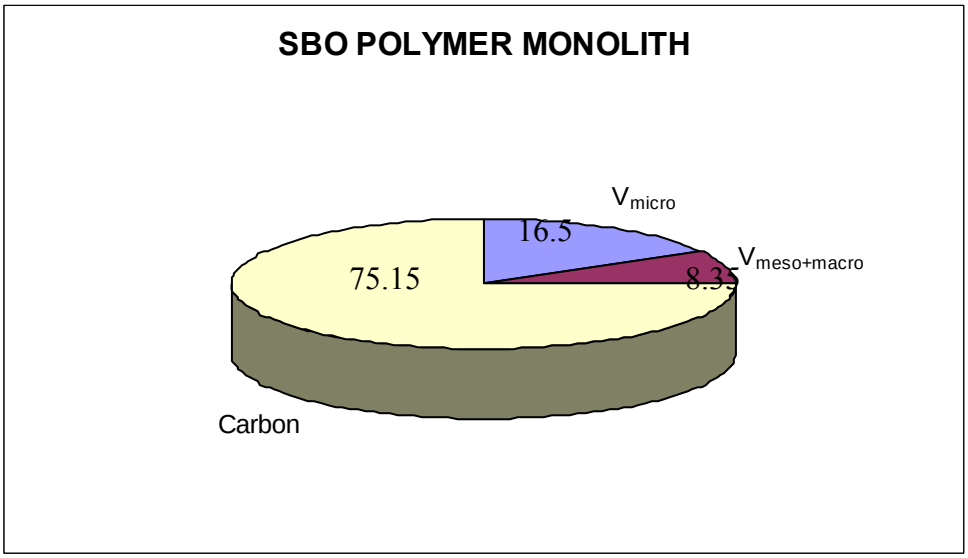


**Figure 4-5** Volume Distribution in Monolith made with carbon obtained from SBO polymer.

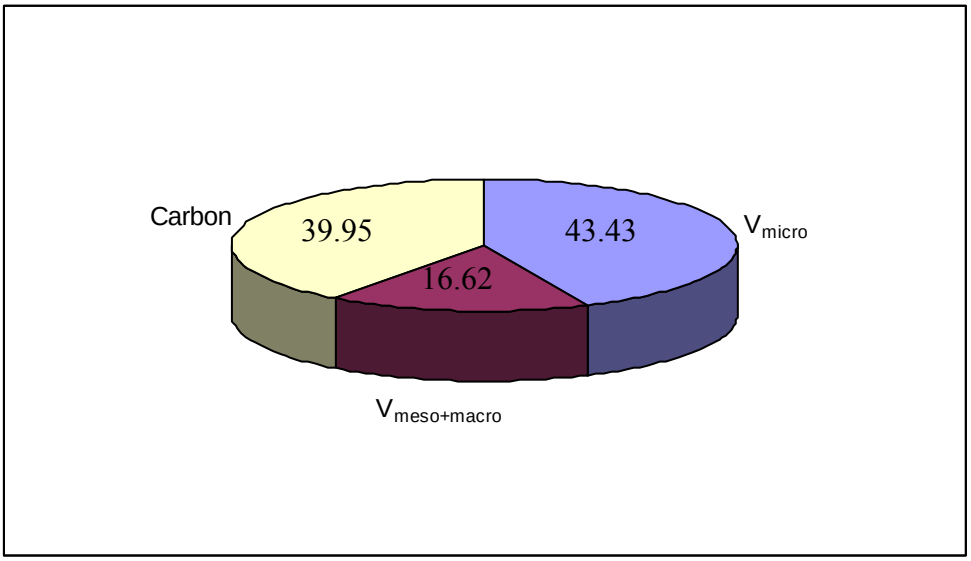


**Figure 4-6** Volume Distribution in Carbon monoliths made using SBO as binders.

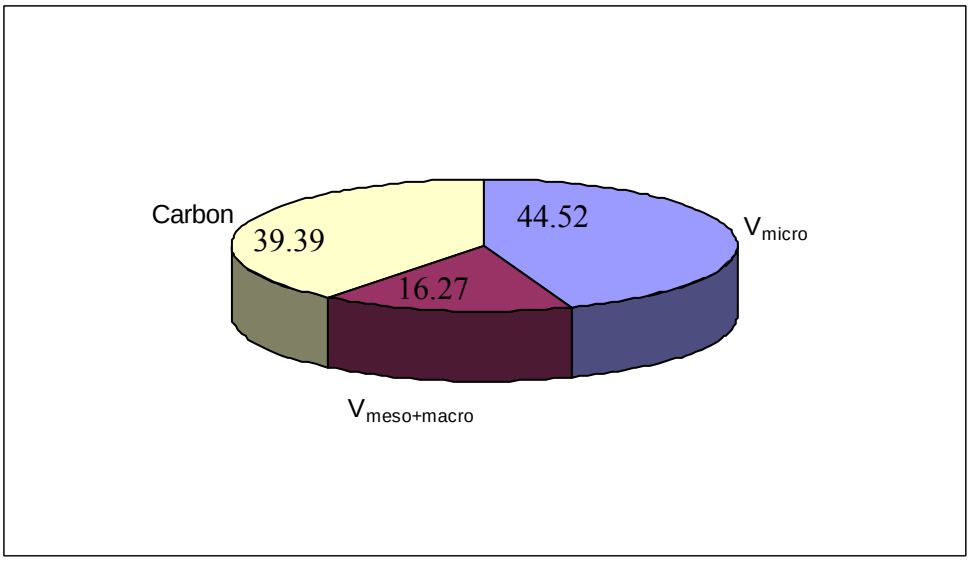


**Figure 4-7** Volume Distribution in Carbon monoliths made using PVDC as binders.

## REFERENCE

[53] "Microporous carbons as adsorbents for methane storage", D. F. Quinn, J. A. MacDonald, *ACS*, **39(2**) 451-455 (1994)

[54] D.F. Quinn and J.A. Holland, Carbonaceous material with high micropore volume and low macropore volume and process for producing same, U.S. Patent 5,071,820, 1991.

[55] S.S. Barton, J.R. Dacey, and D.F. Quinn, High pressure adsorption of methane on porous carbons, *Fundamentals of Adsorption,* in *Proc. 1st Eng. Foundation Conference* (1983), pp. 65–75.

[56] V.C. Menon and S. Komarneni, "Porous adsorbents for vehicular natural gas storage—a review." *J.Porous Mater*. **5**, 43-58 (1998).

[57] Herman Aage Enemark, "The Making of Plastics from Soybean Oil," Iowa State College, P. 18, 19, 29, 30, (1935).

[58] F.D. Gunstone,"Nonfood Uses of Vegetable Oils and Their Fatty Acids," Industrial Uses Of Soy Oil For Tomorrow, P. 17-31 (1995).

[59] Robert W. Johnson, "Polymerization of Fatty Acids," Fatty Acids in Industry, pp. 153-175 (1989).

[60] Printing Ink and Coating Technical Advisory Panels, Chicago, IL, "Preparation of New Oils and Polymers from Soybean Oil," Richard C. Larock, Sep. 15, 1997 and Sep. 16, 1997.

# CHAPTER 5

# 5 NANOPOROUS CARBON FROM CORN COBS FOR CATALYST SUPPORT APPLICATION

## 5.1 INTRODUCTION

Catalytic processes are of tremendous importance in modern industrialized society. Altogether, they account for as much as 90% of the chemical manufacturing processes in use throughout the world.[61] Many of these catalysts consist of metals or metal compounds supported on an appropriate support, the basic role of which is to maintain the catalytically active phase in a highly dispersed state. The most important characteristic of any industrial catalyst is the chemical composition, but other factors such as surface area, stability and mechanical properties are also important. There are several advantages to use a catalytically active metal dispersed on some kind of support as a catalyst: the active phase can be highly dispersed spreading the catalyst on a support. In the case of metal catalysts, preferably a large active surface is produced per unit weight of metal used. On the other hand, a supported catalyst provides for flow of gases through the reactor and then diffusion of reactants through the pores of the active phase; the support can also improve dissipation of reaction heat, retard the sintering of the active phase and increase the poison resistance.

The selection of support is based on a series of desirable characteristics[62 63]:

1. Interness.
2. Stability under reaction and regeneration conditions.
3. Mechanical properties.
4. Physical form
5. Surface area
6. Porosity.

Of a wide range of possible useful materials that can be used as catalyst supports, in practice only three combine the above characteristics in an optimum way and account for most industrial uses: alumina,[64] silica and activated carbon. The combination of useful properties of aluminas makes them generally the first choice for catalyst supports although under some specific experimental conditions silica is to be preferred.[65]

**CARBON SUPPORTS**

Today, carbon occupies only a relatively small portion of the catalyst support market (although the proportion of carbon-supported catalysts is rapidly growing in the brochures of catalyst manufacturers); it's potential has not yet been fully exploited. Thus, although the use of carbon presents some specific problems, there are characteristics of carbon that are very valuable and not attainable with any other support.

The carbon surface has a unique character, offering unparalleled flexibility for tailoring catalyst properties to specific needs. This flexibility arises from a porous structure which determines its adsorption capacity, a chemical structure which influences its interaction with polar and non-polar molecules and a number of active sites (in the form of edges, dislocations, etc.) which determine the chemical reactions of its surface

with heteroatoms. Some of the clear advantages of carbon as support may be summarized as follows[66]:

- Carbon is resistant to acidic or basic media, which other supports are not. This means for highly acidic or basic medium reactions, carbon supported catalyst can offer advantages.
- The carbon structure is stable at very high temperatures. Thus, whereas the cavities in zeolites collapse if heated much above 1000 K, some carbon sieves are stable up to 1700 K. The high-temperature stability of carbon minimizes sintering of the active phase on the surface of the support.
- The pore structure of a carbon support may be tailored to obtain the pore-size distribution needed for each practical application by appropriate selection of precursor and activation method. Further, the support may be prepared with different physical forms from powder to pellets, making carbon-supported catalysts useful for both fixed and fluidized beds.
- Carbons can be produced with ion-exchange properties to increase the precursor adsorption and to increase the dispersion of the active phase.
- From a practical point of view, an advantage of carbon is that expensive catalytic metals are readily recoverable from spent catalysts by burning away the carbon support.
- Finally, carbon can be prepared at low cost as compared to traditional oxide supports such as alumina, silica or zeolites.

The metals most commonly supported on carbon are those of Groups 8-11 of the Periodic System (Fe, Co, Ni and Cu Groups), although the largest volume corresponds to

Pt, Pd, Rh, Ru and Ir. In this project the highly activated carbon obtained from corn cobs was used to support Cu and Cr metals to form a bimetallic Cu and Cr catalyst. These catalysts were used to catalyze the hydrogenation reaction of glycerin to form acetol and propylene glycol. Comparisons were made for the activity and productivity of the carbon supported metal catalyst and the conventional copper chromite catalyst supported on alumina. An increase in activity up to 10 times was observed in case of carbon supported catalyst.

## 5.2 EXPERIMENTAL PROCEDURE

### 5.2.1 CATALYST PREPARATION

The bimetallic copper and chromium catalyst supported on nanoporous carbon obtained from corn cobs were prepared using incipient wet impregnation method. 20g of carbon with surface area in excess of 3000$m^2$/g and pore volume greater than 1.5cc/g was soaked in 2M solution of copper nitrate solution for 60mins. After that the excess of liquid was removed, the carbon containing adsorbed copper metal was heat treated at 110˚C for 2 hrs, then at 300˚C for 1 hr, and finally at 400˚C for 1 hr. The copper containing carbon was than dipped in 3M solution of chromium nitrite pentahydrate for 1hr. After 1hr the excess of liquid was removed and the carbon was heat treated at different temperatures to give final bimetallic Cu and Cr catalysts. Different concentrations of dipping solutions were used to control the loading the metals on the carbon support.

## 5.2.2 CATALYST TESTING

Once the catalysts with different loading of metal were prepared, they were evaluated as catalyst to convert glycerin to propylene glycol. All the reactions were carried out in a plug flow reactor of 40 $cm^3$ capacity equipped with thermocouples at the entry and exit of the reactor (see Figure 5-1). The reactor was packed with different amounts of catalyst. The temperature of the reactor was controlled using camile TG data acquisition system at 220ºC. The reactor was purged continuously with hydrogen and heated at the desired temperature. The reactant which is glycerol was heated in a separate glass flask at 220-230ºC and the glycerol vapors were fed to the reactor at controlled rate. The reaction was carried out at atmospheric pressure. The vapors coming out of the reactor were cooled in a condensing copper coil and the condensate was collected and analyzed.

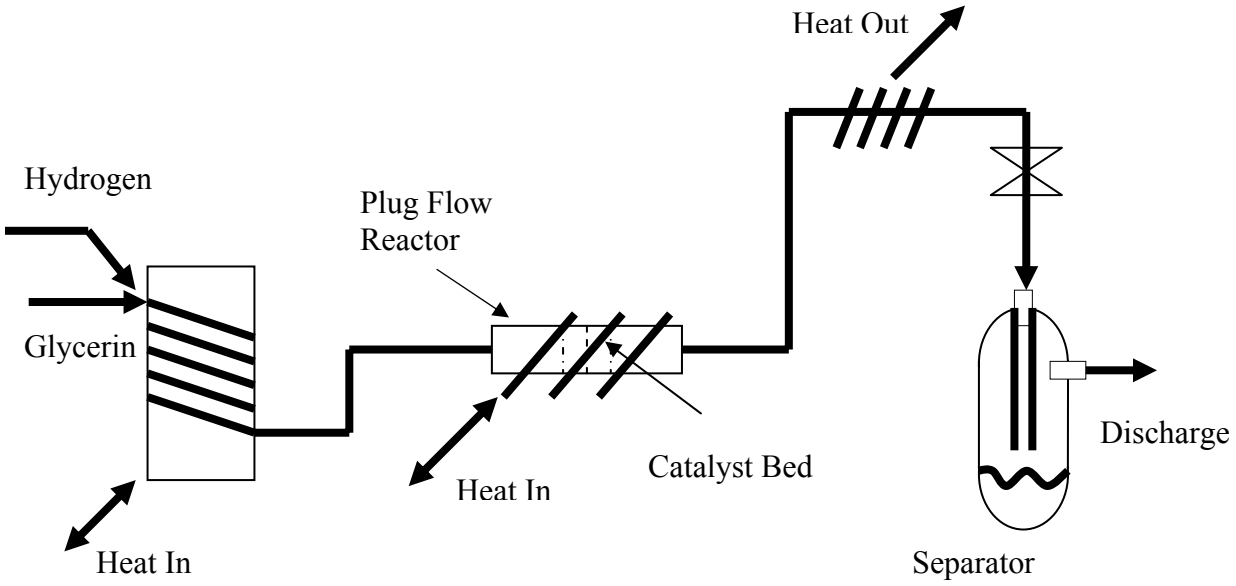


**Figure 5-1 Schematic diagram of experimental setup to test catalyst**

### 5.2.3 PRODUCT ANALYSIS

The samples of each reaction were taken at 10 minute intervals. These samples were analyzed with a Hewlett-Packard 6890 (Wilmington, DE) gas chromatograph equipped with a flame ionization detector. Hewlett-Packard Chemstation software was used to collect and analyze the data. A Restek Corp. (Bellefonte, PA) MXT® WAX 70694 GC column (30 m × 250 μm × 0.5 μm) was used for separation. A solution of *n*-butanol with a known amount of internal standard was prepared a priori and used for analysis. The samples were prepared for analysis by adding 100 μL of product sample to 1000 μL of stock solution into a 2mL glass vial. Using the standard calibration curves that were prepared for all the components, the integrated areas were converted to weight percentages for each component present in the sample.

## 5.3 RESULTS AND DISCUSSION

The carbonization scheme to produce nanoporous carbon from corn cobs discussed in our previous publication[67] produces carbon matrix crisscrossed by a nearly space-filling 2.9 dimensional fractal network of uniform channels[68] as shown in Figure 5-2. The high fractal dimension of 2.9 of the network gives high porosity and high connectivity, enabling rapid liquid and gas transport in and out when used as catalyst support.

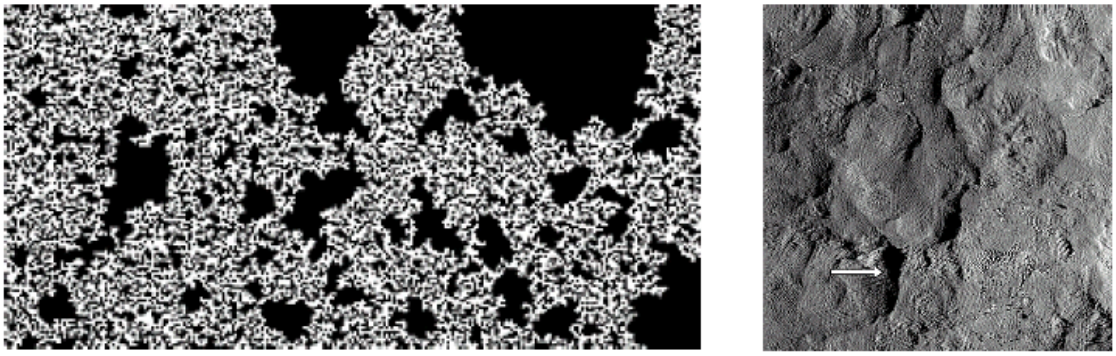

**Figure 5-2: *Left:* 2.9-dimensional network of channels created by oxidative removal of carbon by chemical invasion (simulation; invasion from left to right). *Right*: Channel entrances (black areas) in a scanning tunneling micrograph[69]. The entrance marked with an arrow is 11.4 nm wide at that location.**

Table 5-1 shows data on the conversion of glycerin to propylene glycol using carbon supported copper chromite catalyst in powder form carried out in plug flow reactor. It also shows the comparison between the conversions and productivities for the conventional copper chromite catalyst (no support) and the copper chromite catalyst supported on activated carbon. The reaction is carried out at 220˚C and the hydrogen to glycerin mole ratio is about 20:1. Catalyst 1 and catalyst 2 are catalysts supported on highly porous carbon obtained from corn cobs with different metal loading. As seen from the table, the productivity (which is the measure of the activity of the catalyst) for the copper chromite catalyst supported on carbon (0.9-1.2) is about 8-9 times the productivity for the commercial copper chromite catalyst supported on alumina (0.16). This is attributed to the higher surface area of the carbon support at 3100 m2/g and the pore volume is 1.5cc/g as compared to surface area of 100m2/g and pore volume of 0.5cc/g for alumina support (see Table 5-1). Because of the high pore volume and high surface area of the carbon powder used to support the metal particles, the catalyst or

active metal loading is more per gram of catalyst. Also, because of the high surface area the dispersion of the catalyst is very high. Hence, the activity (A) of the catalyst (which is the measure of the number of active sites available for reaction per gram of catalyst) is very high (about 5-10 times) in the highly porous carbon supported catalyst as compared to commercial alumina supported catalyst. As a result, the reactants will travel over the same number of catalyst active sites in a very small amount of highly porous carbon catalyst disc as the number of active sites in very large amount of catalyst supported on low alumina or silica which has low porosity and low catalyst dispersion.

Figure 5-3 shows the TEM of the copper chromite catalyst supported on highly porous carbon. The dark spots correspond to the metal particles on the carbon. Note that the size of the metal particles deposited is less than 20nm which shows that the metal particles can be deposited in mesopores that constitute the large section of pore size distribution of the carbon as shown in the Table 5-1.

One of the most interesting features of the carbon derived from corn cob (which is used as catalyst support) is that it has a very high surface area of 3000 $m^2/g$ still it has large fraction of mesopores and relatively smaller fraction of micropores (which are usually responsible for larger surface area). Such a feature in activated carbon is extremely beneficial for its application as catalyst support since the predominantly microporous structure is an important drawback of activated carbon in practical applications; the micropores are not accessible to large molecules present in many industrial feedstocks.

In last few years there has been a considerable amount of work directed toward the preparation of activated carbons with large surface areas and pore volumes outside

the narrow micropores. Success has been attained by just few research groups[70] [71] [72]. For catalyst support applications it is beneficial to have higher fraction of mesopores in the activated carbon since mesopores are easily accessible to the reactants for reacting and for the products to diffuse out. Micropores may cause more diffusion limitations especially in the liquid phase.

**Table 5-1: Comparison of commercial catalyst and catalyst supported on highly porous carbon powder.**

| **Catalyst** | **Amt of catalyst (g)** | **Conversion** | **Productivity** $g_{PG}/ g_{catalyst}$ |
|---|---|---|---|
| Catlalyst-1 | 1.00 | >99% | 1.02 |
| Catalyst-2 | 1.00 | >98% | 0.95 |
| Commercial | 10 | >99% | 0.16 |

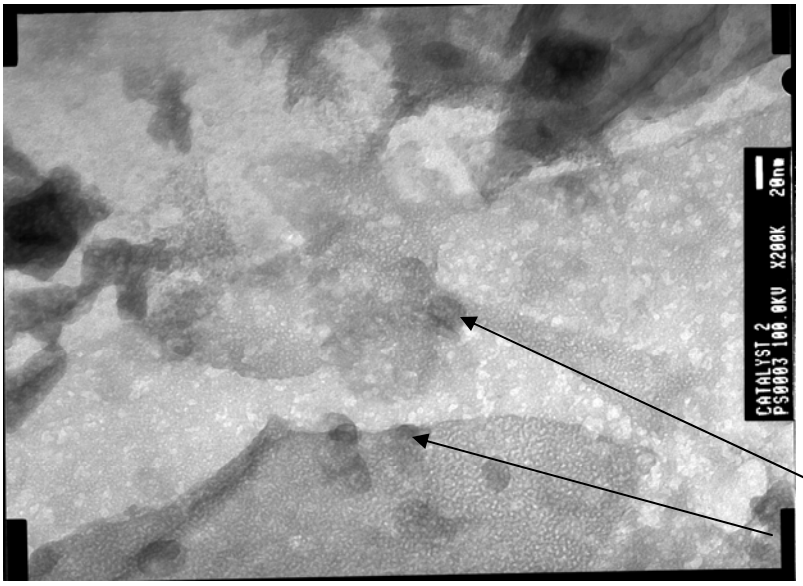


**Figure 5-3 TEM image of bimetallic Cu and Cr deposited on carbon.**

## 5.4 CONLUSION

Bimetallic copper and chromium catalyst supported on nanoporous carbon obtained from corn cobs were synthesized. The carbon supported copper and chromium catalyst were successfully used to catalyze the reaction to convert glycerin to propylene glycol. Glycerin conversions greater than 99% similar to commercial catalyst were achieved with carbon supported catalysts. The carbon supported catalyst had productivity as high as 1.2 which was 8-9 times higher than the commercial alumina supported catalyst. Transmission Electron Microscopy confirmed the actual deposition of copper and chromium metal ions on to the mesopores and micropores of the nanoporous carbon used as support.

# REFERENCES

[61] Patrick, J.W., 1995: "Porosity in Carbons: Characterization and Applications" Halsted Press, New York.

[62] Moss, R. L. 1976: in Anderson, R.B. and Sawson, P.T. (eds) Experimental Methods in Catalytic Research. New York: Academic Press, Vol. II, P. 43.

[63] Satterfield, C.N. 1980: Hetrogeneous Catalysis in Practice. New York: McGraw Hill.

[64] Weisser, I. and Landa, S. 1973: Sulphide Catalysts. Their Properties and Applications. New York: Pergamon Press.

[65] Bird, A. J. 1987: in Stiles, A. B. (ed). Catalyst Supports and Supported Catalysts. Guildford: Butterworth, P. 107.

[66] Rodriguez-Reinoso, F., Rodreguez-Ramos, I., Guerreroruiz, A. and Lopez-Gonzalez, J.D. 1986: Applied Catalysis 21, 251.

[67] Shah P, Suppes G, Pfeifer P,"Nanoporous Carbon from Corn cobs", Carbon (in press).

[68] P. Pfeifer, F. Ehrburger-Dolle, T.P. Rieker, M.T. González, W.P. Hoffman, M. Molina-Sabio, F. Rodríguez-Reinoso, P.W. Schmidt, and D.J. Voss, Nearly space-filling fractal networks of carbon nanopores, *Phys. Rev. Lett.* 88, 115502-(1-4) (2002).

[69] P. Schewe, J. Riordon, and B. Stein, "Fractal carbon nanopore network." *Physics News Update* (American Institute of Physics), No. 578, 2/27/02. http://www.aip.org/enews/physnews/2002/split/578-1.html

[70] Rodriguez-Reinoso, G. 1989: Pure and Applied Chemistry 61, 1859

[71] Dubinin, M.M. and Fedoseev, D.V. 1982: Izvestiia Akademiia Nauk SSSR: Seriia Khimishceskaia, P. 246.

[72] Caturla, F., Gutierrez, A., Molina-Sabio, M. and Rodriguez-Reinoso, F. 1988: In McEnaney, B. and Mays, T.G. (eds) Proceedings of Carbon'88. Bristol: IOP Publishing, P. 4.

# CHAPTER 6

# 6 ACTIVATED CARBON FROM CORN COBS FOR REMOVING CU(II) AND CR(III) METALS

**This paper was submitted for publication to Journal of AOCS as: "*Activated Carbon From Corn cobs for Removing Cu(II) and Cr(III) Metals*", Parag Shah[a], Galen Suppes[a], Joseph Turner[b], Tom Marrero[a]**

**[a] Department of Chemical Engineering, W2028 Engineering Bldg. East, University of Missouri, Columbia, MO 65211**

**[b] Department of Chemistry, University of Missouri, Columbia, MO 65211**

## ABSTRACT

Activated carbon obtained from corn cobs was used to remove Cu(II) and Cr(III) metal ions from aqueous solutions. The adsorption capacity for Cu (II) and Cr (III) of the carbon obtained from corncobs were measured and compared with other commercially available carbons and alumina. The effect of post oxidation of carbon with nitric acid on the metal adsorption capacity was also studied. The Cu(II) adsorption capacity as high as 29mg/g and Cr(III) adsorption capacity up to 3.5 mg/g were obtained on the carbon made by physical and chemical processing of corncobs. Carbons with different pore sizes and pore size distribution were made by varying the process conditions to study the change in their metal adsorption capacity.

**KEYWORDS:** Nanoporous carbon, Activated carbon, Copper removal, Chromium removal, Adsorption

## 6.1 INTRODUCTION

Heavy metal removal is an important step in waste water treatment process. Metal impurity removal is also a critically important task in pharmaceutical process research, where the final products mush meet stringent purity requirements. Use of adsorbents for removing metal ion impurity such as Pd, Cu (II), Cr (III), Cr (VI), Ni (II), Cd (II), etc from waste water and chemical products is a common practice.[73] The adsorbent used for heavy metal removal from waste water and product streams include alumina[74], activated carbon[75 76], zeolites[77], clay[78], agricultural waste such as bagasse, fly ash[79], saw dust[80], etc. Carbons are important group of adsorbents for removing heavy metals during waste water treatment and also for recovering spent catalyst in pharmaceutical processes.

Out of all these adsorbents the agricultural wastes are the cheapest adsorbents; however their adsorption capacity without any chemical or physical treatments is very less as compared to the adsorption capacity after being converted to carbon or activated carbon. The process of converting agricultural waste to carbon can be costly due to the energy and chemical consumption. However, Benter et al[81], and Babel and Kurniknov[82] have reported that improved adsorption capacity of the adsorbents after additional processing does compensate the cost of such a process. Nevertheless, the production cost of activated carbon is an important factor for economics of the process for removing heavy metals.

Corn cobs could be an excellent precursor for low cost activated carbon production as it has botanical origin similar other lignocellulosic precursors for activated carbon. Since the yield of the activated carbon production is usually very low, the cost

and availability of the raw material is a very important factor in the economic production of activated carbon. Coconut shell, wood, lignite coals which are often used for commercial production of activated carbon have high price as compared to agricultural waste such as corn cob in US. Corn cob is available in abundance in the US and is relatively cheap. Also the chemical composition of corn cobs suggest that it has less mineral matters, which are often responsible for preferential gasification during the activation process resulting in meso and macropore channeling and pitting, and not the preferred microporosity and repeatability. Because of this reasons corn cobs could be an excellent precursor for the commercial production of activated carbon. Table 6-1 shows the elemental analysis of corn cobs which shows high promises of its use as precursor of nanoporous carbon production because of its carbon content up to 45%.

In this project highly activated carbon was produced from corn cobs. These carbons were used to remove Cu (II) and Cr (III) metal ions from aqueous solutions. High adsorbent capacities of 29mg/g for Cu (II) and 3.5mg/g for Cr (III) were observed on these carbons at temperature of 298K and pH of 6-8. Carbons with different pore size distribution and surface area were prepared by varying the process conditions and the final effect on the adsorption capacity for metals was studied.

## 6.2 EXPERIMENTAL PROCEDURE

The experimental procedure for making the carbon from corn cobs is discussed in detail in our previous publication[83]. This paper discusses the use of nanoporous carbon obtained from corn cobs for removing Cu(II) and Cr(III) from aqueous solutions. Three different types of carbon produced using different processing conditions were tested for

their adsorption capacities for Cu(II) and Cr(III) from metal containing aqueous solutions. Along with carbon produced from corn cobs, alumina adsorbent from SudChemie and two different commonly used commercial activated carbons Darco-G-60 from Norit and Calgon Activated carbon from Calgon were also tested for comparison purposes. Experiments were also carried out with adsorbents modified with nitric acid post oxidation in which the adsorbents were heated with 10% nitric acid at 200˚C for 2hr. After heating, the excess of nitric acid was removed with aqueous washing and the adsorbents were dried at 110˚C for 8hr. The modified adsorbents were then used for removing Cu(II) and Cr(III) metals at the same conditions as the unmodified adsorbents.

### 6.2.1 GENERAL PROCEDURE FOR ADSORBENT TESTING

Adsorbent testing was carried out in 20ml glass vials. Adsorbent amounts varying from 1g, 0.1g, 0.05g were added to vials containing 10 ml of aqueous solutions of varying concentrations of Cu(II) and Cr(III) prepared by dissolving copper(II) nitrate hemipentahydrate and chromium(III) nitrate nonhydrate salts. The vials containing adsorbents in the solution were agitated for 30-45min in a gyratory shaker after which the adsorbent containing metal solutions were transformed to plastic centrifuge vials and were centrifuged for 30min at 10000rpm. The supernate from each vial was withdrawn for analysis to determine the concentration of Cu(II) and Cr(III). The solution was then filtered through a 0.45um nylon syringe filter to remove suspended particulates.

### 6.2.2 METAL ANALYSIS BY ATOMIC EMISSION SPECTROSCOPY

The adsorbent treated supernate was mixed with 1% nitric acid at a dilution factor of 1000. Atomic emission was conducted, with detection wavelengths of 324.4 and

417.2 for copper and chromium respectively. A slit width of 2mm was used. Based on literature values, atomic emission has a detection limit of 0.01μg/ml for Cu(II) ions and 0.05μg/ml for Cr(III) ions using a acetylene/nitrous oxide flame and 5cm burner head. Emission from ultra pure deionized water was used a baseline reading. For calculating the concentrations of Cu(II) and Cr(III) ions in the aqueous solutions calibration curves were prepared from copper nitrate hemipentahydrate and chromium nitrite solutions prepared in distilled water using serial dilution method at concentrations ranging from 20mg/ml to 12.5ul/ml.

## 6.3 RESULT AND DISCUSSION

### 6.3.1 COPPER (II) REMOVAL

Six adsorbents were tested for Cu(II) adsorption, including 3 carbons produced from corncobs (designated CC1, CC2 and CC3), Darco-G60 from Norit, activated carbon from Calgon, and alumina from Sudchemie. Table 6-2 summarizes the BET surface area, micropore, and total porosity as obtained by $N_2$ adsorption at 77K.

Figure 6-1 summarizes initial tests on the capacity of 1 g of adsorbent to remove Cu(II) from 10 ml aqueous solutions that contained 20 mg/L of copper. CC-3 is the most effective adsorbent whereas alumina has the lowest adsorption capacity. The second highest capacity is that of Calgon activated carbon followed by CC-2, darco and CC-1.

Based on the screening tests, a loading of 0.2 g (rather than 1 g) was used to further discriminate the adsorbents with results summarized by Figure 6-2. At this loading only CC-3 and Calgon carbons had not reached their adsorption threshold.

Performances for loadings of 0.05 grams (per 10 ml stock) are summarized by Figure 6-3 where the capacity of the Calgon carbon was exceeded and while the CC-3 carbon maintained removal that was close to the detection threshold. Hence it was concluded that the CC-3 carbon had the maximum Cu adsorption capacity among the adsorbents compared.

The adsorption capacities of all adsorbents are shown in Table 6-3 with the CC-3 having the maximum adsorption at 29mg/g. The primary reason for this is as seen from Table 6-2 CC-3 has very high surface area of 3350 $m^2$/g and high pore volume of 1.9cc/g. More importantly it has high fraction of mesopore volume with pores of the size between 2-50 nm as compared to other adsorbents. For adsorbing metal ions in to the pores it is essential that the pores are accessible to the metal ions. Figure 6-6 illustrates the good correlation between mesopore volume and metal adsorption capacity for these samples.

Micropores which are of the size less than 2nm are not very favorable for metal ion removal since the metal ion cannot easily enter the pores. The pores of the size bigger than 2nm upto 50nm are optimal since they are easily accessible to the metal ions and still have large surface area and pore volume. The CC-2 and CC-1 had higher surface area than the Calgon carbon still they had lower Cu (II) adsorption capacity than Calgon; the reason being in CC-2 there is high fraction of micropores (< 2nm size). While the surface areas of Calgon and Darco are not as high as CC-2, they have higher fraction of pores between 2-100nm than CC-2 which makes them more effective for metal adsorption. Both CC-1 and alumina had low pore volumes and low capacities for adsorbing copper.

In addition to the physical structure, activated carbons have a chemical structure which can be important since adsorption capacity is also influenced by the chemical nature of the surface. Activated carbons are invariably associated with appreciable amounts of heteroatoms such as oxygen and hydrogen (in addition, they may be associated with atoms of chorine, sulphur, etc.) preferentially bonded at the active sites. Carbon-oxygen surface groups are by far the most important in influencing the chemical surface behavior of an activated carbon.[84] Consequently, the adsorption behavior of an activated carbon cannot be interpreted on the basis of mesopore volume alone.

Figure 6-4 shows the concentration of Cu+2 in the solution treated with the same adsorbents but at 40˚C. The adsorption capacity of CC-1, CC-2, CC-3 and Darco G-80 carbons dropped, whereas that of Calgon didn't change considerably. This suggests a weaker bonding in the CC-1, CC-2, CC-3 and Darco G-80 carbons relative to the Calgon carbon. Of these adsorbents, only the Calgon carbon was treated (at manufacturer) with nitric acid which tended to improve binding strengths.

To check the effect of surface treatment of the carbon, all the carbon adsorbents were mixed with 10% nitric acid solution at 120˚C for 2hrs and then washed with water to remove excess of nitric acid until a pH of 6-7. Figure 6-5 shows the resulting adsorptions in terms of Cu+2 remaining in solution. The CC-3 adsorbent continued to have the highest adsorption capacity. The adsorption capacity of the Calgon carbon dropped considerably possibly due to the destruction of the active surface sites caused due to the effect of nitric acid.

### 6.3.2 CHROMIUM (III) REMOVAL

Carbon adsorbents were also tested for Cr+3 removal from aqueous solution. Figure 6-7 shows the concentration of Cr+3 in aqueous solution after being treated with adsorbents. The initial concentration was 20 mg/l with 1 g of adsorbent being added to 10ml of Cr (III) solution. Figure 6-8 provides adsorption results for 0.1 g adsorbent loadings. CC-3 carbon provided the lowest Cr concentration in the treated solution. For chromium adsorption, Darco-2 provided the second greatest capacity. Alumina adsorbents had the lowest adsorption capacity than activated carbon.

The reason for CC-3 having highest chromium adsorption capacity was again due to its high surface area and large fraction of pores between 2-50nm which helps to adsorb higher Cr+3 ions. The CC-3 carbon has the Cr (III) adsorption capacity of >3.5mg/g determined experimentally which is one of the best adsorption capacity reported for any carbon adsorbent for Cr (III) removal. The Figure 6-10 shows the final concentration of Cr(III) in the solutions treated at 0.05% loading of adsorbents. As the adsorbent loading is decreased the concentration of Cr(III) increases in the solution treated with Darco carbon whereas in the solution treated with CC-3 carbon is still very low indicating the higher adsorption capacity of CC-3 than Darco G60.

Figure 6-9 shows the final concentration of Cr(III) aqueous solution treated with adsorbents treated with nitric acid. In case of Cr(III) the adsorption capacity of all the adsorbents increased slightly due to acid treatment except for the Calgon activated carbon whose adsorption capacity decreased considerably.

## 6.4 CONCLUSION

The carbon obtained from corncob is an effective adsorbent for removing heavy metals such as Cu and Cr from aqueous solution. The adsorption capacity of the carbon depends on the carbon activation process which impacts both average pore size and total BET surface area. An adsorption capacity of 29mg/g was achieved for Cu(II) which was higher than commercially available controls. The adsorption capacity of the carbon depended predominantly on the pore volume and pore size distribution of the carbon. The carbon with higher pore volume and high fraction of mesopores and macropores was found to be more effective for Cu and Cr ion removals as compared to carbon with higher micropore volume and low mesopores volume. The effect of the surface modification by acid treatment needs to be studied in detail as its effect was not very clear from this study.

## TABLES

**Table 6-1 Elemental Analysis of Corn cobs**[Error! Bookmark not defined.]**.**

| ***Element*** | ***%*** |
|---|---|
| Carbon | 43.5 |
| Nitrogen | 0.21 |
| Oxygen | 48.4 |
| Hydrogen | 7.9 |
| Sulphur | 0.013 |
| Ash | 1.2 |

| | |
|---|---|
| Moisture | 10+/- 2 |
| Cellulose | 47.1 |
| Lignin | 6.8 |
| Hemi cellulose | Not Available |

**Table 6-2 Characterization of Adsorbents.**

| Adsorbent | BET Surface Area, m2/g | Micropore Volume, cc/g | Total Pore Volume, cc/g |
|---|---|---|---|
| CC-1 | 1500 | 0.18 | 0.66 |
| CC-2 | 2000 | 0.78 | 1.3 |
| CC-3 | 3350 | 0.15 | 1.93 |
| Calgon | 1100-1400 | 0.1 | 1 |
| Darco-G60 | 900-1000 | 0.14 | 0.94 |
| Alumina | 300-400 | 0.05 | 0.3 |

**Table 6-3 Adsorbent capacity of adsorbents for Cu (II) and Cr (III).**

| Adsorbent | Cu(II) Adsorption Capacity, mg/g | Cr(III) Adsorption Capacity, mg/g |
|---|---|---|
| Alumina | 1.2 | 0.81 |
| CC-1 | 4.4 | 1.1 |
| CC-2 | 4.9 | 1.45 |
| CC-3 | 26.9 | 3.5 |
| Calgon | 12.7 | 1.23 |
| DarcoG-60 | 4.9 | 1.75 |

# FIGURES

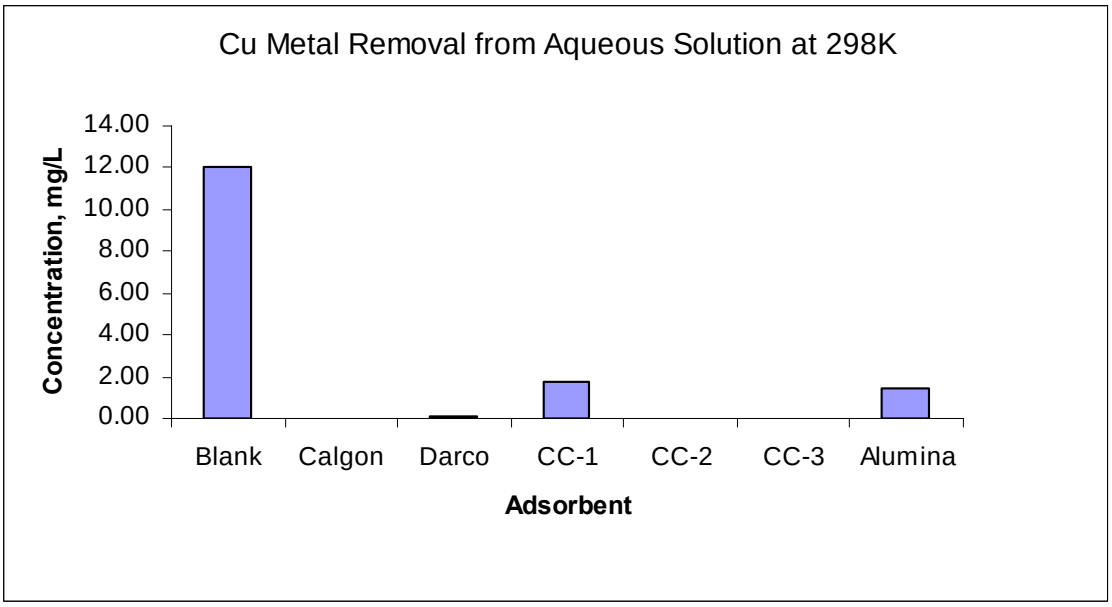


**Figure 6-1 Concentration of $Cu^{2+}$ remaining in solution after treatment of 10 ml of aqueous solution with 1.0g of carbon at 298K.**

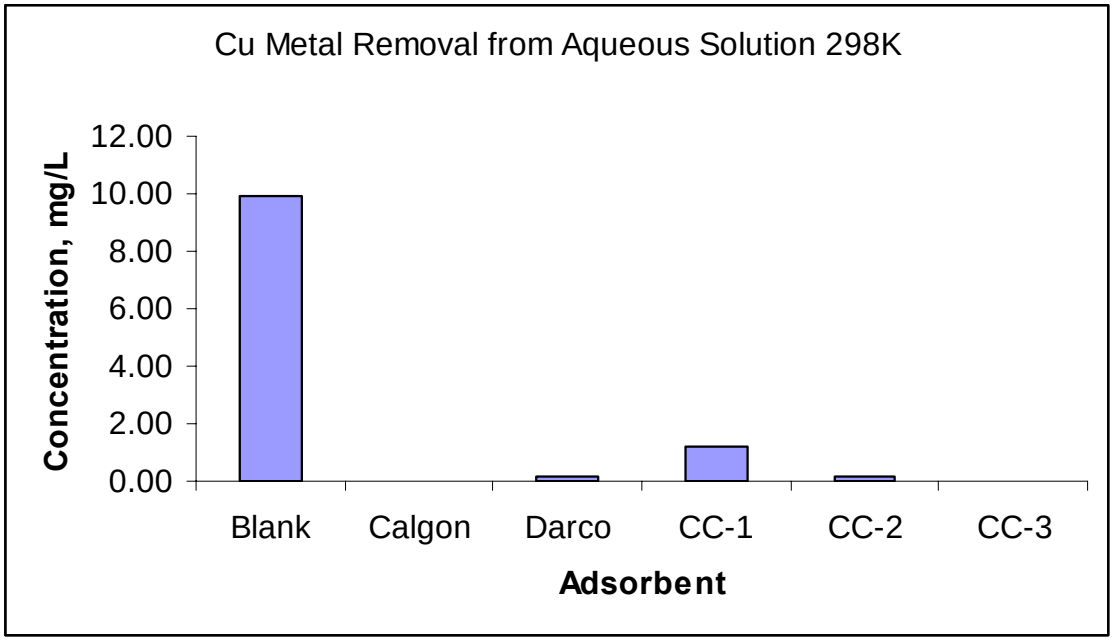


**Figure 6-2 Concentration of $Cu^{2+}$ remaining in solution after treatment of 10 ml of aqueous solution with 0.2g of carbon at 298K.**

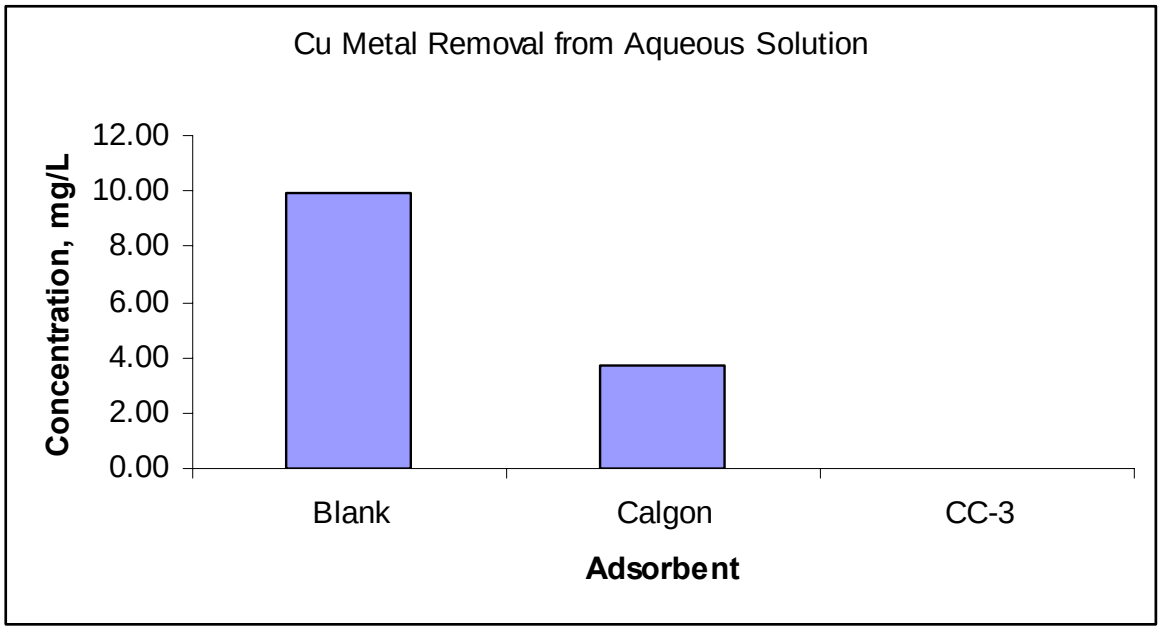

**Figure 6-3 Concentration of $Cu^{2+}$ remaining in solution after treatment of 10 ml of aqueous solution with 0.5g of carbon at 298K.**

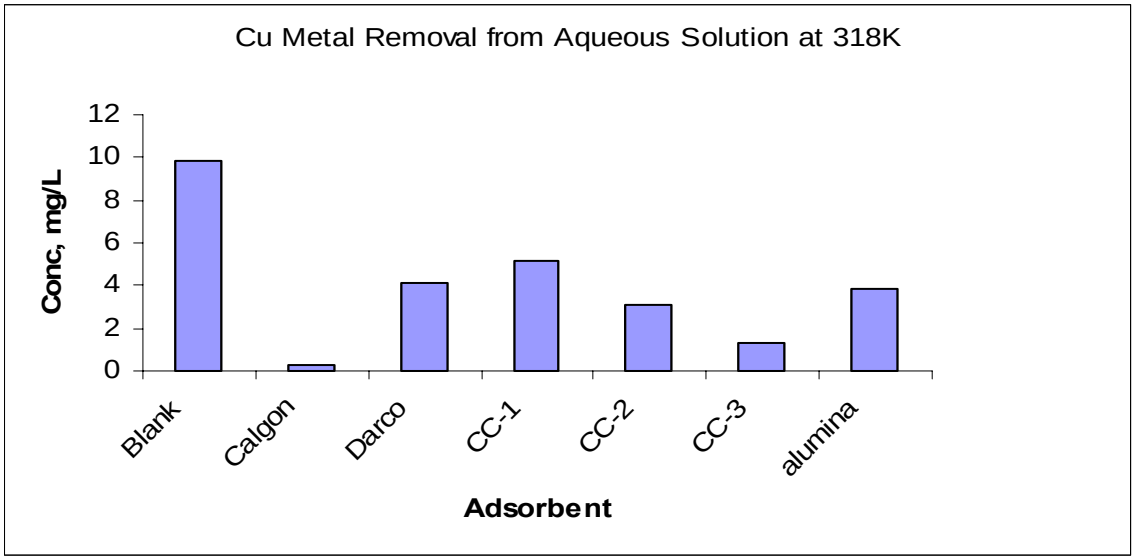


**Figure 6-4 Concentration of $Cu^{2+}$ remaining in solution after treatment of 10 ml of aqueous solution with 1.0g of carbon at 318K.**

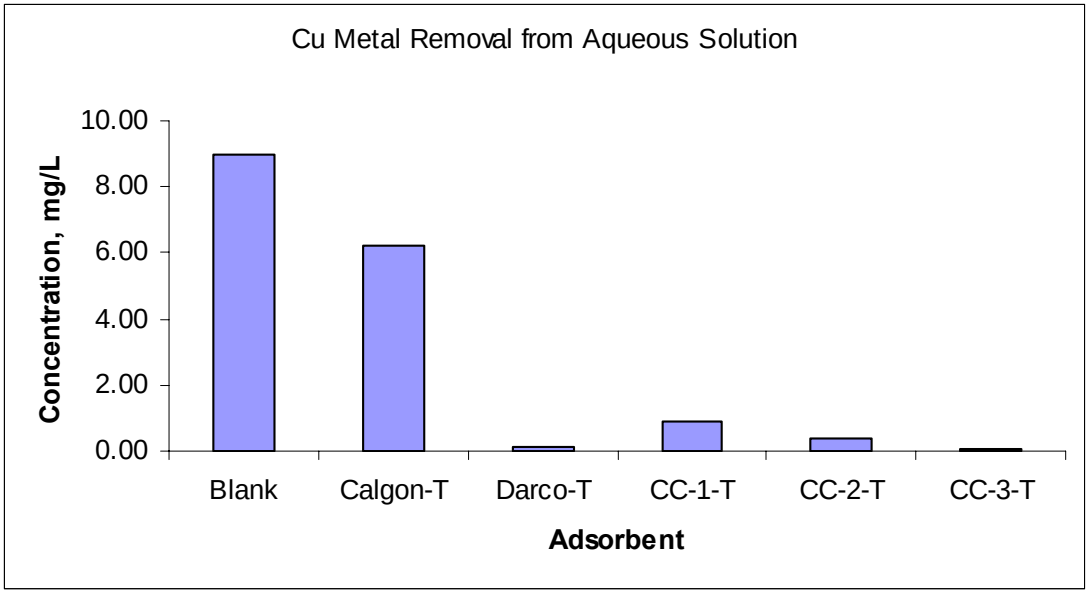


**Figure 6-5 Concentration of $Cu^{2+}$ remaining in solution after treatment of 10 ml of aqueous solution with 1.0g of carbon at 298K for case where carbon is treated with nitric acid.**

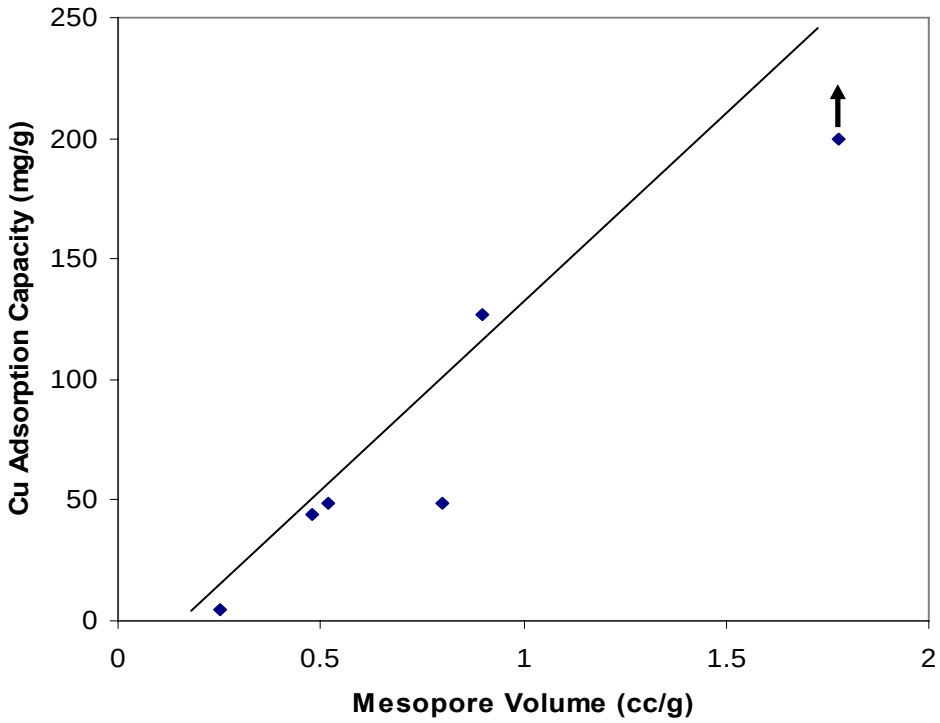


**Figure 6-6 Impact of mesopore volume on capacity of carbon to remove $Cu^{2+}$ from aqueous solution.**

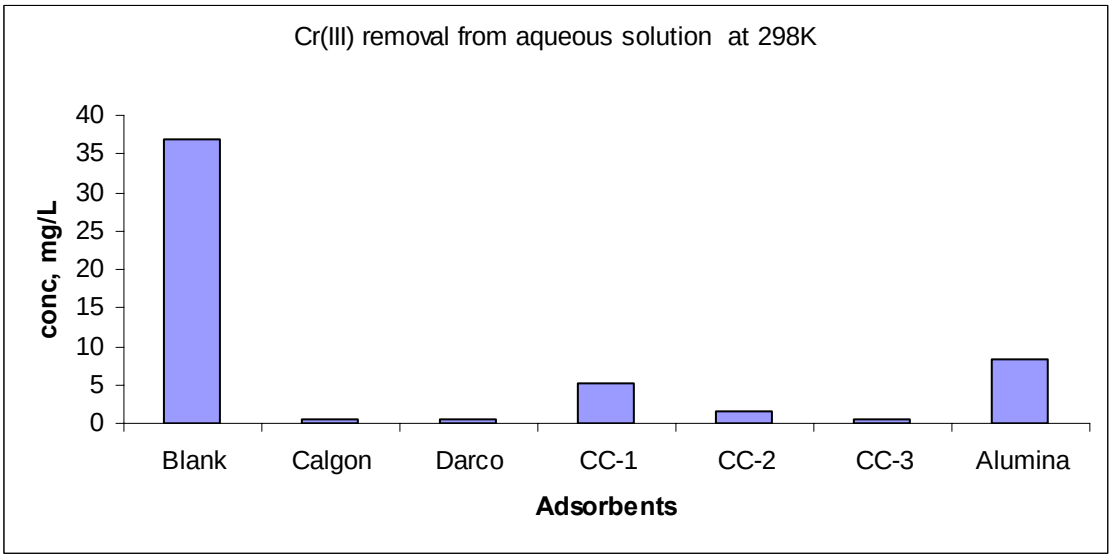


**Figure 6-7 Concentration of Cr(III) remaining in solution after treatment of 10 ml of aqueous solution with 1.0g of carbon at 298K.**

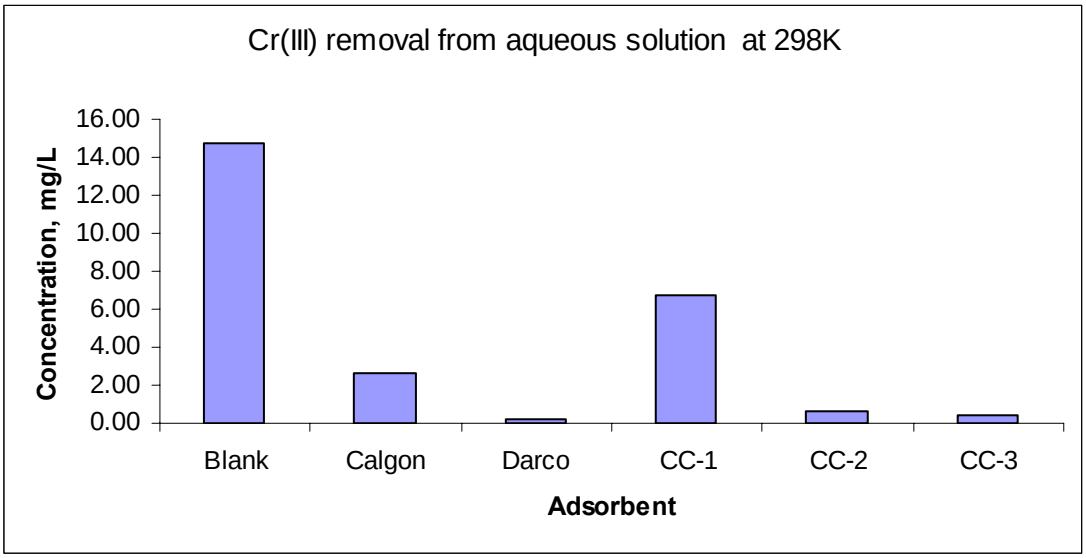


**Figure 6-8 Concentration of Cr(III) remaining in solution after treatment of 10 ml of aqueous solution with 0.1g of carbon at 298K.**

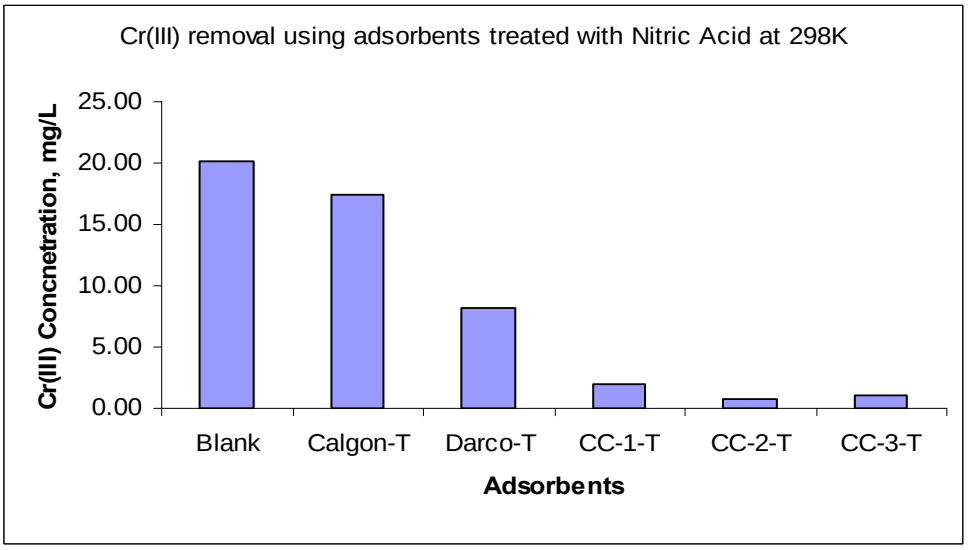


**Figure 6-9 Concentration of Cr(III) remaining in solution after treatment of 10 ml of aqueous solution with 0.05g of carbon at 298K for case where carbon is treated with nitric acid.**

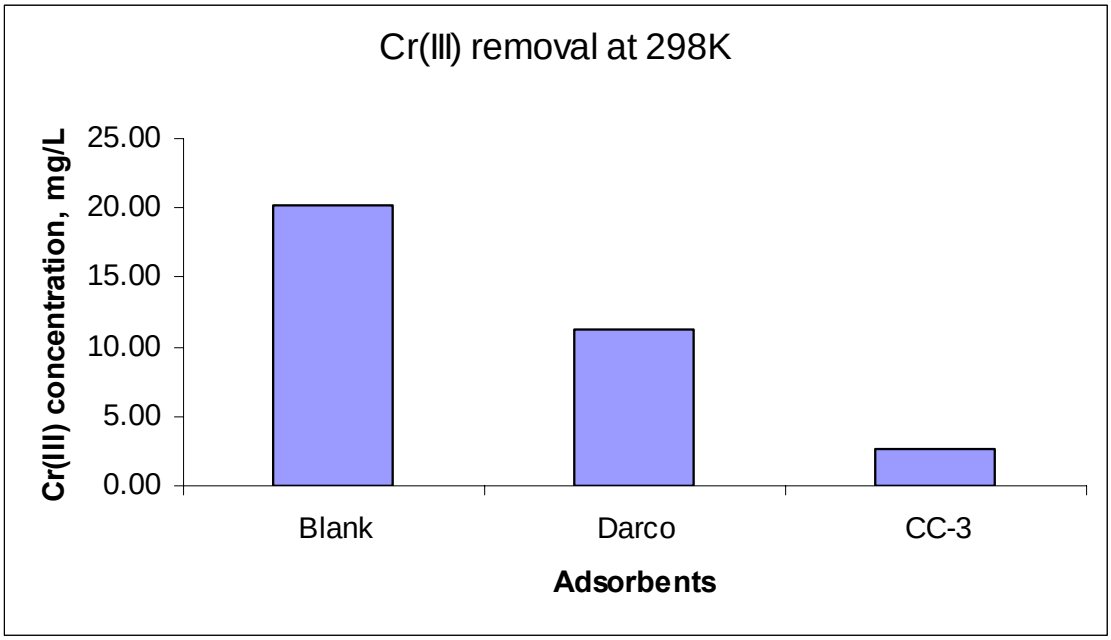


**Figure 6-10 Concentration of Cr(III) remaining in solution after treatment of 10 ml of aqueous solution with 0.05g of carbon at 298K.**

# REFERENCE

[73] Welch C.J., Walker J.A., Leonard W. R., Biba M., DaSilva J., Henderson D., Laing B.,Mathre D. J.,Spencer S., Bu X., and Wang T., "Adsorbent Screening for Metal Impurity Removal in Pharmaceutical Process Research" Organic Process Research & Development 2005, 9, 198-205.

[74] Bishnoi NR, Bajaj M, Sharma N, Gupta A. Adsorption of Cr(VI) on activated rice husk carbon and activated alumina. Biores Technol 2003;91(3):305 –7.

[75] Park JS, Jung WY. Removal of chromium by activated carbon fibers plated with copper metal. Carbon Sci 2001;2(1):15– 21.

[76] Periasamy K, Namasivayam C. Removal of copper(II) by adsorption onto peanut hull carbon from water and copper plating industry wastewater. Chemosphere 1996;32(4):769– 89.

[77] Peric´ J, Trgo M, Medvidovic´ NV. Removal of zinc, copper, and lead by natural zeolite—a comparison of adsorption isotherms. Water Res 2004;38(7):1893–9

[78] Vengris T, Binkiene R, Sveikauskaite A. Nickel, copper, and zinc removal from wastewater by a modified clay sorbent. Appl Clay Sci 2001;18:183–90.

[79] Rao M, Parawate AV, Bhole AG. Removal of Cr6+ and Ni2+ from aqueous solution using bagasse and fly ash. Waste Manage 2002;22:821– 30.

[80] Dakiky M, Khamis M, Manassra A, Mer'eb M. Selective adsorption of Cr(VI) in industrial wastewater using low-cost abundantly available adsorbents. Adv Environ Res 2002;6:533 – 40.

[81] Bailey SE, Olin TJ, Bricka M, Adrian DD. A review of potentially low cost sorbents for heavy metals. Water Res 1999; 33(11):2469– 79.

[82] Babel S, Kurniawan TA. Low-cost adsorbents for heavy metals uptake from contaminated water: a review. J Hazard Mater 2003a;97(1–3):219– 43.

[83] Shah P, Suppes G, Pfeifer P,"Nanoporous Carbon from Corn cobs", Carbon (To be submitted).

[84] Pierce, C. 1968: Journal of Physical Chemistry 72, 3763.

# CHAPTER 7

# 7 CONCLUSIONS AND FUTURE WORK

## 7.1 CONCLUSIONS

From these studies it can be concluded that corn cobs are an excellent precursor for making nanoporous or activated carbon of similar or better quality than other common precursors. Carbon with micopore volume of 1.4cc/g and BET surface area of 3800+ $m^2$/g can be produced from corn cobs.

As far as phosphoric acid activation of corn cobs is concerned, it is advantageous to soak the corn cobs with acid at lower temperatures because of the soft nature of the precursor. The heat treatment temperature of 450 -500˚C and acid concentration of 1.1 g/g is appropriate for getting high micropore volume.

To produce carbon with high surface area and pore volume, phosphoric acid treatment followed by KOH treatment is a preferred route of activation. For KOH activation, the KOH:C ratio between 2.5 and 3 and heat treatment temperature between 750-790˚C is optimum for getting nanoporous carbon with pore size smaller than 20nm after which the widening of ultramicropores or nanopores begins—the product starts becoming more and more mesoporous.

In application of nanoporous carbon obtained from corn cobs for storing natural gas (ANG application) it is important to have a high fraction of pores between size 0.7 nm to 2 nm. The KOH:Char ratio and heat treatment temperature proved to be very critical parameters for getting high methane storage density on the carbon. Carbon

adsorbent with micropore volume as high as 1.4 cc/g and piece density of monoliths between 0.6 and 0.7 were obtained the combination of which helped to get high methane storage density of 173 V/V and 108 g/L. The carbon with high methane uptake capacity was produced. Repeatedly, high methane uptakes were confirmed by both gravimetric and pressure differential measurement techniques. The deliverable volume of 156 V/V was obtained repeatedly. The use of recycled KOH to produce same quality of carbon as fresh KOH was also demonstrated.

Soybean oil was successfully demonstrated as a binder for making carbon monolith. The amount of divinyl benzene added as comonomer and amount of catalyst added to the soybean oil prepolymer are important factors that affect the final properties of the monoliths. Carbon monoliths using soybean oil with similar compressive strengths and densities as monoliths made with saran were successfully made. The methane uptake capacity of the monoliths made with soybean oil was about 10% less than that made with saran, primarily due to smaller amount of micropores in the carbon derived from soybean oil polymer as compared to the carbon derived from saran.

The carbon obtained in this project also proved to be an excellent catalyst support for producing bimetallic copper and chromium catalyst. Carbon having a high fraction of mesopores and still having high surface area was produced which proved to be advantageous for making high activity catalyst. The carbon supported copper and chromium catalyst were successfully used to catalyze the reaction to convert glycerin to propylene glycol. Glycerin conversions greater than 99% and productivity as high as 1.2 (which was 8-9 times higher than the commercial alumina supported catalyst) were obtained using catalyst supported on carbon obtained from corn cobs.

The use of carbon obtained from corn cob as an adsorbent for removing heavy metals such as Cu and Cr from aqueous was successfully demonstrated. The adsorption capacity of carbon made from corn cob was found to be dependent on the processing parameters. High adsorption capacity for Cu(II) up to 29mg/g were achieved with carbon derived from corn cob which was higher than commercially available carbons. At similar surface areas, adsorption was a strong function of pore size distribution of the carbon. The carbon with higher pore volume and a high fraction of mesopores and macropores was found to be more effective for Cu and Cr ion removals as compared to carbon with higher micropore volume and low mesopores volume.

## 7.2 RECOMMENDED RESEARCH

From the knowledge and insight gained during the course of this project, the following future work is recommended in the production and application of nanoporous carbon from corn cob.

In order to make the production of nanoporous carbon from corn cob commercialized for adsorbed natural gas technology the cost of the final carbon monoliths is an important factor. In order to bring the cost down the recycling of phosphoric acid and potassium hydroxide is an important step which needs to be studied in detail. The use of soybean oil instead of saran will also help to reduce the price greatly and make the process more environmental friendly, so a dedicated study to improve the micropore volume of the carbon obtained by pyrolysis of soybean oil derived polymer is needed. In order to increase the methane storage capacity of the ANG tank, in addition to high storage capacity of the adsorbent, proper design of the tank is necessary.

Although the work done in this project for use of activated carbon from corn cobs as catalyst support was very limited, it showed that there is a tremendous potential to make highly active and selective catalyst supported on this carbon. So the use of the carbon obtained using the technology of this project for supporting other noble metals should be fully explored. As far as the use of activated carbon from corn cobs as adsorbent for removing heavy metals for waste water is concerned, the effect of surface treatment using nitric acid or other reagents needs to be studied in detail as its effect was not very clear from this study.

# APPENDIX

## A1. Calculation for finding methane uptake capacity using gravimetric method

First, measure the density of the carbon. This is done by placing 1 $cm^3$ of carbon in a graduated cylinder (by packing) and taking the weight difference between the empty cylinder and the cylinder with sample. This is recorded in the Table A1 as 'Piece Density gm/ml'.

Second, the desired amount of sample is massed out and placed inside of the chamber. The sample mass is placed in the table A1 under 'Amt Carbon gm'.

Third, taking the known constant values find the amount of void space inside of the chamber wherein unadsorbed methane will reside. The chamber volume is known by measurement (usually 4.5ml considering the packing material has negligible volume) and using this volume, calculate the volume taken up by the sample. Using the sample volume, take the total volume, subtracts off the sample volume, and get the volume of free methane in the chamber.

The density of methane at 500 psig and 298K that is used is 0.0280 g/mL calculated using gas law and compression factor of 0.93 for methane. Now multiply the density of methane by the volume of void space to get the weight of methane in chamber at 500 psig as entered in the table A1.

Table A1. Shows calculation of gravimetric method for measuring methane uptake

| Carbon Sample | Piece Density gm/ml | Carbon g | Pressure psig | Outgasing Temp degC (4hrs) | chamber + carbon g | Chamber + Carbon g | Dead wt Methane g | chamber+ carbon+CH4 g | Methane Ads g | gm/100gm gm/100gm | Storage density gm/L | v/v L/L |
|---|---|---|---|---|---|---|---|---|---|---|---|---|
| B-21/k | 0.432 | 0.8055 | 500 | 140 vac | 184.5216 | 184.4110 | 0.075 | 184.7103 | 0.1733 | 21.5146 | 92.9430 | 142 |
| B-21/k | 0.432 | 0.8055 | 0 | 140 vac | 184.5216 | 184.4110 | 0.075 | 184.5450 | 0.0175 | 2.1726 | 9.3855 | 14 |
| B'-21/k | 0.490 | 0.8489 | 500 | 140 vac | 184.4750 | 184.3657 | 0.077 | 184.6741 | 0.1846 | 21.7458 | 106.5544 | 163 |
| B'-21/k | 0.490 | 0.8489 | 0 | 140 vac | 184.4750 | 184.3657 | 0.077 | 184.4400 | 0.0180 | 2.1204 | 10.3899 | 16 |
| B'-21/k | 0.490 | 0.8480 | 500 | 140 vac | 184.4402 | 184.3588 | 0.077 | 184.6483 | 0.1798 | 21.2028 | 103.8939 | 159 |
| B'-21/k | 0.490 | 0.8480 | 0 | 140 vac | 184.4402 | 184.3588 | 0.077 | 184.4198 | 0.0149 | 1.7571 | 8.6097 | 13 |
| S-30 | 0.350 | 0.7460 | 500 | 140 vac | 205.7170 | 205.6385 | 0.080 | 205.8922 | 0.1347 | 18.0563 | 63.1971 | 97 |
| S-30 | 0.350 | 0.7460 | 0 | 140 vac | 205.7170 | 205.6385 | 0.080 | 205.7065 | 0.0290 | 3.8874 | 13.6059 | 21 |
| B'-21/k' | 0.499 | 1.0266 | 500 | 140 vac | 205.8788 | 205.7375 | 0.080 | 206.0734 | 0.2084 | 20.3000 | 101.2971 | 155 |
| B'-21/k' | 0.499 | 1.0266 | 0 | 140 vac | 205.8788 | 205.7375 | 0.080 | 205.8070 | 0.0220 | 2.1430 | 10.6936 | 16 |

Also the mass of the sample chamber + sample is taken after outgasing which is also shown in the table under the second heading ‘wt of chamber + carbon ’.

After that the sample chamber with sample is pressured up to 500psig and after some time it is massed. This value is placed in the table under ‘wt of chamber + carbon + methane at 500 psi (gm)’.

After all of this take the mass of (chamber+carbon+methane) and subtracts off the mass of methane in void space and the mass of chamber+carbon after outgasing which will give the mass adsorbed onto the surface of the carbon. This number is than further converted to storage density in terms of g/L and volumetric storage capacity in terms of V/V.

Example Calculation for sample B21k:

(1) Piece Density = 0.432 g/ml

(2) Amount of Carbon (massed in air) = 0.8055 g

(3) Pressure (psig) = 500

(4) Mass of chamber + carbon after outgasing = 184.4110 g

(5) Mass of methane in chamber void at 500 psig = 0.075 g

(6) Mass of chamber + carbon + methane at 500 psig = 184.7103 g

(6) – (4) (+ Teflon correction of 0.051 g ) – (5) = mass adsorbed

184.7103 g – [184.4110 g (+0.051 g)] – 0.075 g = 0.1733 g

Mass adsorbed / mass of carbon = 0.2151 = g/g

Or, 21.51 g/100g

Or 21.51 * 10 * 0.432 = 92.94 g/L

Or 92.94 * 1.53 = 142L/L

## A2. Calculation for finding methane uptake capacity volumetric or by using pressure differential method

Table A2. Shows calculation of volumetric method for measuring methane uptake

| Sample | Pst0 | Pst1 | Ptt1 | Pst0 | Pst1 | Ptt1 | ΔPst | Mc | Vc | Vtt | Vst | n1 | n2 | nads | Mads | Mads/Mc |
|---|---|---|---|---|---|---|---|---|---|---|---|---|---|---|---|---|
| | value | value | value | psig | psig | psig | psig | g | cc | cc | cc | | | | g | g/g |
| Sample 1 | 0.16775 | 0.1303 | 0.1313 | 764.33 | 556.28 | 500.11 | 208.06 | 65.43 | 158.90 | 587.55 | 2276.00 | 1.43 | 0.64 | 0.79 | 12.65 | 0.19 |
| Sample 2 | 0.16974 | 0.1313 | 0.1313 | 775.39 | 561.83 | 500.11 | 213.56 | 65.30 | 158.90 | 587.55 | 2276.00 | 1.47 | 0.64 | 0.83 | 13.26 | 0.20 |

n1= total moles of CH4 transferred from storage tank
n2= total moles of CH4 in the dead volume of test tank
nads= total moles of CH4 adsorbed
Pst0= initial pressure in the storage tank
Pst1= final pressure in the storage tank
Ptt1= final pressure in the test tank
Mc= total mass of carbon in the test tank
Vc= total volume of carbon in test tank
Vtt= total volume of test tank
Vst= total volume of storage tank

# VITA

Parag Sureshchandra Shah was born in Baroda, India. He attended Bright High School in Baroda, India. He received his Bachelors of Engineering in Chemical Engineering from South Gujarat University, India in July of 2001. Since September 2002 he initiated graduate studies in Chemical Engineering at the University of Missouri-Columbia and received his M.S in December 2004 and a Doctor of Philosophy degree in August 2007.